

Electronic Thesis and Dissertation Repository

12-4-2014 12:00 AM

Synthesis and Characterization of Metal-Bis(trimethylsilyl)phosphido Complexes

Masoomeh Madadi, *The University of Western Ontario*

Supervisor: John F. Corrigan, *The University of Western Ontario*

A thesis submitted in partial fulfillment of the requirements for the Master of Science degree in Chemistry

© Masoomeh Madadi 2014

Follow this and additional works at: <https://ir.lib.uwo.ca/etd>

Recommended Citation

Madadi, Masoomeh, "Synthesis and Characterization of Metal-Bis(trimethylsilyl)phosphido Complexes" (2014). *Electronic Thesis and Dissertation Repository*. 2556.
<https://ir.lib.uwo.ca/etd/2556>

This Dissertation/Thesis is brought to you for free and open access by Scholarship@Western. It has been accepted for inclusion in Electronic Thesis and Dissertation Repository by an authorized administrator of Scholarship@Western. For more information, please contact wlsadmin@uwo.ca.

Synthesis and Characterization of Metal-Bis(trimethylsilyl)phosphido Complexes

(Thesis format: Monograph)

by

Masoomeh Madadi

Graduate Program in Chemistry

A thesis submitted in partial fulfillment
of the requirements for the degree of
Master of Science

The School of Graduate and Postdoctoral Studies
The University of Western Ontario
London, Ontario, Canada

© Masoomeh Madadi 2014

Abstract

The metal-halide complexes bearing monodentate N-heterocyclic carbenes [PdI₂(ⁱPr₂-bimy)₂], [NiI₂(ⁱPr₂-bimy)₂], [PdI₂(ⁿBu₂-bimy)₂] (*trans*-**1**) and [NiBr₂(ⁿBu₂-bimy)₂] (*trans*-**2**); bimy = benzimidazole-2-ylidene, react under mild conditions with Li[P(SiMe₃)₂], in a 1:1 ratio, to provide metal-halido-silylphosphido complexes [PdI(ⁱPr₂-bimy)₂{P(SiMe₃)₂}] (*trans*-**3**), [NiI(ⁱPr₂-bimy)₂{P(SiMe₃)₂}] (*trans*-**4**), [PdI(ⁿBu₂-bimy)₂{P(SiMe₃)₂}] (*trans*-**5**) and [NiBr(ⁿBu₂-bimy)₂{P(SiMe₃)₂}] (*trans*-**6**). The reaction of a dimeric gold(I) complex with a bidentate N-heterocyclic carbene, [Au₂Cl₂(ⁿBu₄-benzo(imy)₂)]₂; benzo(imy)₂ = benzobis(imidazole-2-ylidene), with Li[P(SiMe₃)₂], in a 1:2 ratio, results in the formation of the metal-bis(trimethylsilyl)phosphido complex [Au₂(ⁿBu₄-benzo(imy)₂)₂{P(SiMe₃)₂}₂] (**7**).

The carbonyl addition reactions with the metal-halido-silylphosphido complexes *trans*-**3** and *trans*-**4**, with benzoyl chloride is also studied wherein, they lead to the formation of two new metal-halido-dibenzoylphosphido complexes, [PdI(ⁱPr₂-bimy)₂P{C(O)Ph}₂] (*trans*-**8**) and [NiI(ⁱPr₂-bimy)₂P{C(O)Ph}₂] (*trans*-**9**). NMR spectroscopy, X-ray crystallography, mass spectrometry and elemental analysis are used to analyze these coordination complexes.

Keywords: N-heterocyclic carbenes, benzimidazole-2-ylidene, benzobis(imidazole-2-ylidene), silylphosphido, carbonyl addition, benzoyl chloride, NMR spectroscopy, X-ray crystallography, mass spectrometry, elemental analysis.

Acknowledgments

I would like to express my sincerest appreciation to Professor John F. Corrigan for his support, guidance and encouragement. His valuable ideas were always helpful to make the work move forward.

I would like to send my utmost thanks to my family and it is enough to say that this thesis has been written for and dedicated to my mother and father as well as my loving husband, whose presence and support allowed me to accomplish success and attain my dream goals.

For
My
Loving Mother and Father,
&
Beloved Husband

Table of Contents

Abstract.....	II
Acknowledgments.....	III
Table of Contents.....	V
List of Figures.....	VII
List of Schemes.....	X
List of Appendices.....	XI
List of Abbreviations.....	XII
1. Introduction.....	1
1.1 Metal-Bis(trimethylsilyl)phosphido Complexes.....	1
1.2 Electronic and Steric Properties of Phosphines and NHCs.....	5
1.3 Metal-NHC-Halido Complexes.....	8
1.4 Metal-Diacylphosphido Complexes.....	10
1.5 Project Objectives.....	15
2. Metal-Silylphosphido complexes.....	17
2.1. Introduction.....	17
2.2. Experimental.....	18
2.2.1. General Synthetic Techniques and Starting Materials.....	18
2.2.2. $[\text{PdI}_2(\text{}^n\text{Bu}_2\text{-bimy})_2]$ (<i>trans</i> -1).....	21
2.2.3. $[\text{NiBr}_2(\text{}^n\text{Bu}_2\text{-bimy})_2]$ (<i>trans</i> -2).....	21
2.2.4. $[\text{PdI}(\text{}^i\text{Pr}_2\text{-bimy})_2\{\text{P}(\text{SiMe}_3)_2\}]$ (<i>trans</i> -3).....	22
2.2.5. $[\text{NiI}(\text{}^i\text{Pr}_2\text{-bimy})_2\{\text{P}(\text{SiMe}_3)_2\}]$ (<i>trans</i> -4).....	23
2.2.6. $[\text{PdI}(\text{}^n\text{Bu}_2\text{-bimy})_2\{\text{P}(\text{SiMe}_3)_2\}]$ (<i>trans</i> -5).....	24

2.2.7. [NiBr(ⁿ Bu ₂ -bimy) ₂ {P(SiMe ₃) ₂ }] (<i>trans</i> -6).....	25
2.2.8. [Au ₂ (ⁿ Bu ₄ -benzo(imy) ₂){P(SiMe ₃) ₂ } ₂] (7)	25
2.3. Results and Discussion	26
2.3.1. [MX ₂ (ⁿ Bu ₂ -bimy) ₂] Complexes; M = Pd, Ni; X = Br, I.	26
2.3.2. [MX(R ₂ -bimy) ₂ {P(SiMe ₃) ₂ }] Complexes; M = Pd, Ni; R = ⁱ Pr, ⁿ Bu; X = Br, I.	32
2.4. Conclusions.....	45
3. Metal-Diacylphosphido Complexes.....	47
3.1. Introduction.....	47
3.2. Experimental.....	48
3.2.1. General Synthetic Techniques and Starting Materials.....	48
3.2.2. [PdI(ⁱ Pr ₂ -bimy) ₂ P{C(O)Ph} ₂] (<i>trans</i> -8).....	49
3.2.3. [NiI(ⁱ Pr ₂ -bimy) ₂ P{C(O)Ph} ₂] (<i>trans</i> -9).....	49
3.3. Results and Discussion	50
3.3.1. [MI(ⁱ Pr ₂ -bimy) ₂ P{C(O)Ph} ₂] Complexes, M = Pd, Ni.....	50
3.4. Conclusions.....	56
4. Conclusions and Recommendations for Future Work	58
4.1. Conclusions.....	58
4.2. Recommendations for Future Work.....	59
References.....	61
Appendices.....	65
Curriculum Vitae	92

List of Figures

Figure 1.1: Multiple bond character of Zr-P bond in $[(\eta^5\text{-C}_5\text{H}_4\text{Me})_2\text{Zr}\{\text{P}(\text{SiMe}_3)_2\}_2]$ [3].	3
Figure 1.2: Reactivity patterns for Pt-P(SiMe ₃) ₂ complexes [11].	5
Figure 1.3: Tolman's method of measuring cone angle (θ) of phosphine ligands [13].	6
Figure 1.4: Nolan's method of measuring percent buried volume (% V _{bur}) [15].	7
Figure 2.1: Metal-hydrogen bond interactions.	28
Figure 2.2: ¹ H NMR spectrum of complex $[\text{PdI}_2(\text{}^n\text{Bu}_2\text{-bimy})_2]$ (<i>trans-1</i>).	28
Figure 2.3: Molecular structure of complex $[\text{PdI}_2(\text{}^n\text{Bu}_2\text{-bimy})_2]$ (<i>trans-1</i>) (50% probability). All hydrogen atoms are omitted for clarity. Selected bond lengths (Å) and angles (°) of complex 1 : Pd1-I1 (2.6088(6)), Pd1-I2 (2.6057(6)), Pd1-C1 (2.023(3)), Pd1-C16 (2.021(3)), I1-Pd1-I2 (179.472(14)), I1-Pd1-C1 (91.60(9)), I2-Pd1-C1 (88.92(8)), I1-Pd1-C16 (89.11(9)), I2-Pd1-C16 (90.37(9)), C1-Pd1-C16 (179.24(14)).	29
Figure 2.4: ¹ H NMR spectrum of complex $[\text{NiBr}_2(\text{}^n\text{Bu}_2\text{-bimy})_2]$ (<i>trans-2</i>).	31
Figure 2.5: Molecular structure of complex $[\text{NiBr}_2(\text{}^n\text{Bu}_2\text{-bimy})_2]$ (<i>trans-2</i>) (50% probability). All hydrogen atoms are omitted for clarity. Selected bond lengths (Å) and angles (°) of complex 2 : Ni1-Br1 (2.3143(18)), Ni1-C1 (1.903(3)), Br1-Ni1-Br1A (180.0), Br1-Ni1-C1 (88.98(8)), Br1-Ni1-C1A (91.02(8)), C1-Ni1-C1A (180.0).	32
Figure 2.6: ¹ H NMR spectrum of complex $[\text{PdI}(\text{}^i\text{Pr}_2\text{-bimy})_2\{\text{P}(\text{SiMe}_3)_2\}]$ (<i>trans-3</i>).	34

Figure 2.7: ^1H NMR spectrum of complex $[\text{PdI}(\text{}^n\text{Bu}_2\text{-bimy})_2\{\text{P}(\text{SiMe}_3)_2\}]$ (<i>trans</i> - 5).....	35
Figure 2.8: $^{31}\text{P}\{^1\text{H}\}$ NMR spectrum of $[\text{PdI}(\text{}^i\text{Pr}_2\text{-bimy})_2\{\text{P}(\text{SiMe}_3)_2\}]$ (<i>trans</i> - 3).....	36
Figure 2.9: $^{31}\text{P}\{^1\text{H}\}$ NMR spectrum of complex $[\text{PdI}(\text{}^n\text{Bu}_2\text{-bimy})_2\{\text{P}(\text{SiMe}_3)_2\}]$ (<i>trans</i> - 5) ...	36
Figure 2.10: Molecular structure of complex $[\text{PdI}(\text{}^i\text{Pr}_2\text{-bimy})_2\{\text{P}(\text{SiMe}_3)_2\}]$ (<i>trans</i> - 3) (50% probability). All hydrogen atoms and solvent (pentane) molecules are omitted for clarity. Selected bond lengths (Å) and angles (°) of complex 3 : Pd1-I1 (2.6998(7)), Pd1-P1 (2.3442(12)), Pd1-C1 (2.027(4)), Pd1-C14 (2.047(4)), I1-Pd1-P1 (166.42(3)), I1-Pd1-C1 (86.94(10)), I1-Pd1-C14 (84.48(11)), P1-Pd1-C1 (91.93(11)), P1-Pd1-C14 (96.49(11)), C1-Pd1-C14 (171.41(13)).....	38
Figure 2.11: Molecular structure of complex $[\text{PdI}(\text{}^n\text{Bu}_2\text{-bimy})_2\{\text{P}(\text{SiMe}_3)_2\}]$ (<i>trans</i> - 5) (50% probability). All hydrogen atoms and solvent ($\text{LiI} \cdot (\text{thf})_3$) molecules are omitted for clarity. Selected bond lengths (Å) and angles (°) of complex 5 : Pd1-I1 (2.6985(10)), Pd1-P1 (2.3648(17)), Pd1-C1 (2.022(6)), Pd1-C8 (2.049(6)), I1-Pd1-P1 (174.55(4)), I1-Pd1-C1 (88.14(17)), I1-Pd1-C8 (88.51(16)), P1-Pd1-C1 (93.60(17)), P1-Pd1-C8 (89.77(17)), C1-Pd1-C8 (176.6(2)).....	39
Figure 2.12: ^1H NMR spectrum of complex $[\text{NiI}(\text{}^i\text{Pr}_2\text{-bimy})_2\{\text{P}(\text{SiMe}_3)_2\}]$ (<i>trans</i> - 4)	40
Figure 2.13: ^1H NMR spectrum of complex $[\text{NiBr}(\text{}^n\text{Bu}_2\text{-bimy})_2\{\text{P}(\text{SiMe}_3)_2\}]$ (<i>trans</i> - 6)	41
Figure 2.14: $^{31}\text{P}\{^1\text{H}\}$ NMR spectrum of $[\text{NiI}(\text{}^i\text{Pr}_2\text{-bimy})_2\{\text{P}(\text{SiMe}_3)_2\}]$ (<i>trans</i> - 4).....	42
Figure 2.15: $^{31}\text{P}\{^1\text{H}\}$ NMR spectrum of complex $[\text{NiBr}(\text{}^i\text{Pr}_2\text{-bimy})_2\{\text{P}(\text{SiMe}_3)_2\}]$ (<i>trans</i> - 6)	42

Figure 2.16: ^1H NMR spectrum of complex $[\text{Au}(\text{}^n\text{Bu}_4\text{-benz(bimy)\{P(SiMe}_3\}_2\}_2)]$ (7).....	44
Figure 2.17: $^{31}\text{P}\{^1\text{H}\}$ NMR spectrum of complex $[\text{Au}(\text{}^n\text{Bu}_4\text{-benz(bimy)\{P(SiMe}_3\}_2\}_2)]$ (7) ..	45
Figure 3.1: ^1H NMR spectrum of complex $[\text{PdI}(\text{}^i\text{Pr}_2\text{-bimy})_2\text{P}\{\text{C(O)Ph}\}_2]$ (<i>trans</i> - 8)	52
Figure 3.2: ^1H NMR spectrum of complex $[\text{NiI}(\text{}^i\text{Pr}_2\text{-bimy})_2\text{P}\{\text{C(O)Ph}\}_2]$ (<i>trans</i> - 9).....	53
Figure 3.3: $^{31}\text{P}\{^1\text{H}\}$ NMR spectrum of complex $[\text{PdI}(\text{}^i\text{Pr}_2\text{-bimy})_2\text{P}\{\text{C(O)Ph}\}_2]$ (<i>trans</i> - 8).....	53
Figure 3.4: $^{31}\text{P}\{^1\text{H}\}$ NMR spectrum of complex $[\text{NiI}(\text{}^i\text{Pr}_2\text{-bimy})_2\text{P}\{\text{C(O)Ph}\}_2]$ (<i>trans</i> - 9).....	54
Figure 3.5: Molecular structure of complex $[\text{NiI}(\text{}^i\text{Pr}_2\text{-bimy})_2\text{P}\{\text{C(O)Ph}\}_2]$ (<i>trans</i> - 9) (50% probability). All hydrogen atoms and solvent (toluene) molecules are omitted for clarity. Selected bond lengths (Å) and angles (°) of complex 9 : Ni1-I1 (2.5326(6)), Ni1-P1 (2.1888(10)) Ni1-C1 (1.896 (3)), Ni1-C14 (1.903 (3)), I1-Ni1-P1 (170.15(3)), I1-Ni1-C1 (87.23(9)), I1-Ni1-C14 (89.81(8)), P1-Ni1-C1 (92.29(9)), P1-Ni1-C14 (90.31(9)), C1-Ni1-C14 (176.50(11)).....	56

List of Schemes

Scheme 1.1: Iron complexes terminally bonded or bridged to P(SiMe ₃) ₂ [7].	2
Scheme 1.2: Synthesis of [(η ⁵ -C ₅ H ₄ Me) ₂ Zr{P(SiMe ₃) ₂] ₂] complex [3].	3
Scheme 1.3: Synthesis of [(^t Bu-DAB)Ga{P(SiMe ₃) ₂] ₂] [10].	4
Scheme 1.4: Mizoroki-Heck reactions catalyzed by [Pd(ⁱ Pr ₂ -bimy) ₂ X ₂] (X = Br, I) [19]	9
Scheme 1.5: Becker route to phosphalkenes: condensation followed by the [1,3]-sigmatropic rearrangement of an acylphosphine to a phosphalkene [41].	11
Scheme 1.6: Elimination reaction to form phosphorus-carbon double bond.	11
Scheme 1.7: Condensation reaction to synthesize carbon-phosphorus double bond.	12
Scheme 1.8: Sigmatropic migration of organophosphines resulted in P=C double bond.	12
Scheme 1.9: The first iron phosphalkene complexes prepared by Weber <i>et al.</i> [47]	13
Scheme 1.10: Phosphalkenylrhenium complexes synthesized by Weber <i>et al.</i> [49].	13
Scheme 1.11: Mono and diacylphosphido iron complexes reported by Weber <i>et al.</i> [50].	14
Scheme 1.12: Mono-, bis- and poly(phosphalkene) prepared by Gates <i>et al.</i> [51].	15
Scheme 2.1: Synthesis of [MX(R ₂ -bimy) ₂ {P(SiMe ₃) ₂ }] complexes.	33
Scheme 3.1: Synthesis of [MI(R ₂ -bimy) ₂ P{C(O)Ph} ₂] complexes.	51

List of Appendices

Appendix A: Crystal data and structure refinement for [PdI ₂ (ⁿ Bu ₂ -bimy) ₂] (<i>trans</i> -1)	65
Appendix B: Atomic coordinates for [PdI ₂ (ⁿ Bu ₂ -bimy) ₂] (<i>trans</i> -1)	67
Appendix C: Crystal data and structure refinement for [NiBr ₂ (ⁿ Bu ₂ -bimy) ₂] (<i>trans</i> -2)	72
Appendix D: Atomic coordinates for [NiBr ₂ (ⁿ Bu ₂ -bimy) ₂] (<i>trans</i> -2)	74
Appendix E: Crystal data and structure refinement for [PdI(ⁱ Pr ₂ -bimy) ₂ {P(SiMe ₃) ₂ }].C ₅ H ₁₂ (<i>trans</i> -3)	76
Appendix F: Atomic coordinates for [PdI(ⁱ Pr ₂ -bimy) ₂ {P(SiMe ₃) ₂ }].C ₅ H ₁₂ (<i>trans</i> -3)	78
Appendix G: Crystal data and structure refinement for [PdI(ⁿ Bu ₂ -bimy) ₂ {P(SiMe ₃) ₂ }]. [Li (THF) ₃ I] (<i>trans</i> -5)	81
Appendix H: Atomic coordinates for [PdI(ⁿ Bu ₂ -bimy) ₂ {P(SiMe ₃) ₂ }]. [Li (THF) ₃ I] (<i>trans</i> -5)	83
Appendix I: Crystal data and structure refinement for [NiI(ⁱ Pr ₂ -bimy) ₂ P{C(O)Ph} ₂].C ₇ H ₈ (<i>trans</i> -9)	87
Appendix J: Atomic coordinates for [NiI(ⁱ Pr ₂ -bimy) ₂ P{C(O)Ph} ₂].C ₇ H ₈ (<i>trans</i> -9)	89

List of Abbreviations

\AA	angstrom
<i>bimy</i>	benzimidazole-2-ylidene
<i>benzo(imy)₂</i>	benzobis(imidazole-2-ylidene)
ⁿ <i>Bu</i> ₂	normal butyl
$^{\circ}\text{C}$	degree Celsius
<i>d</i> (NMR)	doublet
<i>dd</i> (NMR)	doublet of doublets
<i>DCM</i>	dichloromethane
<i>DME</i>	dimethoxyethane
<i>DMSO</i>	dimethyl sulfoxide
<i>Et</i>	ethyl
<i>g</i>	gram
<i>HRMS</i>	high resolution mass spectrometry
<i>m</i> (NMR)	multiplet
<i>mL</i>	milliliter
<i>m.p.</i>	melting point
<i>M</i>	any metal atom
<i>Me</i>	methyl
<i>Mes</i>	mesitylene
<i>MHz</i>	megahertz

<i>NHC</i>	N-heterocyclic carbene
<i>NMR</i>	nuclear magnetic resonance
<i>OAc</i>	acetate anion
<i>Ph</i>	phenyl
<i>ppm</i>	part per million
<i>ⁱPr</i>	isopropyl
<i>r</i>	repulsiveness
<i>s (NMR)</i>	singlet
<i>sep (NMR)</i>	septet
<i>THF</i>	tetrahydrofuran

1. INTRODUCTION

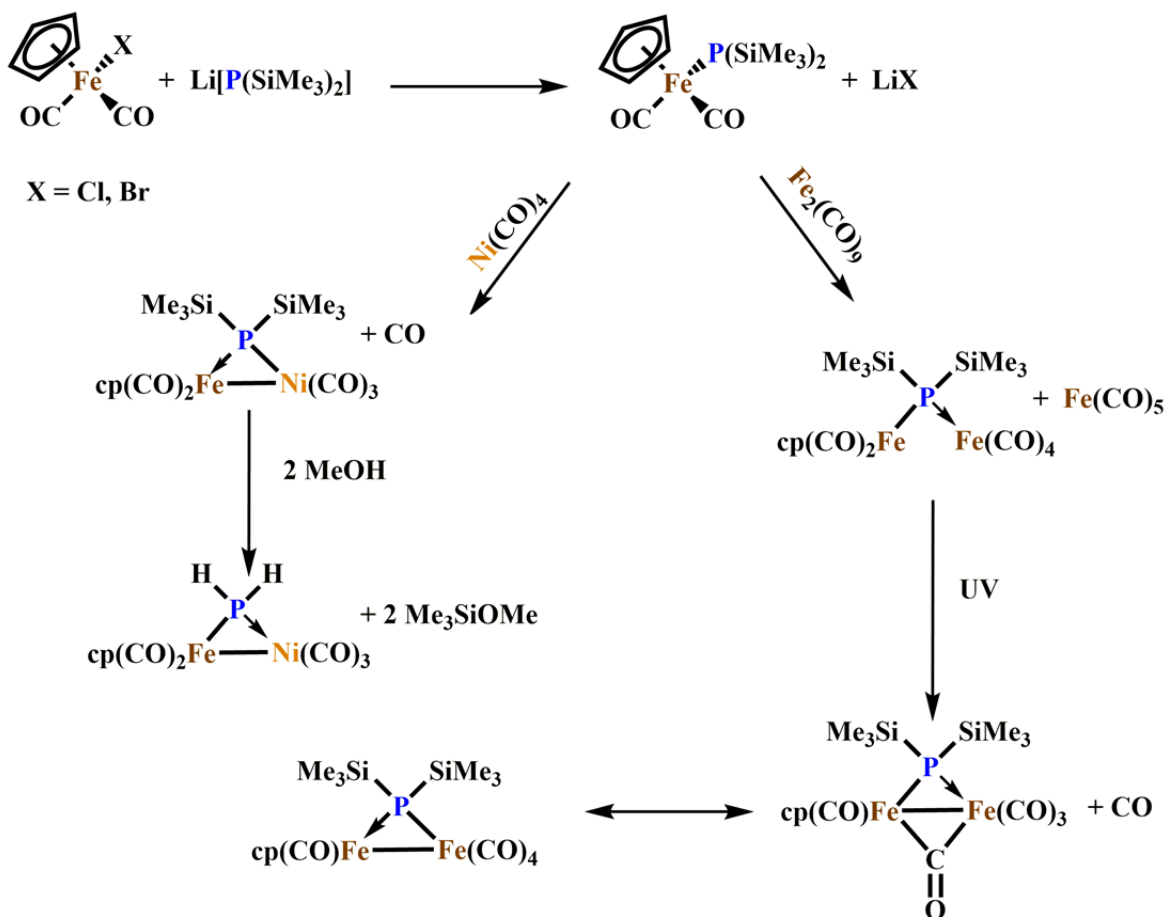
Tris(trialkylsilyl)phosphines and their substituted lithium phosphidos are valuable synthons which are widely used for the formation of multiple bonds between metal and a phosphorus atom [1-8]. The lithiation of tris(trialkylsilyl)phosphine with n-butyllithium leads to the formation of lithium-bis(trialkylsilyl)phosphido, $\text{Li}[\text{P}(\text{SiMe}_3)_2]$, which is commonly used in phosphorus chemistry as a strong, sterically hindered base [9]. Although using the highly reactive tris(trialkylsilyl)phosphines causes some handling difficulties, their unique electron donating and steric bulk properties make them excellent reagents in metal-silylphosphido chemistry [1].

1.1 Metal-Bis(trimethylsilyl)phosphido Complexes

The bis(trimethylsilyl)phosphido group can be transferred to many metals and nonmetals by the reaction of $\text{Li}[\text{P}(\text{SiMe}_3)_2]$ with various metal/non-metal halides. Several reports are available in this area of research [1-8].

A review on the development of metal-phosphorus chemistry which relies on the use of $\text{Li}[\text{P}(\text{SiMe}_3)_2]$ reagent is presented here. It has been shown that nucleophilic addition of $\text{Li}[\text{P}(\text{SiMe}_3)_2]$ to the complex of $[(\eta^5\text{-C}_5\text{H}_5)(\text{CO})_2\text{FeX}]$; X = Br, Cl, resulted in the formation of the first iron complex containing a terminal silylphosphido group $[(\eta^5\text{-C}_5\text{H}_5)(\text{CO})_2\text{Fe}\{\text{P}(\text{SiMe}_3)_2\}]$ [7]. This complex was reacted with $\text{Ni}(\text{CO})_4$ and $\text{Fe}_2(\text{CO})_9$ to

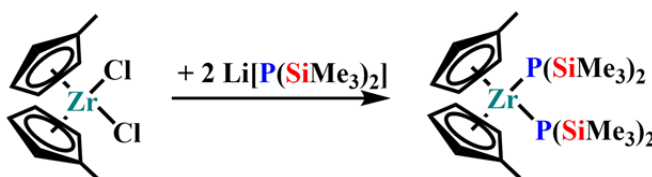
obtain the $P(SiMe_3)_2$ -bridged complexes $[(\eta^5-C_5H_5)(CO)_2Fe\{\mu-P(SiMe_3)_2\}Ni(CO)_3]$ and $[(\eta^5-C_5H_5)(CO)_2Fe\{\mu-P(SiMe_3)_2\}Fe(CO)_4]$, respectively. A CO-bridged complex $[(\eta^5-C_5H_5)(CO)Fe\{\mu-CO, \mu-P(SiMe_3)_2\}Ni(CO)_3]$ was formed upon UV-irradiation of the $[(\eta^5-C_5H_5)(CO)_2Fe\{\mu-P(SiMe_3)_2\}Ni(CO)_3]$. Moreover, the study of P—Si bond cleavage by reaction with methanol resulted in the formation of PH_2 -bridged complexes, $[(\eta^5-C_5H_5)(CO)_2Fe\{\mu-PH_2\}Ni(CO)_3]$ and $[(\eta^5-C_5H_5)(CO)_2Fe\{\mu-PH_2\}Fe(CO)_4]$ (see Scheme 1.1).



Scheme 1.1: Iron complexes terminally bonded or bridged to $P(SiMe_3)_2$ [7].

The bis(trimethylsilyl)phosphido complex, $[(\eta^5-C_5H_4Me)_2Zr\{P(SiMe_3)_2\}_2]$, was prepared by the reaction of two equivalents of $Li[P(SiMe_3)_2]$ with $[(\eta^5-C_5H_4Me)_2ZrCl_2]$ [3]

(see Scheme 1.2). The presence of two equivalent P atoms was confirmed by variable temperature ^{31}P NMR studies (-100 to 25 °C). Their resonances were exhibited at -75.3 ppm (25 °C) and -86.2 ppm (-100 °C) which significantly shifted downfield (from -297 ppm in $\text{Li}[\text{P}(\text{SiMe}_3)_2]$) due to the partial multiple bond character of $\text{Zr}-\text{P}$ bonds (see Figure 1.1). X-ray crystallography data showed that $[(\eta^5\text{-C}_5\text{H}_4\text{Me})_2\text{Zr}\{\text{P}(\text{SiMe}_3)_2\}_2]$ had two almost identical $\text{Zr}-\text{P}$ bonds and each phosphido group indicated a nearly planar arrangement.



Scheme 1.2: Synthesis of $[(\eta^5\text{-C}_5\text{H}_4\text{Me})_2\text{Zr}\{\text{P}(\text{SiMe}_3)_2\}_2]$ complex [3].

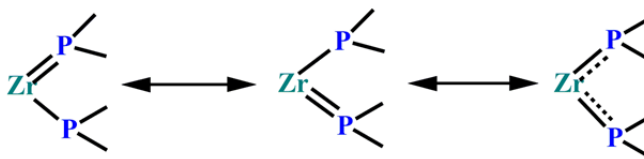
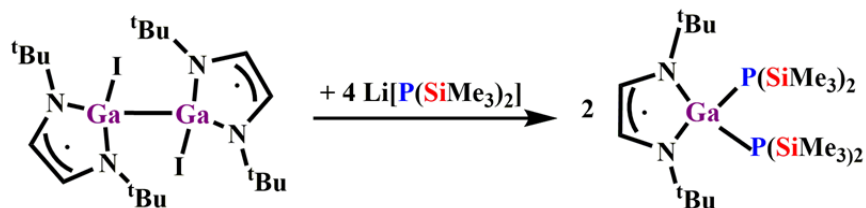


Figure 1.1: Multiple bond character of $\text{Zr}-\text{P}$ bond in $[(\eta^5\text{-C}_5\text{H}_4\text{Me})_2\text{Zr}\{\text{P}(\text{SiMe}_3)_2\}_2]$ [3].

The reaction of $[\{(\text{}^t\text{Bu-DAB})\text{GaI}\}_2]$; $\text{}^t\text{Bu-DAB} = \{(\text{}^t\text{Bu})\text{NC}(\text{H})\}_2$, with the alkali metal pnictides $\text{M}[\text{E}(\text{SiMe}_3)_2]$; $\text{M} = \text{Li}$ or Na ; $\text{E} = \text{N}$, P , or As , was performed under a range of stoichiometries [10]. The 1:2 and 1:4 reactions led to the gallium(II) $[(\text{}^t\text{Bu-DAB})\text{GaI}\{\text{E}(\text{SiMe}_3)_2\}]$ and $[(\text{}^t\text{Bu-DAB})\text{Ga}\{\text{E}(\text{SiMe}_3)_2\}_2]$; $\text{E} = \text{N}$, P , or As , respectively [10] (see Scheme 1.3).



Scheme 1.3: Synthesis of $[(^t\text{Bu-DAB})\text{Ga}\{\text{P}(\text{SiMe}_3)_2\}_2]$ [10].

Two square planar platinum(II)-bis(trimethylsilyl)phosphido complexes *trans*- $[\text{PtCl}(\text{Et}_3\text{P})_2\{\text{P}(\text{SiMe}_3)_2\}_2]$ and *trans*- $[\text{Pt}(\text{Et}_3\text{P})_2\{\text{P}(\text{SiMe}_3)_2\}_2]$ were reported as the first platinum complexes bearing silylphosphido ligands [11]. The substitution products were initially formed in the reactions of $[\text{PtCl}_2(\text{Et}_3\text{P})_2]$ with $\text{Li}[\text{P}(\text{SiMe}_3)_2]$ at low temperatures. Note that *trans*- $[\text{Pt}(\text{Et}_3\text{P})_2\{\text{P}(\text{SiMe}_3)_2\}_2]$ was not stable in solution and immediately decomposed at ambient temperature. Elimination of $\text{P}(\text{SiMe}_3)_3$ and PEt_3 from the complex resulted in a mixture of the diphosphene complex $[\text{Pt}(\text{Et}_3\text{P})_2\{\eta^2\text{-}(\text{PSiMe}_3)_2\}]$ and the phosphido-bridged platinum(I) complex $[(\text{Pt}-\text{Pt})\{\text{Et}_3\text{PPtP}(\text{SiMe}_3)_2\}_2]$. Heating *trans*- $[\text{PtCl}(\text{Et}_3\text{P})_2\{\text{P}(\text{SiMe}_3)_2\}_2]$ to 80 °C in solution yielded the P_2 -complex $[(\text{Et}_3\text{P})_2\text{Pt}]_2\text{P}_2$, which was also unstable at higher temperatures (see Figure 1.2). Similar results were reported for *trans*- $[\text{NiCl}(\text{Et}_3\text{P})_2\{\text{P}(\text{SiMe}_3)_2\}_2]$ and *trans*- $[\text{Ni}(\text{Et}_3\text{P})_2\{\text{P}(\text{SiMe}_3)_2\}_2]$ [12].

Analogous reactions of *trans*- $[\text{PtCl}_2(\text{PPh}_3)_2]$ with $\text{Li}[\text{P}(\text{SiMe}_3)_2]$, $[(\text{Me}_3\text{Si})_2\text{P}]_2$ and $[\text{Me}_3\text{Si}(\text{Me}_3\text{C})\text{P}]_2$ were much more difficult to survey [11]. The complexes $(\text{Ph}_3\text{P})_2\text{Pt}[\eta^2\text{-}(\text{PSiMe}_3)_2]$, $[\{\text{Ph}_3\text{P}\}\text{Pt}]_2\text{P}_2$ and $(\text{Ph}_3\text{P})\text{Pt}[\eta^2\text{-}(\text{PCMe}_3)_2]$ were detectable via NMR spectroscopy; however, they could not be isolated as pure compounds [11]. This was due to the steric and electronic properties of the triphenylphosphine ligand which made the complex formation more difficult than that of the triethylphosphine complexes [11].

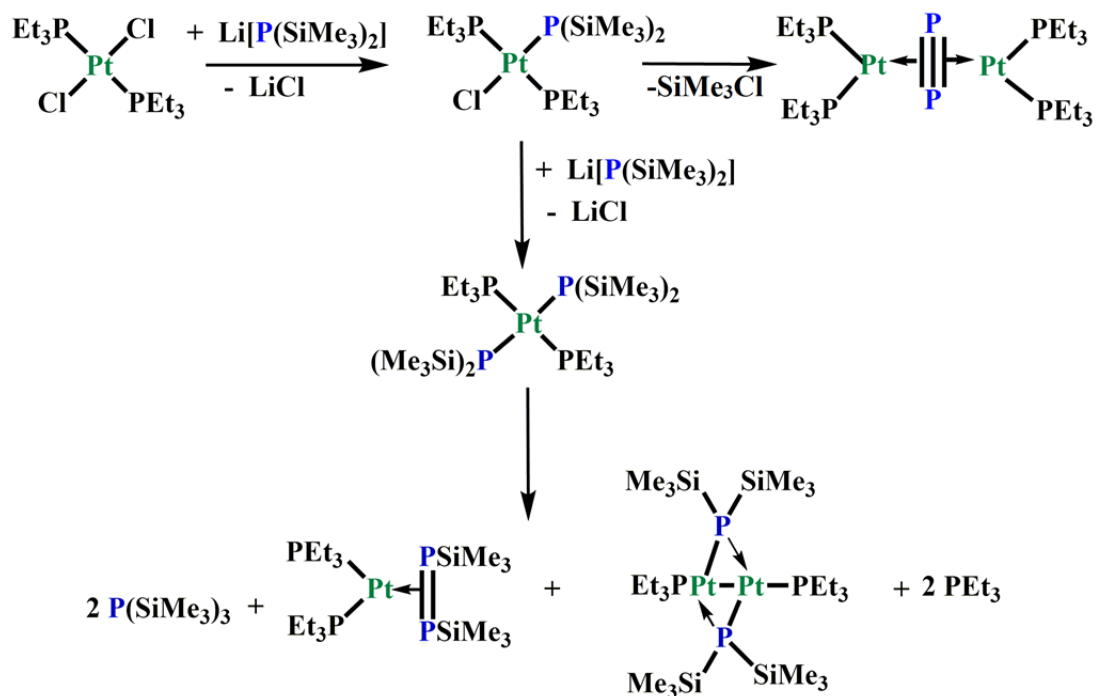


Figure 1.2: Reactivity patterns for Pt-P(SiMe₃)₂ complexes [11].

1.2 Electronic and Steric Properties of Phosphines and NHCs

The behavior of the free tertiary phosphines and their transition metal complexes could be remarkably changed by altering substituents on the phosphorus ligands [13]. A review on the steric effects of phosphorus ligands in organometallic chemistry was published in 1977 by Tolman [13]. Tolman proposed an experimental measure of electronic parameter (ν) by using the fundamental CO stretching frequency A_1 in $[\text{Ni}(\text{CO})_3\text{L}]$ complexes in dichloromethane, where L denoted a PR_3 ligand. Tolman's electronic parameter (TEP) was consistent with the net donor properties of L, thereby allowing estimation of electron-richness of the nickel atom in $[\text{Ni}(\text{CO})_3\text{L}]$ complexes. For example, $[\text{Ni}(\text{CO})_3(\text{PEt}_3)]$ with TEP = 2061.7 ($X_i = 1.8$) was more electron-rich species than $[\text{Ni}(\text{CO})_3(\text{PPh}_3)]$ with TEP =

2068.9 cm⁻¹ ($X_i = 4.3$) in the [Ni(CO)₃L] series. The electronic parameter (ν) of phosphines was decreased by increasing the repulsion in substituents on phosphorus ligands. The TEP of various tertiary phosphines (PR₃) was estimated through Equation (1.1), where X_i was the identity of substituents contributions [13].

$$\text{TEP} = 2056.1 + \sum_{i=1}^3 R_i \quad (1.1)$$

Tertiary phosphines could be ranked in the steric series as well as the electronic ones. The size of substituents on the phosphorus ligand had a significant effect on the bonding properties of phosphines. The size of phosphine ligands was measured by the cone angle (θ) [13]. According to Tolman's definition, the cone angle (θ) is the apex angle of a cylindrical cone, centered 2.28 Å (the standard Ni–P bond distance in [Ni(CO)₃L] complexes) from the center of the P atom, where the outermost atoms touched the perimeter of the cone (Figure 1.3). For instance, the calculated cone angles of PEt₃ and PPh₃ ligands were 132° and 145°, respectively [13]. Tertiary phosphine ligands are classified using TEP and cone angle parameters, however, the method can be applied in theory to any ligand.

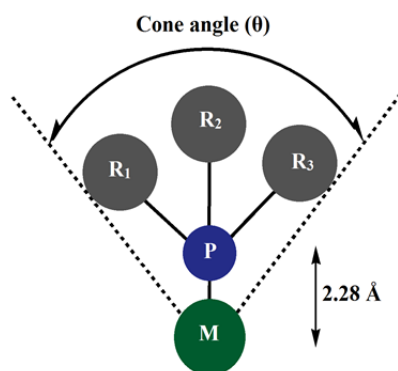


Figure 1.3: Tolman's method of measuring cone angle (θ) of phosphine ligands [13]

The steric parameter calculations using the Tolman model have proven difficult and for more sterically elaborate ligands such as phosphines containing biphenylene and related groups, bidentate ligands and N-heterocyclic carbenes (NHCs) [14]. Nolan and Cavallo [15] introduced an alternate phosphine-like model (percent buried volume % V_{bur}) to estimate the steric bulk of NHC ligands. Percent buried volume (% V_{bur}) was the percent of the total volume of a sphere occupied by NHC (Figure 1.4). In Nolan's model, a metal atom was placed in the core of a sphere with a defined radius. Although the original metal-carbene bond length was 2.105 Å, 2.00 Å was considered as the average of metal-carbene bond distance in this model. The % V_{bur} of several saturated and unsaturated NHCs was calculated using crystallography data [15].

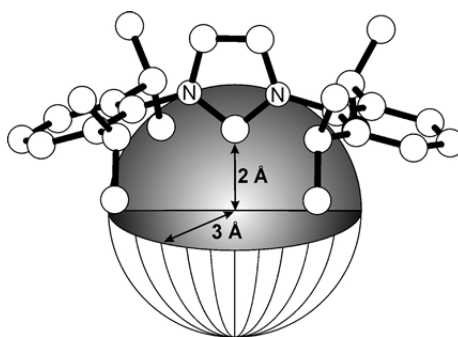


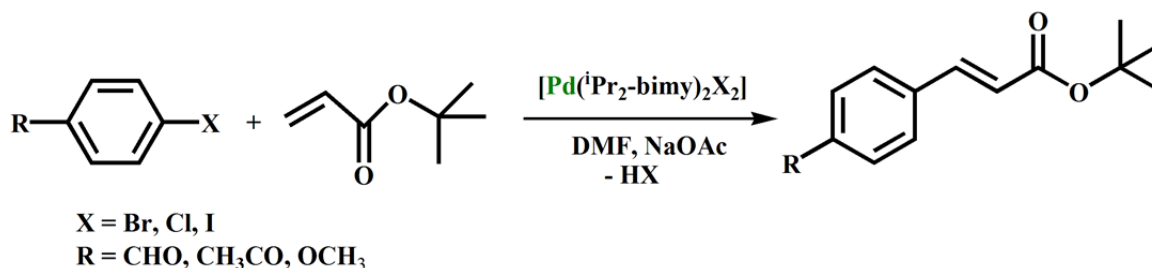
Figure 1.4: Nolan's method of measuring percent buried volume (% V_{bur}) [15]

On the other hand, Gusev [16] used DFT calculations to determine the steric and electronic properties of 76 NHCs in $[(\text{NHC})\text{Ni}(\text{CO})_3]$ complexes. Different descriptor repulsiveness (r) was applied and an increase in r between NHC and CO ligands was observed in $[(\text{NHC})\text{Ni}(\text{CO})_3]$ complexes with bulky substituents on NHCs. For example, TEP (cm^{-1}) and r values were calculated for $^1\text{Pr}_2\text{-bimy}$ (2054.0, 2.3), $\text{Me}_2\text{-bimy}$ (2057.0, 1.6) and $\text{Et}_2\text{-bimy}$ (2055.2, 1.6) ligands, respectively. Gusev showed that the donor properties of

NHCs was decreased as the size of substituents on N-heterocycles was increased [16]. The steric bulk of NHCs was also estimated by Nolan's % V_{bur} [15]. For instance, the percent buried volumes (% V_{bur}) of [$(i\text{Pr}_2\text{-bimy})\text{AuCl}$] (27.9 and 23.9), [$(\text{Et}_2\text{-bimy})\text{AuCl}$] (27.9 and 24.0) and [$(\text{Me}_2\text{-bimy})\text{AuCl}$] (26.3 and 22.7) were smaller than that of [$(\text{Et}_3\text{P})\text{AuCl}$] (31.7 and 27.1) and [$(\text{Ph}_3\text{P})\text{AuCl}$] (34.8 and 29.9), where M—NHC and M—P were 2.00 Å and 2.28 Å, respectively [15].

1.3 Metal-NHC-Halido Complexes

N-heterocyclic carbenes (NHC) were intensively investigated as strongly bonded ligands in organometallic chemistry and homogeneous catalysts [17-21]. In comparison to traditional carbenes, NHCs are much more electron rich nucleophilic compounds which can easily donate their lone pair of electrons. In addition, introducing different substituents on the heterocycles can modify the steric and electronic properties of NHCs. Transition-metal carbene complexes are widely used as highly active precatalysts for organic reactions such as CO-olefin co-polymerization [22-24], amination [25], dehalogenation of aryl halides [26], Suzuki-Miyaura C-C and C-N coupling reactions [18, 19, 21, 27]. In particular, palladium(II)-NHC-halido complexes *trans*-[Pd($i\text{Pr}_2\text{-bimy}$)₂Br₂] and *trans*-[Pd($i\text{Pr}_2\text{-bimy}$)₂I₂] were successfully developed for different applications such as Mizoroki-Heck coupling of aryl bromides or chlorides (Scheme 1.4) [19]. The catalytic study revealed that the complexes were highly active in coupling of aryl bromides and chlorides. However, the steric bulk of isopropyl groups on NHC prevented the reductive formation of Pd(0) species. As a result, a slower conversion of these catalysts were observed compared to catalysts with less bulky substituents [19].



Scheme 1.4: Mizoroki-Heck reactions catalyzed by $[\text{Pd}(\text{iPr}_2\text{-bimy})_2\text{X}_2]$ ($X = \text{Br, I}$) [19]

A series of square planar luminescent complexes $\text{trans}-[(\text{iPr}_2\text{-bimy})_2\text{Pd}(\text{C}\equiv\text{C-R})_2]$ ($R = \text{C}_6\text{H}_5, \text{C}_6\text{H}_4\text{F}, \text{C}_6\text{H}_4\text{OMe}, \text{SiMe}_3, \text{C}_4\text{H}_3\text{S}, \text{C}_5\text{H}_4\text{N}, \text{C}_6\text{H}_4\text{C}\equiv\text{CC}_6\text{H}_5$ and 1-pyrene) were prepared by the addition of the corresponding lithium acetylides to the starting $\text{trans}-[(\text{iPr}_2\text{-bimy})_2\text{PdBr}_2]$ complex [28]. Single-crystal diffraction data of these complexes were found to be closely related to the luminescent palladium(II) bis-acetylide complexes bearing phosphine ligands [29].

Although the replacement of palladium with nickel in $[\text{M}(\text{NHC})_2\text{X}_2]$ complexes would represent significant cost saving, nickel-NHC-halido complexes have been less studied. Only recently, N-heterocyclic carbenes complexes of nickel attracted increasing attention as highly active organocatalysts [30, 31] for reactions such as olefin dimerization [32], polymerization [33] and C-C bond activation of unsaturated hydrocarbons [34].

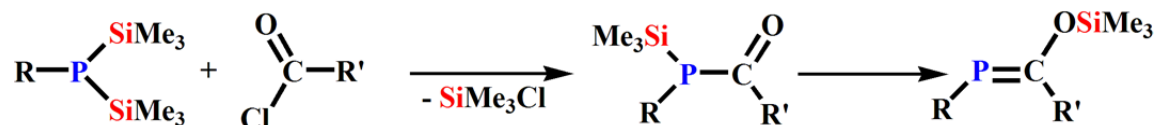
Despite the wide variety of transition metal complexes bearing mono(NHC) ligands, multitopic carbenes, which can bind to multiple transition metals, have not been studied to a great extent [35-37]. Boydston *et al.* [38] synthesized a discrete bis(NHC) composed of two linearly opposed imidazole-ylidenes annulated to a common arene backbone. The linear rigid framework of bidentate bis(NHC) prevented chelation and suggested the potential for use in

linear complex and polymer formation [38]. The small-molecule bimetallic complexes of Rh and Au were synthesized as models for monomeric repeat units and provided information on the physical and chemical properties of their corresponding polymers [38]. Bimetallic homonuclear Fe(II) and Ru(II) bis(NHC) complexes $[(\eta^5\text{-C}_5\text{H}_5)\text{FeI}(\text{CO})(^t\text{Bu}_4\text{-benzo}(\text{imy})_2)]$ and $[(\eta^5\text{-(Me-,}^i\text{Pr-C}_6\text{H}_4))\text{FeCl}_2(^t\text{Bu}_4\text{-benzo}(\text{imy})_2)]$ were synthesized and characterized by electrochemical and spectroelectrochemical analysis as well as X-ray crystallography [39]. The potential of bis(NHC) as spacer for interconnecting redox-active metal centers was probed. The electrochemical and spectroelectrochemical studies showed that the metal-metal interactions in ruthenium complex were very weak, while the evidence of modest coupling was found in the di-iron complex [39]. These results showed that bis(NHCs) combined with suitable metal centers and ancillary ligands have the potential to be used in molecular electronics [39].

1.4 Metal-Diacylphosphido Complexes

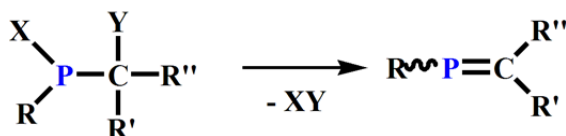
The different electronegativities of silicon and phosphorous atoms can be exploited for cleavage of Si–P bonds upon the reaction of silylphosphines with suitable polar compounds [1]. The Si–P bond cleavage was considered as an entrance to a sequence of stabilization reactions by Becker [1, 40]. A spectacular improvement in the preparation of isolable, acyclic compounds with localized phosphorus-carbon double bond started with a Si–P bond cleavage in $\text{RP}(\text{SiMe}_3)_2$ through $^t\text{BuC}(\text{O})\text{Cl}$ [40]. The first phosphalkene with a localized C=P bond was discovered by Becker in 1976 [40]. Conceptually, phosphalkenes are organophosphorus compounds which are isolated by replacing a methylene group (R_2C) of an alkene with the isolobal phosphinidene (PR) group (i.e., $\text{R}_2\text{C}=\text{PR}$). Becker's route for

preparing phosphalkenes attracted increasing attention since it was high yielding, convenient and can sustain different substituents [40-44]. The condensation reaction of an acid chloride with a bis(trimethylsilyl)phosphine results in the formation of transient acylphosphine that rapidly tautomerizes to the phosphalkene, as shown in Scheme 1.5. The side product (Me_3SiCl) is easily removed from the reaction solution.



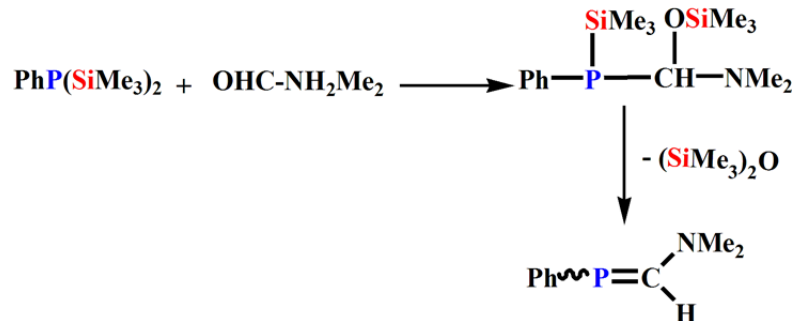
Scheme 1.5: Becker route to phosphalkenes: condensation followed by the [1,3]-silyl migration of an acylphosphine to a phosphalkene [41].

There are different synthetic routes to prepare phosphalkenes such as elimination reactions, condensation reactions and 1,3-trimethylsilyl migration. A C–P double bond can be formed by the 1,2-elimination reaction at organophosphine having a functional group X at phosphorus and Y at the α -C atom. Elimination of molecule XY creates the phosphorus-carbon double bond (see Scheme 1.6) [45].



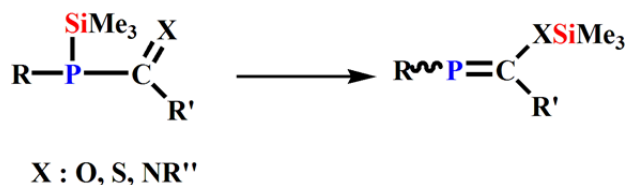
Scheme 1.6: Elimination reaction to form phosphorus-carbon double bond

The addition of a silylphosphine or a phosphine with P–H bond to a carbonyl group, followed by an elimination step can create a P–C-bond via a condensation reaction, as shown in Scheme 1.7 [45].



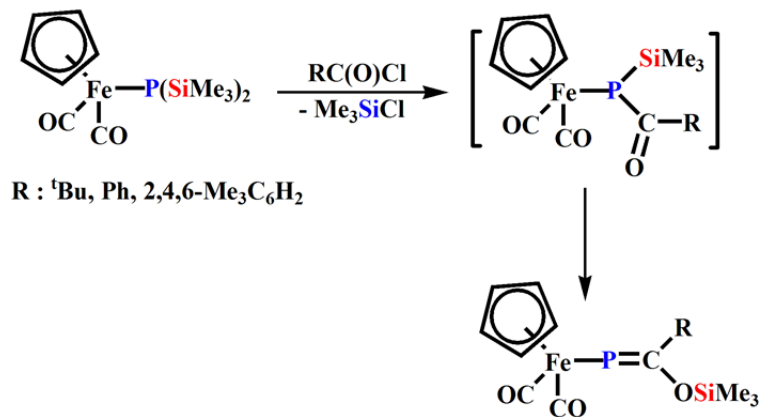
Scheme 1.7: Condensation reaction to synthesize carbon-phosphorus double bond

The migration of a P-silyl group to an element such as nitrogen, oxygen or sulfur which is in the α -position forms a phosphorus-carbon double bond, as depicted in Scheme 1.8. The formation of very stable N-Si, O-Si or S-Si is the driving force of 1,3-trimethylsilyl migration [45].



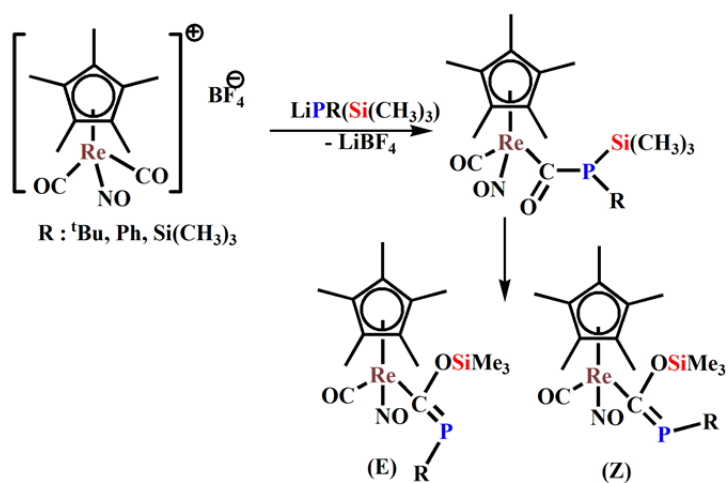
Scheme 1.8: Silotropic migration of organophosphines resulted in P=C double bond.

In an extension of Becker's route, the first phosphalkenyl complex of iron was obtained by Weber *et al.* [46, 47]. The complexes with covalent metal-phosphorus bonds were synthesized from $[(\eta^5\text{-C}_5\text{H}_5)(\text{CO})_2\text{FeP}(\text{SiMe}_3)_2]$ and acid chlorides $\text{RC}(\text{O})\text{Cl}$ ($\text{R} = \text{Ph}$, 2,4,6-Me₃C₆H₂, ^tBu). In these complexes, the lone pair of electrons on the phosphorus were not required for electronic saturation of the iron-phosphalkene, as depicted in Scheme 1.9 [47, 48]. Therefore, the iron complex can be considered as a transition metal-substituted phosphalkene.



Scheme 1.9: The first iron phosphalkene complexes prepared by Weber *et al.* [47]

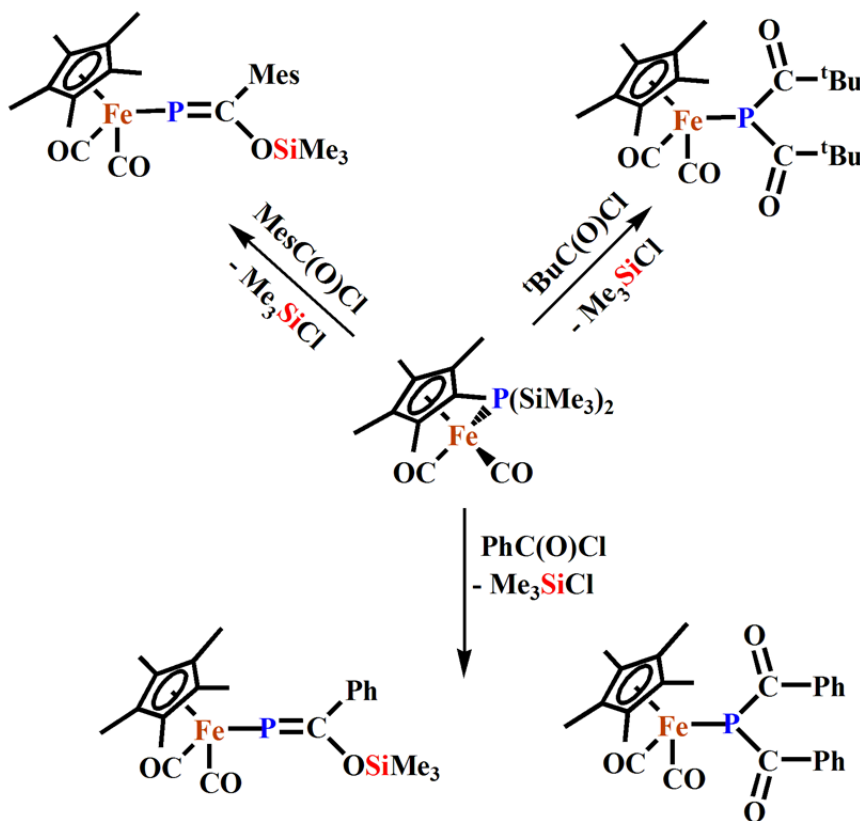
Furthermore, Weber *et al.* [49] synthesized a rhenium complex of a phosphalkene by nucleophilic addition of silylated lithium silylphosphido to a carbonyl ligand of a rhenium complex cation. As a result of a silatropic rearrangement, a rhenium phosphalkene complex $[(\eta^5\text{-C}_5\text{Me}_5)(\text{CO})(\text{NO})\text{Re}(\text{OSiMe}_3)=\text{PR}]$ formed, as outlined in Scheme 1.10.



Scheme 1.10: Phosphalkenylrhenium complexes synthesized by Weber *et al.* [49].

Moreover, Weber *et al.* [50] succeeded in preparing diacylphosphido complexes. Reaction of the compound $(\eta^5\text{-C}_5\text{Me}_5)(\text{CO})_2\text{FeP}(\text{SiMe}_3)_2$ with 2,4,6-trimethylbenzoyl

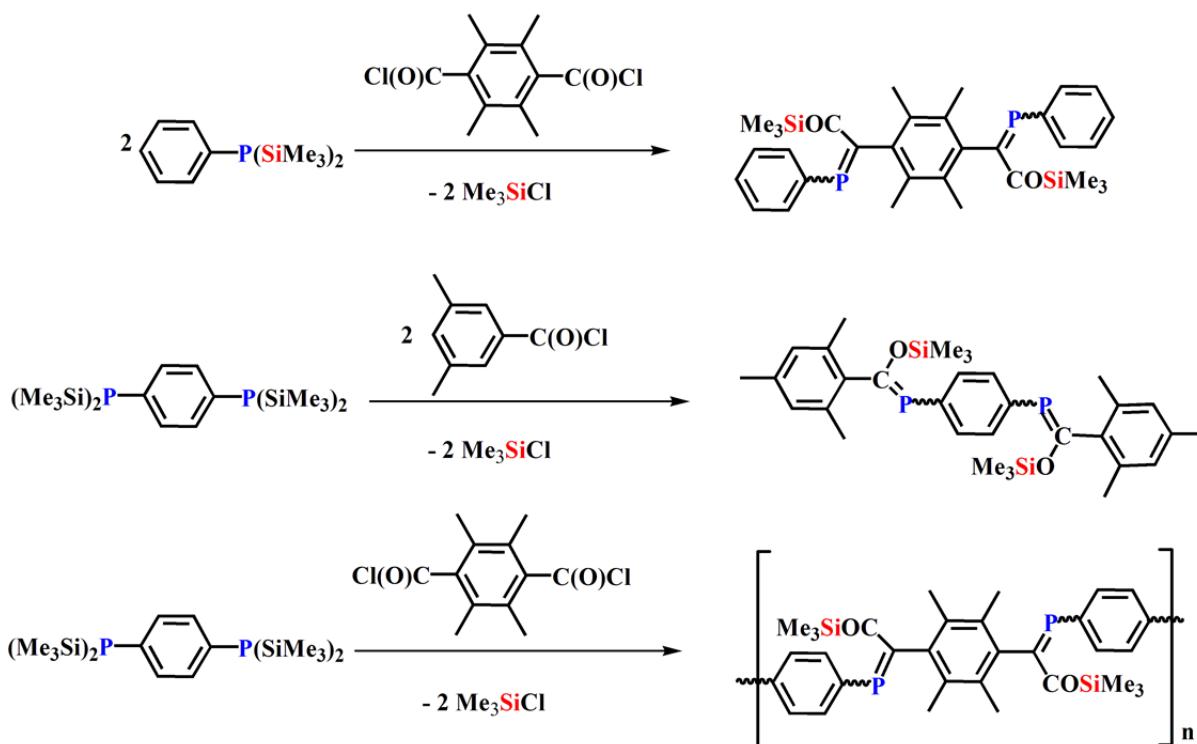
chloride yielded a phosphalkenyl complex of $[(\eta^5\text{-C}_5\text{Me}_5)(\text{CO})_2\text{FeP}=\text{C}(\text{OSiMe}_3)(\text{Mes})]$ as the only detectable product. It can be seen in Scheme 1.11 that the treatment of $[(\eta^5\text{-C}_5\text{Me}_5)(\text{CO})_2\text{FeP}(\text{SiMe}_3)_2]$ with benzoyl chloride affords the phosphalkenyl complexes, $[(\eta^5\text{-C}_5\text{Me}_5)(\text{CO})_2\text{FeP}=\text{C}(\text{OSiMe}_3)\text{Ph}]$ and the dibenzoylphosphido complex, $[(\eta^5\text{-C}_5\text{Me}_5)(\text{CO})_2\text{FeP}\{\text{C}(\text{O})\text{Ph}\}_2]$ whereas the complex of $[(\eta^5\text{-C}_5\text{Me}_5)(\text{CO})_2\text{FeP}\{\text{C}(\text{O})^t\text{Bu}\}_2]$ is formed as the unique product with pivaloyl chloride.



Scheme 1.11: Mono and diacylphosphido iron complexes reported by Weber *et al.* [50]

A new series of π -conjugated polymers and molecules composed of phosphalkene have been recently described by Gates *et al.* [51]. Poly(p-phenylenephosphalkene)s (PPP)s were synthesized by utilizing the Becker reaction of a bifunctional silylphosphine, 1,4-

$C_6R_4[P(SiMe_3)_2]_2$, and the diacid dichloride $1,4-C_6R'_4[COCl]_2$ ($R = H, Me$; $R' = H, Me$). Mono(phosphaalkene), $R-P=C(OSiMe_3)-R'$, ($R = Ph, Mes$; $R' = Ph, Mes$) and bis(phosphaalkene) were formed in the reaction of a monofunctional silylphosphine with mono or diacid dichlorides, as illustrated in Scheme 1.12.



Scheme 1.12: Mono-, bis- and poly(phosphaalkene) prepared by Gates *et al.* [51]

1.5 Project Objectives

Although metal-bis(trimethylsilyl) phosphido complexes have been well studied [7, 8, 10, 11], the preparation of complexes with two terminal P(SiMe₃)₂ groups is still a fertile area of research [3, 8, 11]. As discussed in subsection 1.1, *trans*-[Pt(PEt₃)₂{P(SiMe₃)₂}₂] [11] and analogues *trans*-[NiCl(PEt₃)₂{P(SiMe₃)₂}] [8] complexes were not stable at room temperature as P(SiMe₃)₃ and PEt₃ were eliminated from the complexes.

The dissociation of the aforementioned platinum(II) and nickel(II) complexes might be caused by the donor and/or steric properties of the PEt_3 ligand. Accordingly, ligands with smaller size and/or stronger bonding properties may help to stabilize *trans*-metal-silylphosphido complexes. Due to the unique physical and chemical properties of N-heterocyclic carbenes (NHCs), they may be a valuable alternatives to phosphine ligands to increase the stability of square planar $\text{M}-\{\text{P}(\text{SiMe}_3)_2\}_2$ complexes. Our research interest lies in the synthesis of room temperature-stable *trans*-metal-silylphosphido complexes. Herein, the synthesis of four monosilylphosphido complexes of palladium(II) and nickel(II) bearing two N-heterocyclic carbene ligands are reported. This research continues to introduce a dimetal-bis(trimethylsilyl)phosphido complex of gold(I) with a linear rigid bidentate-NHC in its framework. Furthermore, the cleavage of silicon-phosphorus bonds of two silylphosphido complexes of palladium(II) and nickel(II) with benzoyl chloride provides Pd(II) and Ni(II) dibenzoylphosphido complexes. The characterization of these complexes is completed using NMR spectroscopy, X-ray analysis and mass spectrometry and elemental analysis.

2. METAL-SILYLPHOSPHIDO COMPLEXES

2.1. INTRODUCTION

The cleavage of the Si—P bond by means of ⁿBuLi in tris(trimethylsilyl)phosphine opened the way to lithium-bis(trimethylsilyl)phosphido [9]. Li[P(SiMe₃)₂] was an excellent choice to transfer a P(SiMe₃)₂ group to metals through the reaction with various metal halides [3, 7, 8, 10-12]. Reaction of the dihalide complexes of [(R₃P)₂MCl₂]; M = Pd, Ni, R = PEt₃, PPh₃, with Li[P(SiMe₃)₂] resulted via the mono- or disubstituted intermediates [MCl(R₃P)₂{P(SiMe₃)₂}] and [M(Et₃P)₂{P(SiMe₃)₂}₂] in phosphine complexes [M(R₃P)₂{η²-(PSiMe₃)₂}] [11, 12] as well as in the phosphido bridged metal(I) complexes [(M—M){R₃PPtP(SiMe₃)₂}₂] [11]. The mono- and disubstituted intermediates with triphenylphosphine as ligands were dissociated faster than those of triethylphosphines. The choice of the substituents R (triethylphosphine or triphenylphosphine) as well as the temperature had an important influence on the dissociation of mono- or disilylphosphido complexes, [MCl(R₃P)₂{P(SiMe₃)₂}] or [M(Et₃P)₂{P(SiMe₃)₂}₂].

With these aspects in mind we targeted the synthesis of square planar silylphosphido complexes by means of Li[P(SiMe₃)₂]. The size and bonding properties of coordinated ligands to a metal center have an important role in synthesizing temperature-stable metal-silylphosphido complexes. Ligands with stronger bonding properties such as N-heterocyclic

carbenes (NHCs) can bond to the transition metals and donate their lone pair of electrons. In comparison with trialkylphosphines [11, 12], the presence of NHCs in metal-silylphosphido complexes may increase the stability of silylated phosphido complexes. The steric crowding of NHCs can be easily controlled by introducing different substituents on N-heterocycles. This chapter presents the preparation and characterization of five silylphosphido complexes with different NHCs as ancillary ligands. NMR spectroscopy and X-ray crystallography of these complexes are also described.

2.2. EXPERIMENTAL

2.2.1. General Synthetic Techniques and Starting Materials

All reactions have been performed using standard Schlenk techniques under a dry nitrogen atmosphere unless otherwise stated. Non-chlorinated solvents (toluene, tetrahydrofuran (THF), hexane, heptane, diethyl ether and pentane) were dried by passage through packed columns of activated alumina using a commercially available MBraun MB-SP Series solvent purification system. Chlorinated solvents (CHCl_3 and CH_2Cl_2), dimethoxy ethane (DME) were distilled and dried over Na. Chemicals were used as received from Aldrich and/or VWR. Chloroform-d was purchased from Aldrich and distilled over P_2O_5 . Benzene-d₆ was dried and distilled over Na/K. DMSO-d₆ was purchased from Cambridge Isotope Laboratory (CIL) and used as received. Benzoyl chloride was purchased from Aldrich and dried over CaH_2 .

Tris(trimethylsilyl)phosphine ($\text{P}(\text{SiMe}_3)_3$) [52], lithium bis(trimethylsilyl)phosphine [$\text{Li}(\text{PSiMe}_3)_2$] [9], 1,3-diisopropyl(benz)imidazolium iodide [18], 1,3-diⁿbutyl(benz)-

imidazolium iodide [18], 1,3-diⁿbutyl(benz)imidazolium bromide [53], *trans*-[PdI₂(¹Pr₂-bimy)₂] [19], *trans*-[NiI₂(¹Pr₂-bimy)₂] [25], tetrakis(ⁿbutyl)benzobis(imidazolium)bromide [38] and [Au₂Cl₂(ⁿBu₄-benzo(imy)₂)] [54] were prepared following literature procedures. ¹H, ¹³C{¹H} and ³¹P{¹H} NMR spectra were recorded on Varian Mercury 400 MHz, Inova 400 and 600 MHz spectrometers and the chemical shifts (δ) were internally referenced by the residual solvents signals (benzene-d₆ and chloroform-d) relative to tetramethylsilane (SiMe₄) (¹H and ¹³C) or 85% H₃PO₄ (³¹P). The crystals of 1-4 and 9 were mounted on a Mitegen polyimide micromount with a small amount of Paratone N oil. All X-ray measurements were made on a Bruker APEX-II CCD diffractometer at a temperature of 110(2) K. The data collection strategies were a number of ω and φ scans. The frame integrations were performed using SAINT software (Bruker AXS Inc., Madison, Wisconsin, USA, 2007). The resulting raw data was scaled and absorption corrected using a multi-scan averaging of symmetry equivalent data using SADABS (Bruker-AXS, SADABS version 2012.1, 2012, Bruker-AXS, Madison, WI53711, USA). The structures were solved by using a dual space methodology using the SHELXT program or by direct methods using the SHELXS-97 [23]. All non-hydrogen atoms were obtained from the initial solutions. The hydrogen atoms were introduced at idealized positions and were allowed to ride on the parent atom. The structural models were fit to the data using full matrix least-squares based on F². The calculated structure factors included corrections for anomalous dispersion from the usual tabulation. The structures were refined using the SHELXL-97, SHELXL-2013 or SHELXL-2014 programs from the SHELXTL program package [23]. Graphic plots were produced using the Mercury program suite. Crystal of 3 was non-merohedrally twinned by 179.7 degrees about

reciprocal axis 0.002 0.000 1.000 and real axis 0.453 0.000 1.000. The twin fraction parameter refined to a value of 0.37957(53). The resulting raw data was scaled and absorption corrected using a multi-scan averaging of symmetry equivalent data using TWINABS for this sample. The structures of *trans* **1-4** and **9** were solved and refined by Bahareh Khalili Najafabadi and Mahmood Azizpoor Fard. Mass spectra and exact mass determinations were performed on a Bruker micrOTOF II instrument or Finningan MAT 8400. Elemental analysis was performed by Laboratoire d'Analyse Élémentaire de l'Université de Montréal, Montréal, Canada.

All reactions have been performed using standard Schlenk techniques under a dry nitrogen atmosphere unless otherwise stated. Non-chlorinated solvents (toluene, tetrahydrofuran (THF), hexane, heptane, diethyl ether and pentane) were dried by passage through packed columns of activated alumina using a commercially available MBraun MB-SP Series solvent purification system. Chemicals were purchased from Aldrich and/or VWR. Benzene- d_6 and benzoyl chloride were dried and distilled over Na/K and CaH_2 , respectively.

1H , $^{13}C\{^1H\}$ and $^{31}P\{^1H\}$ NMR spectra were recorded on Varian Mercury 400 MHz, Inova 400 and 600 MHz spectrometer and the chemical shifts (δ) were internally referenced by the residual solvents signals (benzene- d_6 and chloroform- d) relative to tetramethylsilane ($SiMe_4$) (1H and ^{13}C) or 85% H_3PO_4 (^{31}P). Single crystal X-ray diffraction measurements were performed on a Bruker APEXII diffractometer, with the molecular structures determined via direct methods using the SHELX suite of crystallographic programs [55]. All samples were mounted on a Mitegen polyimide micromount with a small

amount of Paratone N oil. Mass spectrometry and exact mass determinations were performed on a Bruker micrOTOF II instrument or Finningan MAT 8400.

2.2.2. [PdI₂(ⁿBu₂-bimy)₂] (*trans*-1)

A mixture of N,N'-diⁿbutyl(benz)imidazolium iodide [36] (0.716 g, 2.00 mmol) and Pd(OAc)₂ (0.220 g, 1.00 mmol) was dissolved in wet DMSO (20 mL) and stirred at 120 °C for 3h and then at 100 °C overnight. The yellow crystalline solid came out by cooling the reaction mixture to room temperature. The obtained solid was filtered off and washed with 50 mL of Et₂O and dried under vacuum; yield 0.580 g (70%). Slow evaporation at ambient temperature of a concentrated CHCl₃ solution afforded single crystals of **1** suitable for X-ray crystallography. ¹H NMR (400 MHz, CDCl₃, 23 °C) δ = 7.39 (dd, 4H, Ar-H), 7.27 (dd, 4H, Ar-H), 4.71 (t, 8H, ³J_{H,H} = 7.9 Hz, NCH₂), 2.21(m, 8H, CH₂), 1.53 (m, 8H, CH₂), 1.05 (t, 12H, ³J_{H,H} = 7.5 Hz, CH₃). ¹³C{¹H} NMR (600 MHz, CDCl₃, 23 °C) δ = 180.0 (s, NCN), 134.9, 122.2, 110.2 (s, Ar-C), 48.6 (s, NCH), 31.1 (s, CH₂), 20.5 (s, CH₂(CH₃)), 13.8 (s, CH₃). Anal. Calc for C₃₀H₄₄I₂N₄Pd (820.92): C 43.89, H 5.40, N 6.82. Found: C 43.95, H 6.52, N 6.82. m.p. > 260 ° C. HRMS (EI): m/z calcd for C₄₅H₃₃N[¹⁰⁴Pd]: 691.16534 [M]⁺; found: 691.16519. Crystal data for [*trans*-1]: M = 820.89, T = 113(2) K, λ = 0.71073 Å, μ(Mo Kα) = 2.513 cm⁻¹, monoclinic, a = 10.790(3), b = 20.017(6), c = 15.036(4) Å, β = 96.577(6)°, V = 3226.1(16) Å³, space group P 2₁, Z = 4, 113233 measured reflections, 34320 unique reflections, R₁ = 0.0314, wR₂ = 0.0501 (I ≥ 2σ(I)), wR₂ (all data) = 0.0532, GOF = 1.014, F(000) = 1616, refined as a 2-component inversion twin, Flack (x) = 0.335(10).

2.2.3. [NiBr₂(ⁿBu₂-bimy)₂] (*trans*-2)

A mixture of N,N'-diⁿbutyl(benz)imidazolium bromide [35] (2.00 g, 6.42 mmol), Ni(OAc)₂ (0.560 g, 3.21mmol) and about 50 % of the combined weight of the two reagents of [Bu₄N]Br (1.28 g, excess) were dried under vacuum at 60 °C for 1h. The temperature was gradually increased to 150 °C and kept at this temperature in vacuo for 12h. After cooling, methanol was added and the mixture was filtered, washed with water and dried under vacuum. The color of the product was red-orange; yield 1.60 g (73%). Slow evaporation at ambient temperature of a concentrated CH₃Cl solution afforded the product as red crystals of **2** suitable for X-ray crystallography. ¹H NMR (400 MHz, CDCl₃, 23 °C) δ = 7.34 (dd, 4H, Ar-H), 7.19 (dd, 4H, Ar-H), 5.29 (t, 8H, ³J_{H,H} = 8.21 Hz, NCH₂), 2.40 (m, 8H, CH₂), 1.73 (m, 8H, CH₂), 1.12 (t, 12H, ³J_{H,H} = 7.4 Hz, CH₃). ¹³C {¹H} NMR (600 MHz, CDCl₃, 23 °C) δ = 183.5 (s, NCN), 134.9, 121.8, 109.8 (s, Ar-C), 48.3 (s, NCH), 31.6 (s, CH₂), 20.8 (s, CH₂(CH₃)), 13.9 (s, CH₃). Anal. Calc for C₃₀H₄₄Br₂N₄Ni (679.20): C 53.05, H 6.53, N 8.25. Found: C 53.00, H 6.52, N 8.20. m.p. > 260 °C. HRMS (EI): m/z calcd for C₄₂H₃₅[⁵⁸Ni]: 597.20922 [M]⁺; found: 597.20995. Crystal data for [*trans*-**2**]: M = 679.22, T = 110(2) K, λ = 0.71073 Å, μ(Mo Kα) = 1.286 cm⁻¹, monoclinic, a = 13.854(9), b = 8.690(7), c = 14.383(8) Å, β = 117.652(17)°, V = 1533.9(18) Å³, space group P 2₁/c, Z = 2, 26784 measured reflections, 4691 unique reflections, R₁ = 0.0436, wR₂ = 0.0795 (I ≥ 2σ(I)), wR₂ (all data) = 0.0952, GOF = 0.995, F(000) = 700.

2.2.4. [PdI(ⁱPr₂-bimy)₂{P(SiMe₃)₂}] (*trans*-**3**)

Complex *trans*-[PdI₂(ⁱPr₂-bimy)₂] [19] (0.23 g, 0.30 mmol) was suspended in 10 mL of toluene and cooled to -40 °C. Freshly prepared Li[P(SiMe₃)₂] · 1.8 (thf) (0.10 g, 0.30 mmol) in toluene (5mL) was cooled to -40 °C and then added dropwise to the suspension at -

40 °C. The reaction was stirred until it reached room temperature, then warmed up to 60 °C and stirred for 1h. The cooled reaction mixture was concentrated under vacuum and the residue was dissolved in 20 mL of pentane. A white-creamy precipitate LiI was filtered over Celite and the orange filtrate concentrated under vacuum giving a yellow oily product (**3**); yield 0.15 g (61%). Recrystallization from a minimal amount of pentane at -25 °C afforded yellow crystals of *trans*-**3** suitable for X-ray crystallography. ¹H NMR (400 MHz, C₆D₆, 23 °C) δ = 7.22 (dd, 4H, Ar-H), 6.90 (dd, 4H, Ar-H), 6.29 (m, 4H, NCH(CH₃)₂), 1.84 (d, 12H, ³J_{H,H} = 7.0 Hz, CH₃), 1.67 (d, 12H, ³J_{H,H} = 7.0 Hz, CH₃), 0.14 (d, 18H, ³J_{H,P} = 3.5 Hz, P(Si(CH₃)₂)). ¹³C{¹H} NMR (600 MHz, C₆D₆, 23 °C) δ = 186.3 (s, NCN), 128.9, 121.2, 111.3 (s, Ar-C), 53.8 (s, NCH(CH₃)₂), 18.9 (s, CH₃), 5.1 (d, ²J_{C,P} = 11.4 Hz, P(Si(CH₃)₂)). ³¹P{¹H} NMR (C₆D₆, 23 °C) δ = -181.8. m.p. = 117-120 °C. Crystal data for [*trans*-**3**].C₅H₁₂: M = 887.38, T = 110(2) K, λ = 0.71073 Å, μ(Mo Kα) = 1.286 cm⁻¹, monoclinic, a = 21.223(4), b = 10.532(2), c = 21.304(5) Å, β = 116.819(7)°, V = 4249.9(16) Å³, space group P 2₁/c, Z = 4, 20403 measured reflections, 15254 unique reflections, R₁ = 0.0493, wR₂ = 0.0913 (I ≥ 2σ(I)), wR₂ (all data) = 0.1012, GOF = 1.017, F(000) = 1832, refined as a 2-component inversion twin, Flack (x) = 0.37957(53).

2.2.5. [NiI(ⁱPr₂bimy)₂]{P(SiMe₃)₂} (*trans*-**4**)

Complex **4** was prepared in an analogous manner to **3** from *trans*-[NiI₂(ⁱPr₂-bimy)₂] [26] (0.14 g, 0.20 mmol) and Li[P(SiMe₃)₂] · 1.8 (thf) (0.06 g, 0.20 mmol) in toluene (15mL). Yield: 0.15 g (61%). ¹H NMR (400 MHz, C₆D₆, 23 °C) δ = 7.15 (dd, 4H, Ar-H), 6.97 (m, 4H, NCH), 6.87 (dd, 4H, Ar-H), 1.89 (d, 12H, ³J_{H,H} = 7.0 Hz, CH₃), 1.73 (d, 12H, ³J_{H,H} = 7.0 Hz, CH₃), 0.04 (d, 18H, ³J_{H,P} = 3.5 Hz, P(Si(CH₃)₂)). ¹³C{¹H} NMR (600 MHz,

C₆D₆, 23 °C) δ = 187.2 (s, NCN), 129.5, 122.2, 113.0 (s, Ar-C), 54.3 (s, NCH(CH₃)₂), 21.1 (s, CH₃), 4.3 (d, ²J_{C,P} = 11.4 Hz, P(Si(CH₃)₂)). ³¹P{¹H} NMR (C₆D₆, 23 °C) δ = -178.6. m.p. = 105-107 °C.

2.2.6. [PdI(ⁿBu₂-bimy)₂{P(SiMe₃)₂}] (*trans*-**5**)

Complex **I** (0.15 g, 0.18 mmol) was suspended in 10 mL of THF at room temperature. Freshly prepared Li[P(SiMe₃)₂] · 1.8 (thf) (0.06 g, 0.18 mmol) was dissolved in THF (5mL) and then added dropwise to the stirred reaction mixture. The reaction was stirred for 1 h at room temperature during which time the color of the reaction solution changed from green to yellow. The reaction solvent was removed under vacuum and the residue taken up in 10 mL of pentane. A creamy- white precipitate (LiI) was filtered over Celite and the clear yellow filtrate concentrated under vacuum giving a yellow oily product (**5**); yield 0.10 g (46%). Recrystallization from a minimal amount of pentane at -5 °C afforded yellow needle crystals of **5** suitable for X-ray crystallography. ¹H NMR (600 MHz, C₆D₆, 23 °C) δ = 7.05 (dd, 4H, Ar-H), 6.99 (dd, 4H, Ar-H), 5.41 (m, 4H, NCH₂), 4.22 (m, 4H, NCH₂), 2.56 (m, 4H, CH₂), 2.15 (m, 4H, CH₂), 1.50 (m, 8H, CH₂), 1.00 (t, 12H, ³J_{H,H} = 7.6 Hz, CH₃), 0.11(d, 18H, ³J_{H,P} = 3.5 Hz, P(Si(CH₃)₂)). ¹³C{¹H} NMR (600 MHz, C₆D₆, 23 °C) δ = 188.8 (s, NCN), 135.6, 122.6, 110.8 (s, Ar-C), 50.1 (s, NCH), 31.0 (s, CH₂), 21.1 (s, CH₂), 14.1 (s, CH₃), 5.8 (d, ²J_{C,P} = 11.4 Hz, P(Si(CH₃)₂)). ³¹P{¹H} NMR (C₆D₆, 23 °C) δ = -192.7. m.p. = 109-111 °C. Crystal data for [*trans*-**5**].[LiI(THF)₃] : M = 1221.50, T = 110(2) K, λ = 0.71073 Å, μ (Mo K α) = 1.532 cm⁻¹, monoclinic, a = 23.826(9), b = 10.960(4), c = 21.942(9) Å, β = 99.762(11)°, V = 5647(4) Å³, space group P 2₁/c, Z = 4, 55222 measured reflections, 9108

unique reflections, $R_1 = 0.0367$, $wR_2 = 0.0975$ ($I \geq 2\sigma(I)$), wR_2 (all data) = 0.1407, GOF = 1.056, $F(000) = 2496$.

2.2.7. $[\text{NiBr}(\text{}^n\text{Bu}_2\text{-bimy})_2\{\text{P}(\text{SiMe}_3)_2\}]$ (*trans*-6)

Complex **6** was prepared in an analogous manner to **5** from **2** (0.14 g, 0.20 mmol) and $\text{Li}[\text{P}(\text{SiMe}_3)_2] \cdot 1.8$ (thf) (0.06 g, 0.20 mmol) in toluene (10 mL). Yield: 0.12 g (80%). ^1H NMR (400 MHz, C_6D_6 , 23 °C) 6.97-7.10 (m, 8H, Ar-H), 5.92 (m, 4H, NCH₂), 4.43 (m, 4H, NCH₂), 2.60 (m, 4H, CH₂), 2.25 (m, 4H, CH₂), 1.62 (m, 4H, CH₂), 1.54 (m, 4H, CH₂), 1.01 (t, 12H, $^3J_{\text{H,H}} = 7.3$ Hz, CH₃), 0.04 (d, 18H, $^3J_{\text{H,P}} = 3.3$ Hz, P(Si(CH₃)₂)). $^{13}\text{C}\{^1\text{H}\}$ NMR (600 MHz, C_6D_6 , 23 °C) $\delta = 187.6$ (s, NCN), 134.6, 122.4, 111.2 (s, Ar-C), 52.6 (s, NCH), 30.7 (s, CH₂), 21.3 (s, CH₂), 13.8 (s, CH₃), 5.1 (d, $^2J_{\text{C,P}} = 11.4$ Hz, P(Si(CH₃)₂)). $^{31}\text{P}\{^1\text{H}\}$ NMR (C_6D_6 , 23 °C) $\delta = -197.3$. m.p. = 110-112 °C.

2.2.8. $[\text{Au}_2(\text{}^n\text{Bu}_4\text{-benzo(imy)}_2)\{\text{P}(\text{SiMe}_3)_2\}_2]$ (**7**)

The reaction of $[\text{Au}_2\text{Cl}_2(\text{}^n\text{Bu}_4\text{-benzo(imy)}_2)]$ [**54**] (0.17 g, 0.21 mmol) with $\text{Li}[\text{P}(\text{SiMe}_3)_2] \cdot 1.8$ thf (0.14 g, 0.42 mmol) was done in 1:2 ratio in THF (30 mL). The reaction was stirred at -40 °C for 1h and then warmed to room temperature and stirred for 2h. The color of the reaction turned from colorless to yellow. The reaction mixture was concentrated under vacuum and pentane was added to precipitate side product of LiCl. The reaction mixture was filtered over Celite and filtrate was concentrated under vacuum to obtain a yellow oily product of **7**. Yield: 0.10 g (50%). ^1H NMR (400 MHz, C_6D_6 , 23 °C) 6.76 (s, 2H, Ar-H), 4.10 (t, 8H, $^3J_{\text{H,H}} = 7.0$ Hz, NCH₂), 1.71 (m, 8H, CH₂), 1.24 (m, 8H,

CH₂), 0.82 (t, 12H, ³J_{H,H} = 7.4, CH₃), 0.76 (d, ³J_{H,P} = 4.3 Hz, 36H, P(Si(CH₃)₂)). ³¹P{¹H} NMR (C₆D₆, 23 °C) δ = -230.4. m.p. = 120-121 °C.

2.3. RESULTS AND DISCUSSION

2.3.1. [MX₂(ⁿBu₂-bimy)₂] Complexes; M = Pd, Ni; X = Br, I.

In general, a convenient route to synthesize Pd(II) bis(carbene) complexes involves in situ acid-base deprotonation reaction of Pd(OAc)₂ with two equivalent of azolium salts. The reaction solvents and conditions are changed based on the size, shape and steric bulk of azolium salts. Azolium salts with larger alkyl groups on N-heterocycles need more drastic reaction conditions due to the +I-effect and the steric bulk of N-substituents than those for azolium salts bearing N-methyl or methylene groups [19]. For instance, the *trans*-[PdBr₂(ⁱPr₂-bimy)₂] complex needs a high temperature range from 100 °C to 120°C to be synthesized. Instead, at lower temperature range (30-90 °C) the dimeric monocarbene complex of *trans*-[PdBr₂(ⁱPr₂-bimy)]₂ is formed [19].

The complex [PdI₂(ⁿBu₂-bimy)₂] (*trans*-**1**) was prepared by the in situ deprotonation of the *N,N'*-diⁿbutylbenzimidazolium iodide salt with Pd(OAc)₂, in a 2:1 ratio, in DMSO at 120 °C. After aqueous work-up, a yellow crystalline solid was isolated from the reaction solution and washed with diethyl ether to obtain 70% yield of pure *trans*-**1**. Complex *trans*-**1** is highly soluble in common organic solvents.

The formation of *trans*-**1** was confirmed by ¹H NMR spectroscopy, which is shown in Figure 2. Its ¹H NMR spectrum is avoid of the characteristic NCHN proton resonance which is observed at 11 ppm in the ¹H NMR spectrum of 1,3-diⁿbutyl(benz)imidazolium iodide. In

addition, the ⁿbutyl NCH₂ proton resonance slightly shifted downfield from 4.63 ppm in the precursor (1,3-diⁿbutyl(benz)imidazolium iodide) to 4.71 ppm in *trans*-**1**. In contrast, the isopropyl NCH proton resonance in *trans*-[PdI₂(ⁱPr₂-bimy)₂] [19], shifted significantly downfield upon coordination from 5.21 ppm in 1,3-diisopropyl(benz)imidazolium iodide (**I**) to 6.25 ppm in *trans*-[PdI₂(ⁱPr₂-bimy)₂]. The large chemical shift difference ($\Delta\delta\text{H} = 1.04$ ppm) of these protons in *trans*-[PdI₂(ⁱPr₂-bimy)₂] is probably due to the Pd \cdots H–C preagostic interactions [19]. Metal-hydrogen interactions (M \cdots H–X, X = C, N) are well described in the literature and include agostic [56] and preagostic [57] interactions as well as hydrogen bonding [58] (see Figure 2.1). Each of these interactions has specific spectroscopic and geometric properties, which make them distinctive from each other. In general, an agostic interaction involves a coordinatively-unsaturated transition metal that interacts with a C–H bond [56]. In this interaction the two electrons involved in the C–H bond is donated to the empty d-orbital of the metal center, and consequently a 3-center-2-electron bonding interaction is created. As a result of the agostic interaction, the C–H bond distance is increased and M \cdots H–C angle decreased. An agostic M \cdots H–C interaction typically causes some characteristic changes in NMR spectroscopy such as an upfield shift of the corresponding C–H proton resonances, a M–H coupling for NMR-active metal atoms and a diminution in the coupling constant value (¹J_{CH}) for the carbon in the C–H bond [59]. In comparison, preagostic interactions are identified by elongated M \cdots H distance and larger M \cdots H–C angle to those of agostic interactions [56]; however, none of these were observed for *trans*-**1**. The ¹³C NMR of *trans*-**1** indicates NCN carbene carbon resonance at 180.0 ppm, similar to that reported for *trans*-[PdI₂(ⁱPr₂-bimy)₂].

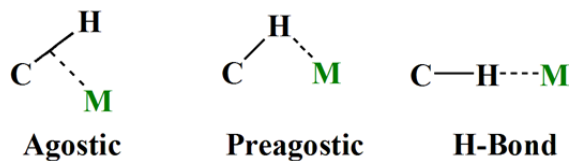


Figure 2.1: Metal-hydrogen bond interactions

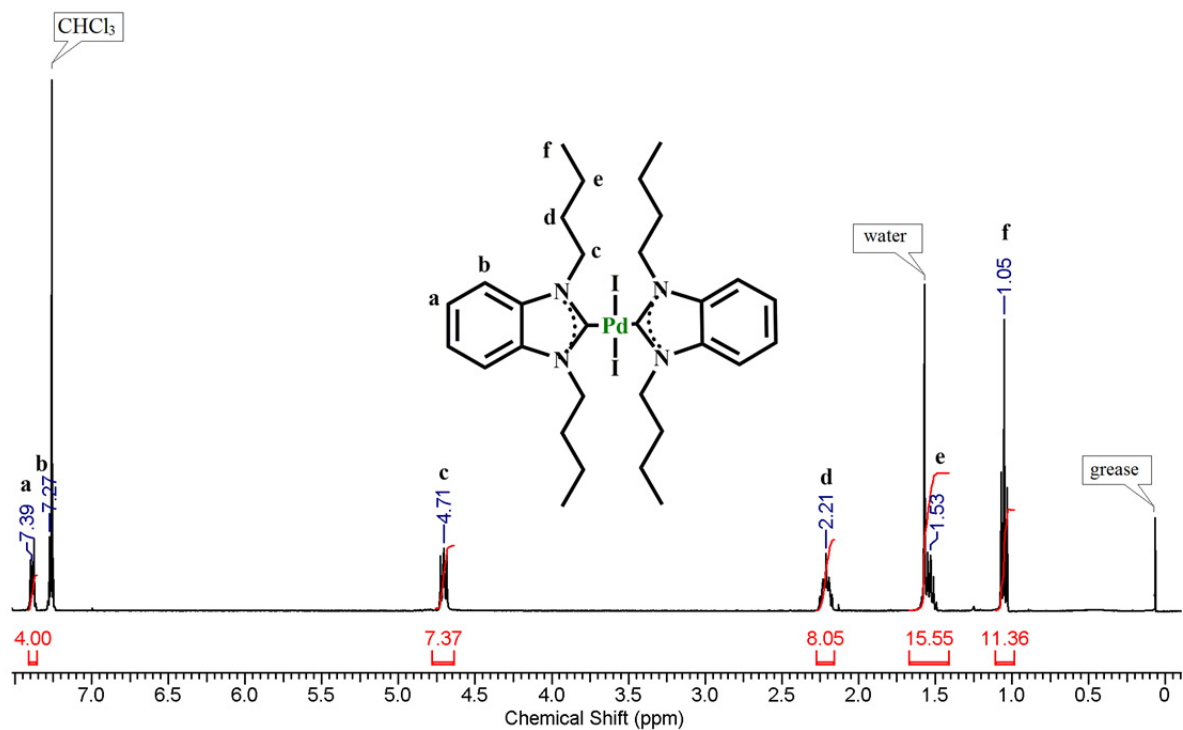


Figure 2.2: ^1H NMR spectrum of complex $[\text{PdI}_2(\text{}^n\text{Bu}_2\text{-bimy})_2]$ (*trans*-**1**)

Single crystals of *trans*-**1** suitable for X-ray diffraction studies were obtained by slow evaporation of a CHCl_3 solution at ambient temperature. The air stable *trans*-**1** crystallized in the monoclinic space group P2_1 with a Z of 4. The molecular structure of *trans*-**1** is illustrated in Figure 2.3 and selected bond length and angles are summarized in the caption.

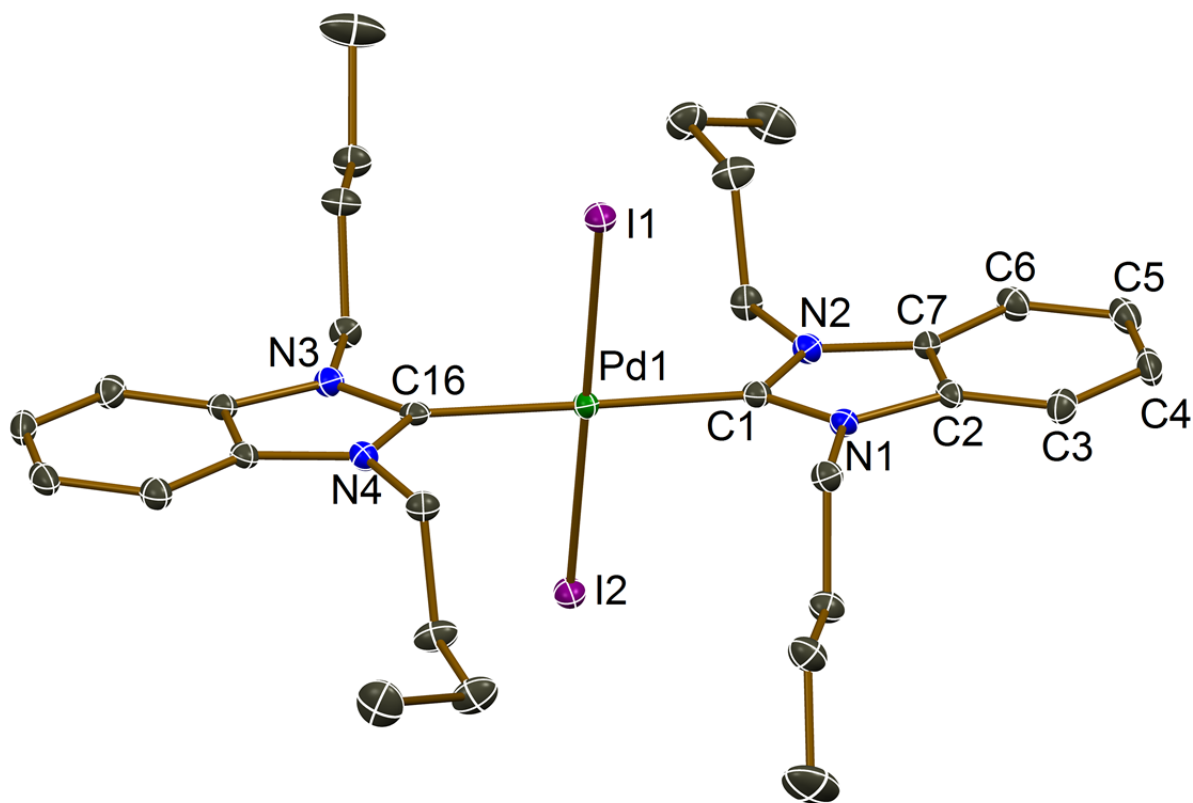


Figure 2.3: Molecular structure of complex $[\text{PdI}_2(\text{}^n\text{Bu}_2\text{-bimy})_2]$ (*trans*-**1**) (50% probability). All hydrogen atoms are omitted for clarity. Selected bond lengths (Å) and angles (°) of complex **1**: Pd1-I1 (2.6088(6)), Pd1-I2 (2.6057(6)), Pd1-C1 (2.023(3)), Pd1-C16 (2.021(3)), I1-Pd1-I2 (179.472(14)), I1-Pd1-C1 (91.60(9)), I2-Pd1-C1 (88.92(8)), I1-Pd1-C16 (89.11(9)), I2-Pd1-C16 (90.37(9)), C1-Pd1-C16 (179.24(14)).

The palladium(II) center is coordinated by two 1,3-diⁿbutyl(benz)imidazol and two iodo ligands in a square-planar fashion. The 2-fold screw axis is the only symmetry element in the unit cell of this molecule. Based on the ^{13}C NMR spectroscopy in solution, the two carbene and halide ligands are arranged *trans* to each other with an angle of 180° owing to the symmetry. Both carbene ring planes are orientated to the PdC_2Br_2 plane with a torsion angle (carbene dihedral angle) of 80.4° . The bond angles of C(1)-Pd(1)-C(16) ($179.240(14)^\circ$)

and I(1)-Pd(1)-I(2) (179.472(14)°) confirm the planar geometry around palladium center. The bond distances for Pd(1)-C(1) and Pd(1)-C(16) are 2.023(3) Å and 2.021(3) Å, respectively, which are identical to that of *trans*-[PdI₂(ⁱPr₂-bimy)₂] (2.017(2) Å). The palladium-iodo bond lengths, Pd(1)-I(1) (2.6088(6)) and Pd(1)-I(2) (2.6057(6)) Å, were rather longer than that of *trans*-[PdI₂(ⁱPr₂-bimy)₂] (2.5906(3)) Å.

[NiBr₂(ⁿBu₂-bimy)₂] (*trans*-**2**) is prepared by reacting the 1,3-diⁿbutyl(benz)-imidazolium bromide at high temperature with Ni(OAc)₂ under vacuum. As melting point of the 1,3-diⁿbutyl(benz)imidazolium bromide itself is too high for a reaction to occur, an ionic salt with lower-melting point, tetrabutylammonium bromide, is added as a solvent according to the original procedure reported by Huynh *et al.* [25]. After aqueous work-up and purification complex *trans*-**2** was obtained as a stable orange powder (73% yield). Complex *trans*-**2** is highly soluble in common solvents.

The formation of *trans*-**2** was confirmed by ¹H NMR spectroscopy, which shows the absence of the NCHN proton, as depicted in Figure 2.4. Moreover, a downfield shift was recorded for NCH₂ resonance from 4.64 ppm in the 1,3-diⁿbutyl(benz)imidazolium bromide to 5.29 ppm in *trans*-**2**. The observed chemical shift change for NCH₂ protons (ΔδH = 0.65 ppm) in *trans*-**2** is less than that of *trans*-[NiI₂(ⁱPr₂-bimy)₂] (ΔδH = 1.72 ppm) [26], which shows there is no or weak Ni···H—C preagostic interactions in *trans*-**2**. The other signals present in the ¹H NMR spectrum of the 1,3-diⁿbutyl(benz)imidazolium bromide are recognized while transferred slightly to the downfield. The NCN carbene carbon of *trans*-**2** is observed at 183.5 ppm in the ¹³C{¹H} NMR spectrum, in the usual range (169.0-188.0 ppm) found for *trans*-nickel(II)imidazolin-2-ylidenes [25, 26].

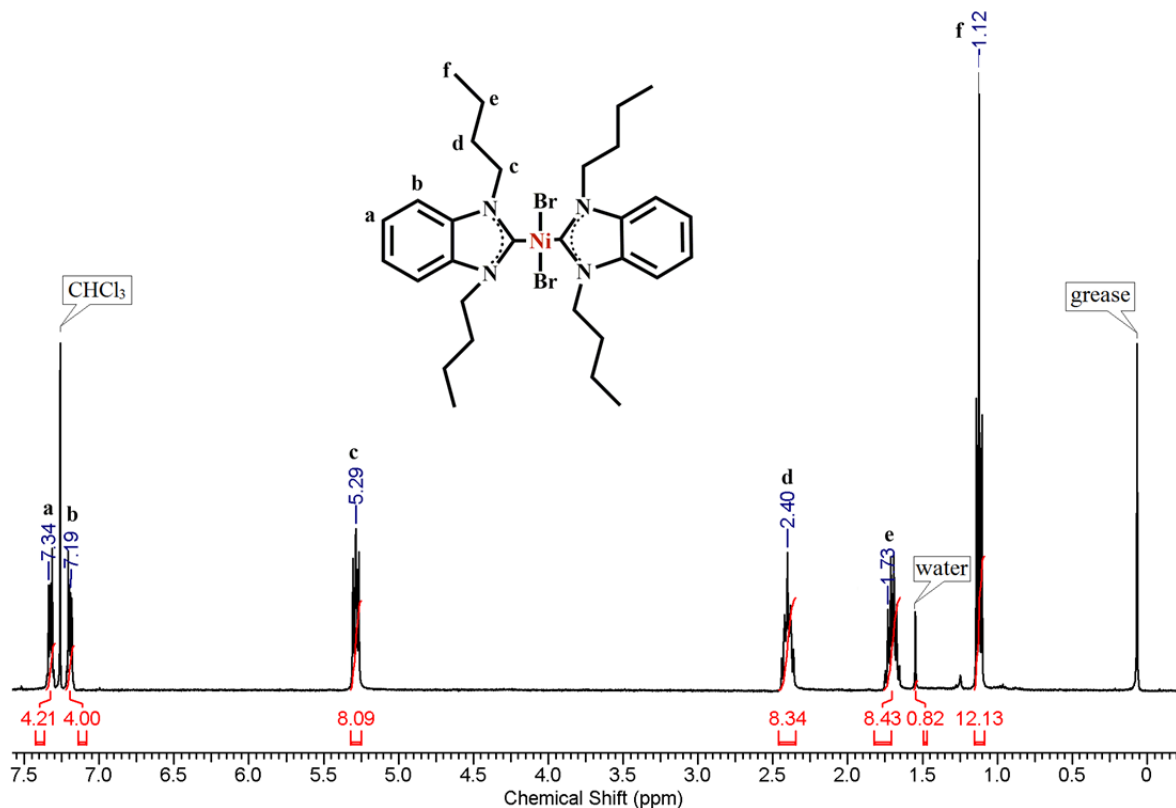


Figure 2.4: ^1H NMR spectrum of complex $[\text{NiBr}_2(\text{}^n\text{Bu}_2\text{-bimy})_2]$ (*trans*-2)

Single crystals of *trans*-2 suitable for X-ray diffraction were formed at ambient temperature by slow evaporation of CHCl_3 solution. Complex *trans*-2 crystallizes as an air stable compound in the monoclinic space group $\text{P2}_1/\text{c}$ with a Z of 2. Ni(II) resides in inversion center and there are the 2-fold screw axes and c-glide in the unit cell of *trans*-2. The molecular structure of this complex is shown in Figure 2.5. In the molecular structure of *trans*-2, the nickel(II) is coordinated by two 1,3-di n butyl(benz)imidazol and two bromo ligands in a square-planar geometry, in a *trans* fashion. Both carbene ring planes are orientated with a torsion angle (carbene dihedral angle) of 76.7° to the NiC_2Br_2 plane. The Ni(1)-Br(1) (2.3143(18) Å) and Ni(1)-C(1) (1.903(3) Å) bond distances are close to those of

$[\text{NiI}_2(\text{}^i\text{Pr}_2\text{-bimy})_2]$ (2.4829(4) Å and 1.8972(15) Å, respectively). The angles of C(1)-Ni(1)-C(1) (180.0°) and Br(1)-Ni(1)-Br(1A) (180.0°) are identical to those of $[\text{NiI}_2(\text{}^i\text{Pr}_2\text{-bimy})_2]$.

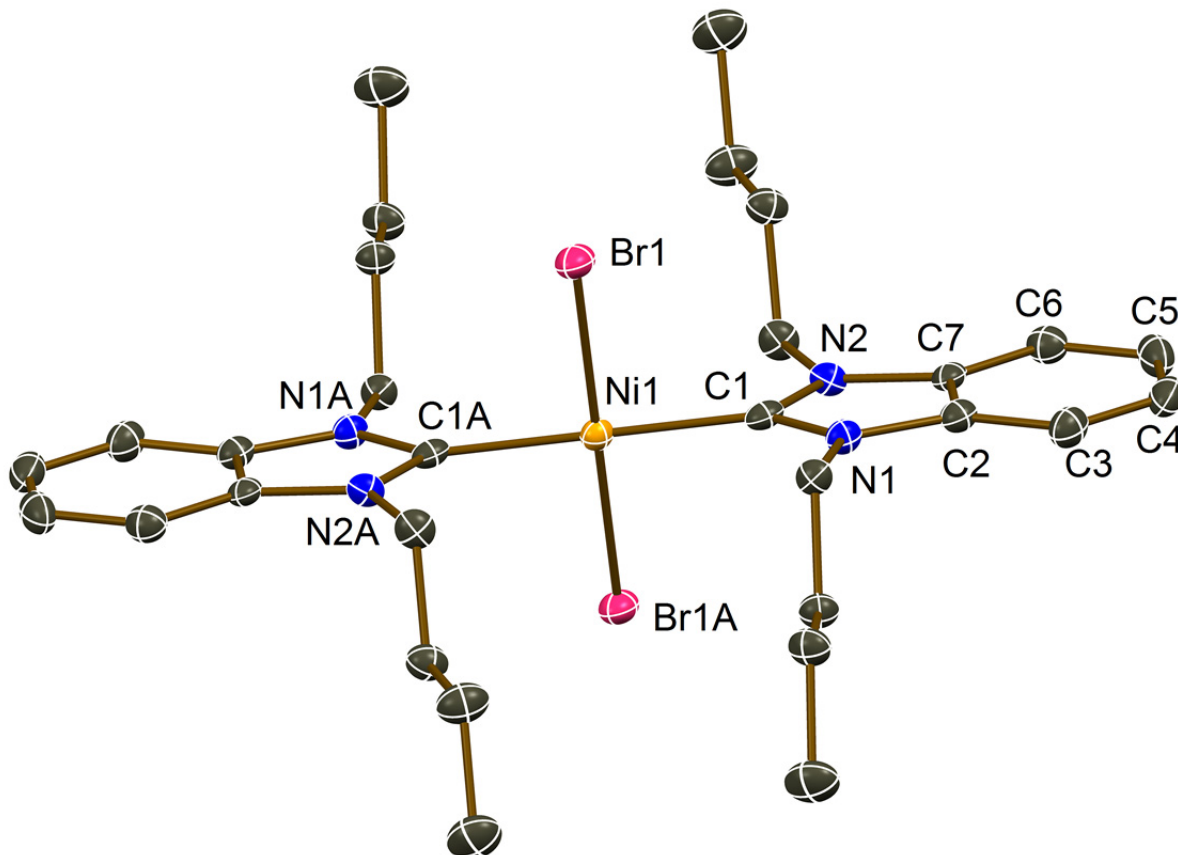
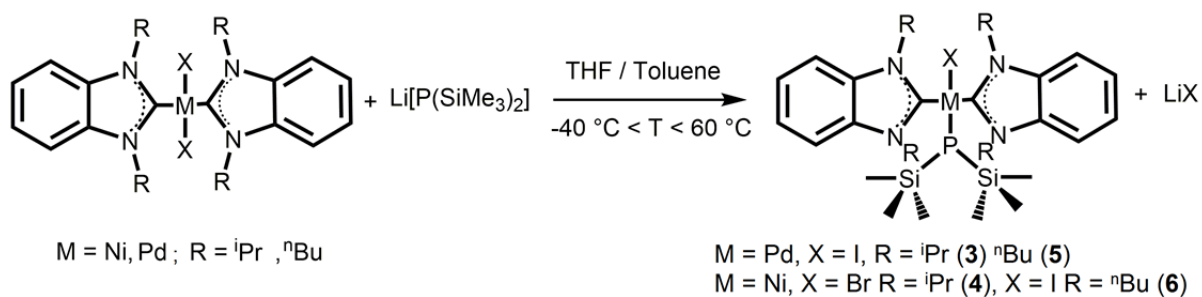


Figure 2.5: Molecular structure of complex $[\text{NiBr}_2(\text{}^n\text{Bu}_2\text{-bimy})_2]$ (*trans*-**2**) (50% probability). All hydrogen atoms are omitted for clarity. Selected bond lengths (Å) and angles (°) of complex **2**: Ni1-Br1 (2.3143(18)), Ni1-C1 (1.903(3)), Br1-Ni1-Br1A (180.0), Br1-Ni1-C1 (88.98(8)), Br1-Ni1-C1A (91.02(8)), C1-Ni1-C1A (180.0).

2.3.2. $[\text{MX}(\text{R}_2\text{-bimy})_2\{\text{P}(\text{SiMe}_3)_2\}]$ Complexes; M = Pd, Ni; R = ^iPr , ^nBu ; X = Br, I.

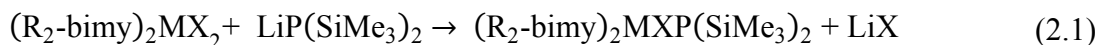
In general, *trans*- $[\text{MX}(\text{R}_2\text{-bimy})_2\{\text{P}(\text{SiMe}_3)_2\}]$ complexes, M = Pd, Ni; R = ^iPr , ^nBu ; X = Br, I, were synthesized via the reaction of *trans*- $[\text{MX}_2(\text{R}_2\text{-bimy})_2]$ with $\text{Li}[\text{P}(\text{SiMe}_3)_2]$ in

a 1:1 ratio, in a temperature range from -40 °C to 60 °C. Due to the poor solubility of *trans*-[PdI₂(ⁱPr₂-bimy)₂] and *trans*-[NiI₂(ⁱPr₂-bimy)₂] in common solvents, their reaction with Li[P(SiMe₃)₂] in THF required heating to 60 °C to obtain clear yellow (for Pd) or red (for Ni) solutions. The reaction of [PdI₂(ⁿBu₂-bimy)₂] (*trans*-**1**) and [NiBr₂(ⁿBu₂-bimy)₂] (*trans*-**2**), however, was started at -40 °C and stopped when it reached room temperature.



Scheme 2.1: Synthesis of [MX(R₂-bimy)₂{P(SiMe₃)₂}] complexes.

In order to eliminate lithium iodide salts, pentane was added to concentrated THF mixtures and any insoluble material was removed by filtering over Celite. Removing the solvent from the filtrate under vacuum resulted in the precipitation of PdI(ⁱPr₂-bimy)₂{P(SiMe₃)₂} (*trans*-**3**), [NiI(ⁱPr₂-bimy)₂{P(SiMe₃)₂}] (*trans*-**4**), PdI(ⁿBu₂-bimy)₂{P(SiMe₃)₂} (*trans*-**5**) and NiBr(ⁿBu₂-bimy)₂{P(SiMe₃)₂} (*trans*-**6**) in the form of oily products. The ¹H NMR spectrum of the palladium-silylphosphido complexes (*trans*-**3** and *trans*-**5**) are illustrated in Figure 2.6 and Figure 2.7, respectively.



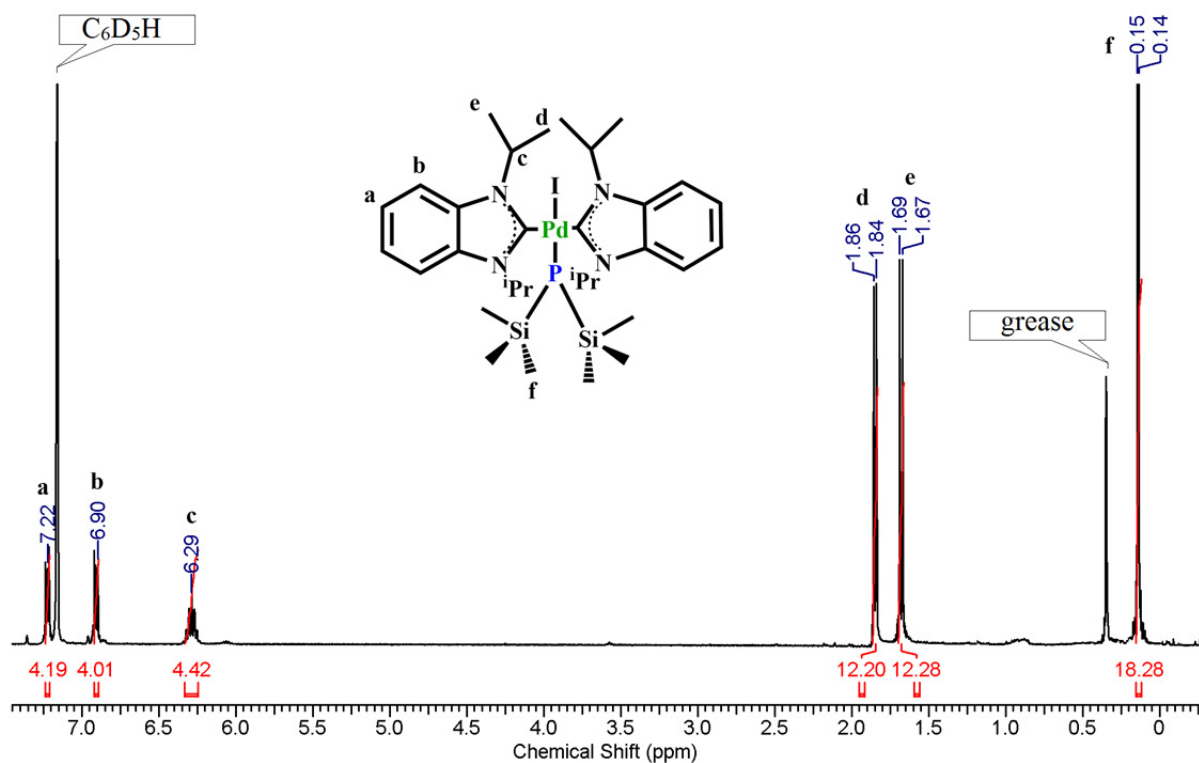


Figure 2.6: ^1H NMR spectrum of complex $[\text{PdI}(\text{iPr}_2\text{-bimy})_2\{\text{P}(\text{SiMe}_3)_2\}]$ (*trans*-**3**)

A doublet signal was observed at 0.14 ppm ($^3J_{\text{H,P}} = 3.5$ Hz) for *trans*-**3** and 0.11 ppm ($^3J_{\text{H,P}} = 3.5$ Hz) for *trans*-**5** assigned to the protons of the $\text{P}(\text{SiMe}_3)_2$ groups. These signals are close to those observed for other metal complexes with terminal bis(trimethylsilyl)phosphido ligands ($\delta = 0.27\text{--}0.76$ ppm, $^3J_{\text{H,P}} = 3.4\text{--}4.9$ Hz) [2, 3, 7], but slightly shifted upfield. Two doublets with equal intensity were observed at 1.67 and 1.84 ppm for methyl protons which indicate two magnetically inequivalent CH_3 groups of isopropyl substituents due to the asymmetrical structure of the *trans*-**3**. The resonance of the NCH protons noticeably shifted from 6.00 ppm in *trans*- $[\text{PdI}_2(\text{iPr}_2\text{-bimy})_2]$ to 6.29 ppm in *trans*-**3**. The similar trend was seen in the resonances of all CH_2 protons in *trans*-**5**, which were split into two sets of multiplets

with equal intensities. The resonances of all protons in *trans-5* were deshielded compared to those in *trans-1*.

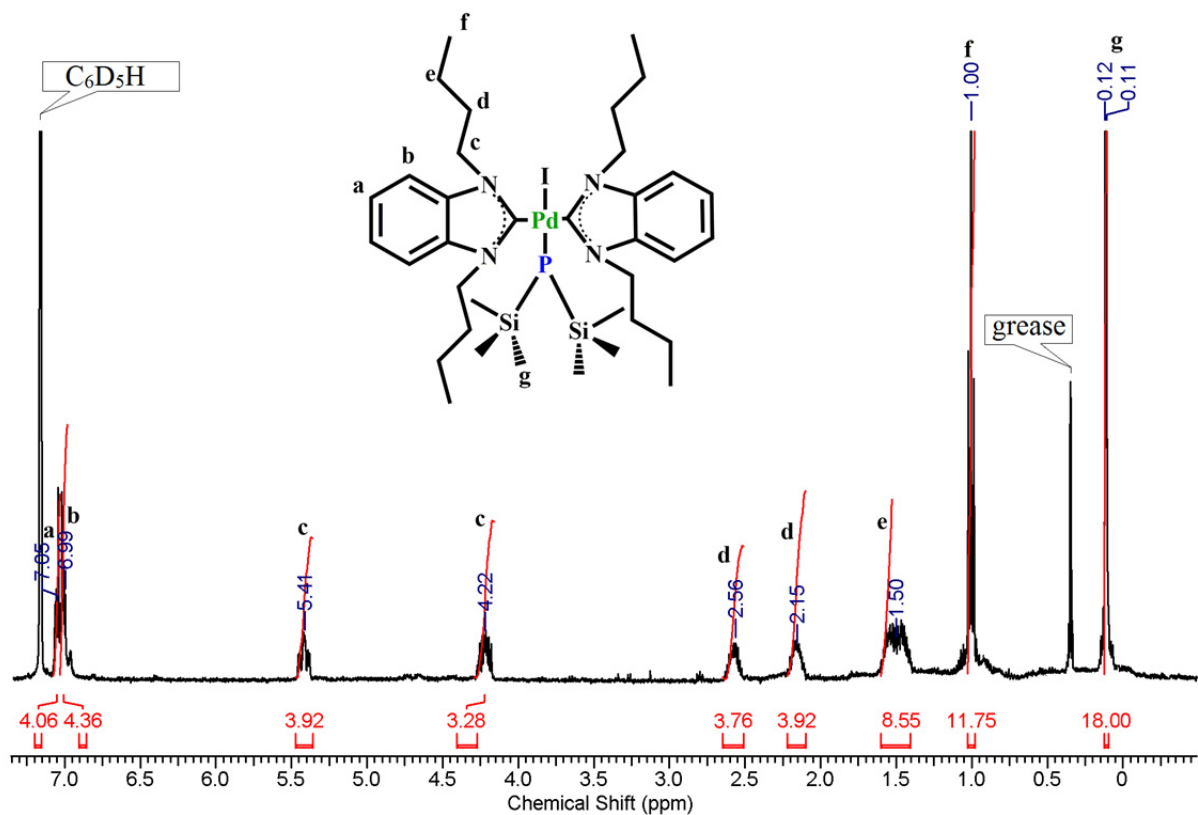


Figure 2.7: ¹H NMR spectrum of complex [PdI(^tBu₂-bimy)₂{P(SiMe₃)₂}] (*trans-5*)

The ¹³C NMR spectra of *trans-3* and *trans-5* are in line with their ¹H NMR spectra. The resonance of the NCN carbene carbon was recorded at 186.3 ppm in *trans-3* and 188.8 ppm in *trans-5*, respectively. Doublets were observed at 5.1 ppm (²J_{C,P} = 11.4 Hz) and 5.8 ppm (²J_{C,P} = 11.4 Hz), correspondingly, in *trans-3* and *trans-5* assigned to the carbon resonance of the P(Si(CH₃)₃)₂ ligand.

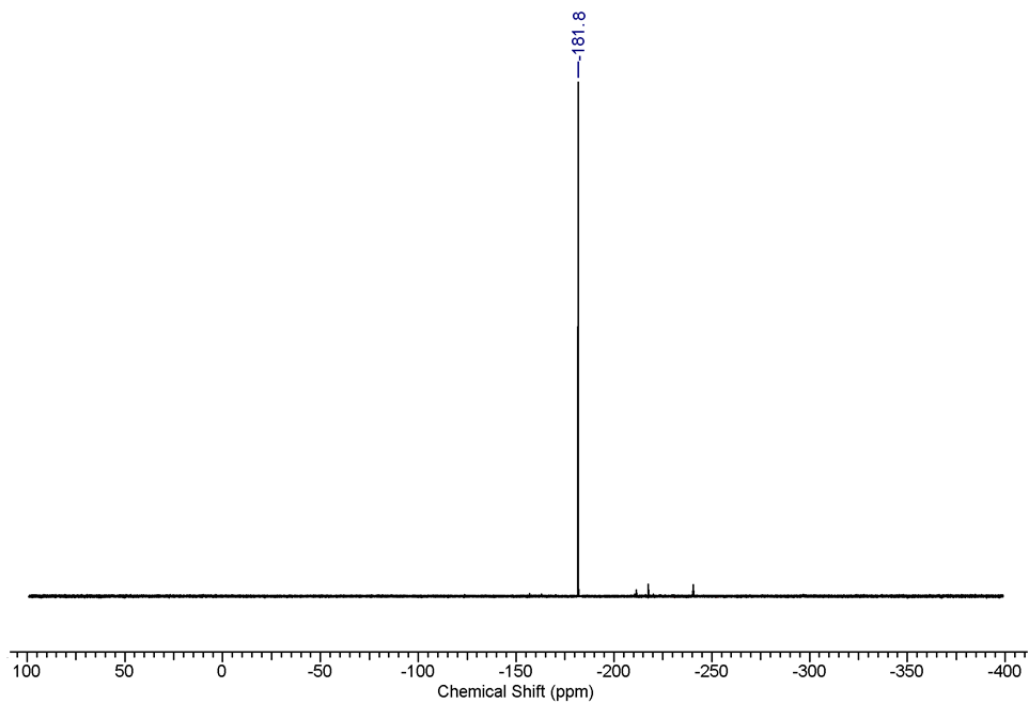


Figure 2.8: $^{31}\text{P}\{^1\text{H}\}$ NMR spectrum of $[\text{PdI}(\text{iPr}_2\text{-bimy})_2\{\text{P}(\text{SiMe}_3)_2\}]$ (*trans*-**3**)

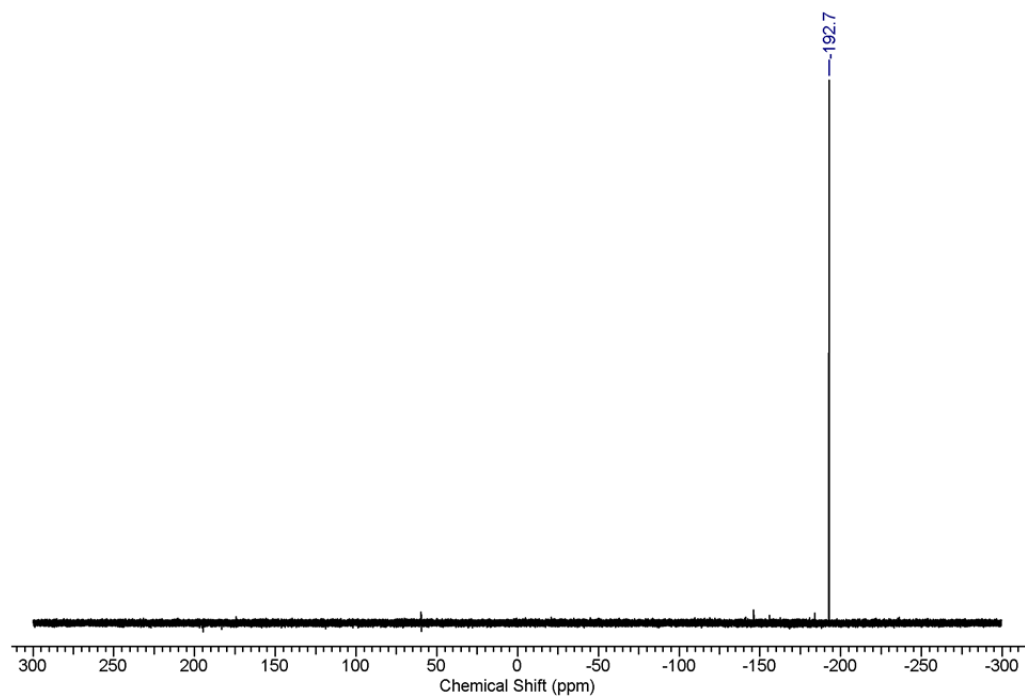


Figure 2.9: $^{31}\text{P}\{^1\text{H}\}$ NMR spectrum of complex $[\text{PdI}(\text{nBu}_2\text{-bimy})_2\{\text{P}(\text{SiMe}_3)_2\}]$ (*trans*-**5**)

^{31}P NMR spectroscopy was used to monitor the formation of *trans*-**3** and *trans*-**4**, respectively, from *trans*- $[\text{PdI}_2(\text{}^i\text{Pr}_2\text{-bimy})_2]$ and *trans*-**1** and spectra are depicted in Figure 2.8 and Figure 2.9. An upfield shift of the bis(trimethylsilyl)phosphido group was observed in the ^{31}P NMR spectra of *trans*-**3** (-181.8 ppm) and *trans*-**5** (-192.7 ppm) compared to that of $[\text{PtCl}(\text{PEt}_3)_2\{\text{P}(\text{SiMe}_3)_2\}]$ (-224 ppm) [11] due to the heavy metal effects in NMR spectroscopy.

The molecular structure of both complexes (*trans*-**3** and *trans*-**5**) was elucidated by single crystal X-ray diffraction studies. Single crystals of *trans*-**3** were obtained from concentrated pentane solution at -75 °C. Slow evaporation of concentrated THF solutions afforded single crystals of *trans*-**5** suitable for X-ray crystallography. The air sensitive yellow needles of *trans*-**3** and plates of *trans*-**5** both crystallize in the monoclinic space group $\text{P}2_1/c$ with a Z of 4. The molecular structures and selected bond angles and distances of both complexes are shown in Figure 2.10 and Figure 2.11. The coordination geometry of the palladium center is square planar connected to one iodo, one bis(trimethylsilyl)phosphido and two NHCs in both *trans*-**3** or *trans*-**5**. The bond distances (Å) of Pd(1)-C(1) (2.027(4) and 2.022(6)) are identical while Pd(1)-P(1) (2.3442(12) and 2.3648(17)) are different, respectively in *trans*-**3** and *trans*-**5**. A distortion from linearity is more seen in the angles of C(1)-Pd(1)-C(1) (171.41(13)°) and I(1)-Pd(1)-P(1) (166.42(3)°) in *trans*-**3** than those of *trans*-**5** (176.6(2)° and 174.55(4)°), respectively. The geometry around the P atom in *trans*-**3** (98.53(6)°) and *trans*-**5** (100.68(9)°) is distorted tetrahedral. These collected data show that n butyl substituents in *trans*-**5** provide more free space and less distortion around palladium center than isopropyl groups in *trans*-**3**.

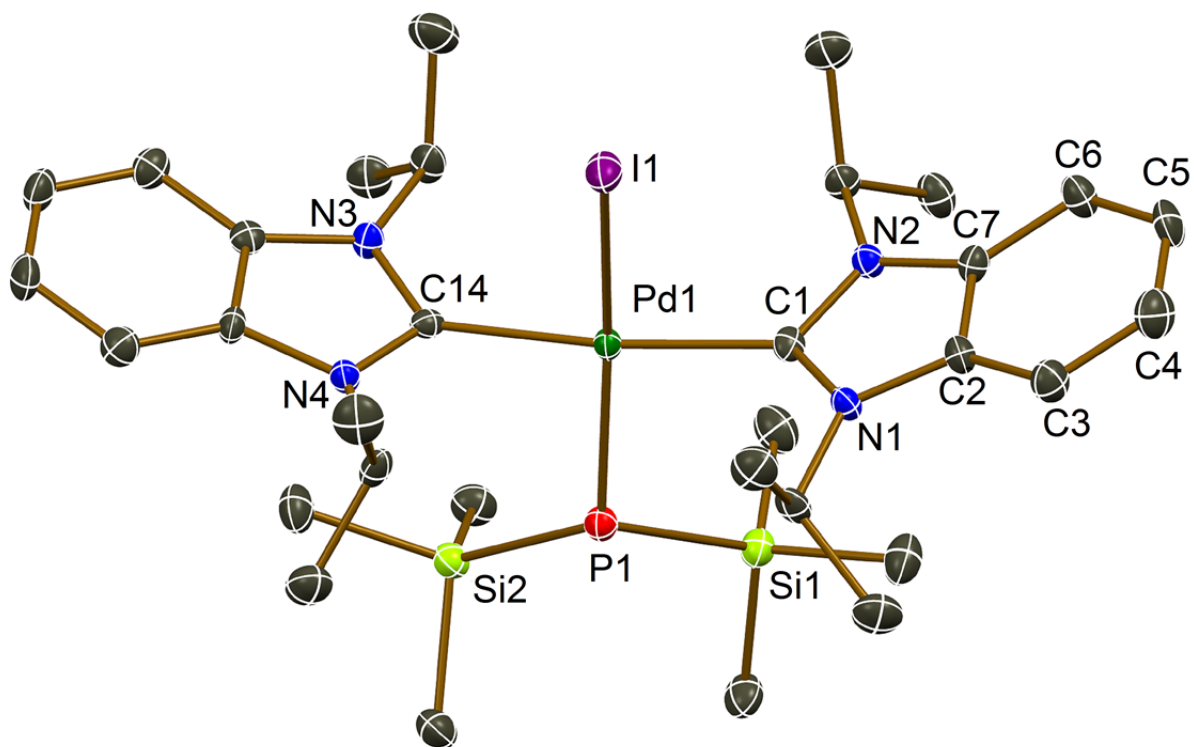


Figure 2.10: Molecular structure of complex $[\text{PdI}(\text{Pr}_2\text{-bimy})_2\{\text{P}(\text{SiMe}_3)_2\}]$ (*trans*-**3**) (50% probability). All hydrogen atoms and solvent (pentane) molecules are omitted for clarity. Selected bond lengths (Å) and angles (°) of complex **3**: Pd1-I1 (2.6998(7)), Pd1-P1 (2.3442(12)), Pd1-C1 (2.027(4)), Pd1-C14 (2.047(4)), I1-Pd1-P1 (166.42(3)), I1-Pd1-C1 (86.94(10)), I1-Pd1-C14 (84.48(11)), P1-Pd1-C1 (91.93(11)), P1-Pd1-C14 (96.49(11)), C1-Pd1-C14 (171.41(13)).

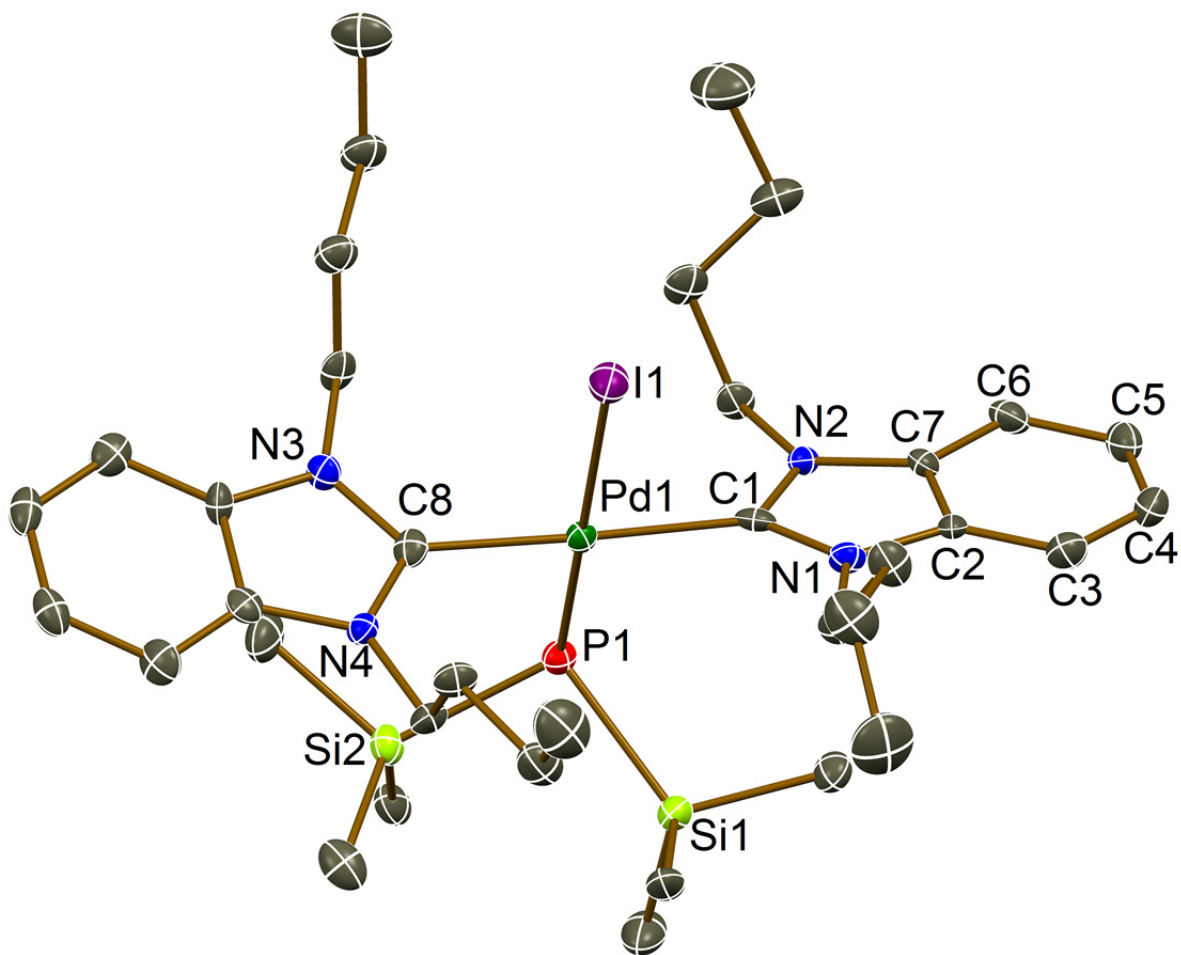


Figure 2.11: Molecular structure of complex $[\text{PdI}(\text{}^n\text{Bu}_2\text{-bimy})_2\{\text{P}(\text{SiMe}_3)_2\}]$ (*trans*-**5**) (50% probability). All hydrogen atoms and solvent ($\text{LiI} \cdot (\text{thf})_3$) molecules are omitted for clarity. Selected bond lengths (Å) and angles (°) of complex **5**: Pd1-I1 (2.6985(10)), Pd1-P1 (2.3648(17)), Pd1-C1 (2.022(6)), Pd1-C8 (2.049(6)), I1-Pd1-P1 (174.55(4)), I1-Pd1-C1 (88.14(17)), I1-Pd1-C8 (88.51(16)), P1-Pd1-C1 (93.60(17)), P1-Pd1-C8 (89.77(17)), C1-Pd1-C8 (176.6(2)).

The ease of preparation and stability of the palladium complexes suggested that the analogous Ni(II) species could be prepared. The ^1H NMR spectra of $[\text{NiI}(\text{}^i\text{Pr}_2\text{-bimy})_2\{\text{P}(\text{SiMe}_3)_2\}]$ (*trans*-**4**) and $[\text{NiBr}(\text{}^n\text{Bu}_2\text{-bimy})_2\{\text{P}(\text{SiMe}_3)_2\}]$ (*trans*-**6**), are illustrated

in Figure 2.12 and Figure 2.13, correspondingly. As expected, a doublet at 0.04 ppm was recorded for both complexes assigned to the protons of $P(SiMe_3)_2$ ligand. Due to the asymmetrical structures of *trans-4*, the resonance of CH_3 protons of isopropyl groups showed two sets of doublets with the same J coupling value at 1.73 and 1.89 ppm, similar to those observed for *trans-3*. In the case of *trans-6*, all CH_2 protons of the n butyl groups indicate two sets of multiplets with equal intensities, similar to those observed for *trans-5*.

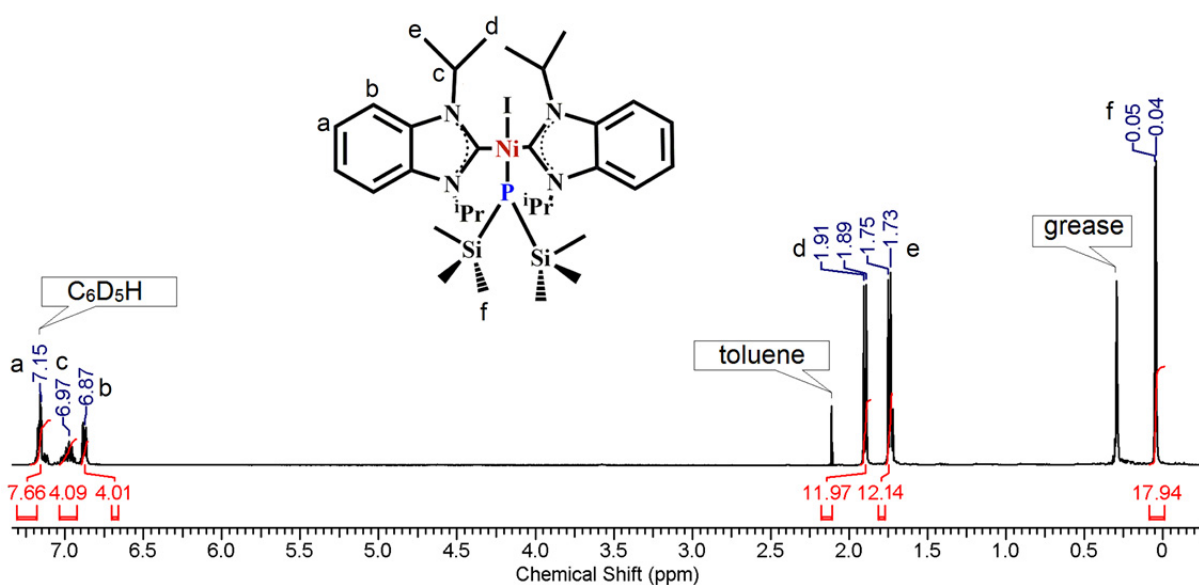


Figure 2.12: 1H NMR spectrum of complex $[NiI(iPr_2\text{-bimy})_2\{P(SiMe_3)_2\}]$ (*trans-4*)

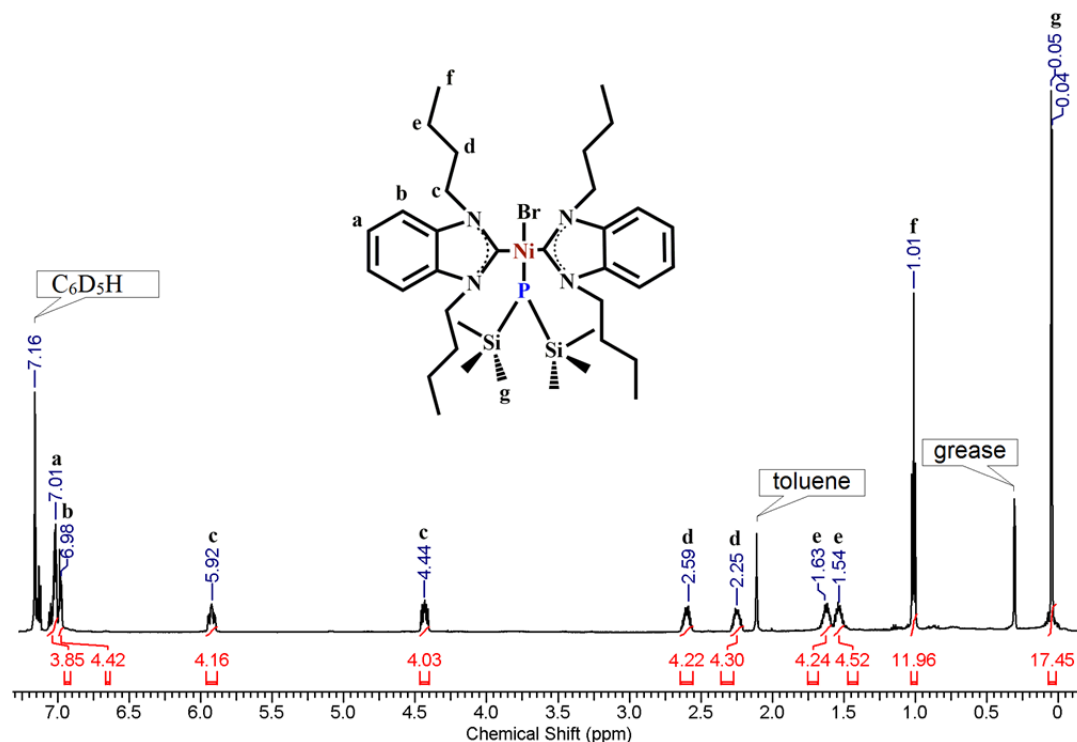


Figure 2.13: ^1H NMR spectrum of complex $[\text{NiBr}(\text{tBu}_2\text{-bimy})_2\{\text{P}(\text{SiMe}_3)_2\}]$ (*trans*-**6**)

$^{31}\text{P}\{^1\text{H}\}$ NMR spectra for *trans*-**4** and *trans*-**6** are depicted in Figure 2.14 and Figure 2.15, respectively. A significant downfield shift of the $\text{P}(\text{SiMe}_3)_2$ group was recorded at -178.6 ppm for *trans*-**4** and at -197.3 ppm for *trans*-**6** from their original position in $\text{Li}[\text{P}(\text{SiMe}_3)_2]$ ($\delta = -297$). These phosphorus chemical shifts are different from those reported for $[\text{NiCl}(\text{PEt}_3)_2\{\text{P}(\text{SiMe}_3)_2\}]$ and $[\text{Ni}(\text{PEt}_3)_2\{\text{P}(\text{SiMe}_3)_2\}_2]$ (-254 to -247 ppm) [8] due to the different environment of nickel centers. While they are close to the phosphorus chemical shifts of *trans*-**3** and *trans*-**5** (-181.8 and -192.7 ppm).

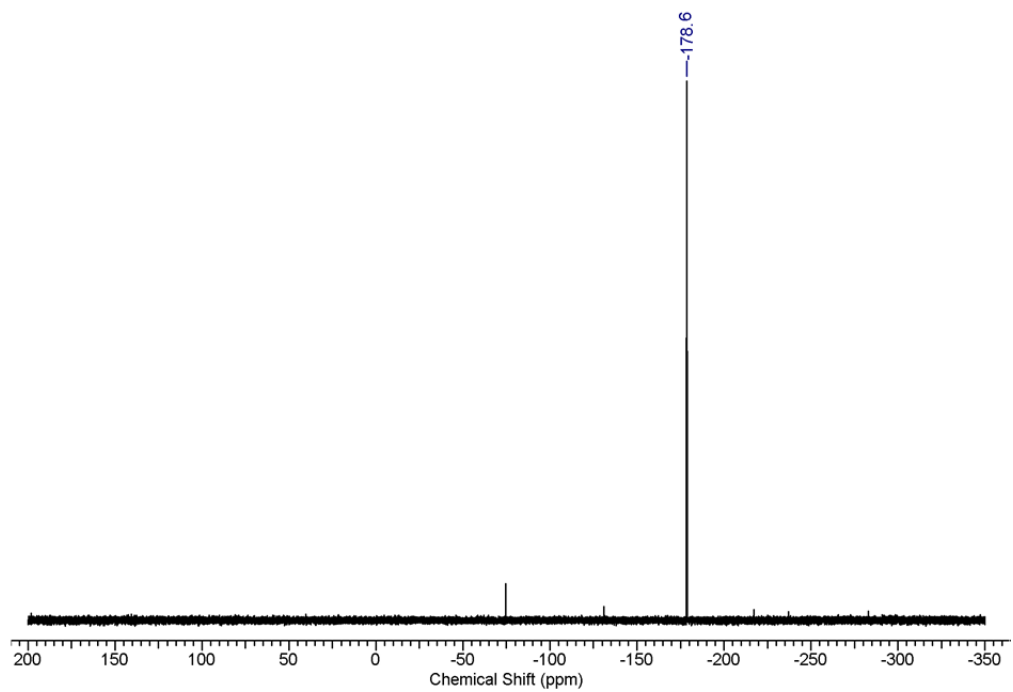


Figure 2.14: $^{31}\text{P}\{^1\text{H}\}$ NMR spectrum of $[\text{Ni}(\text{iPr}_2\text{-bimy})_2\{\text{P}(\text{SiMe}_3)_2\}]$ (*trans*-4)

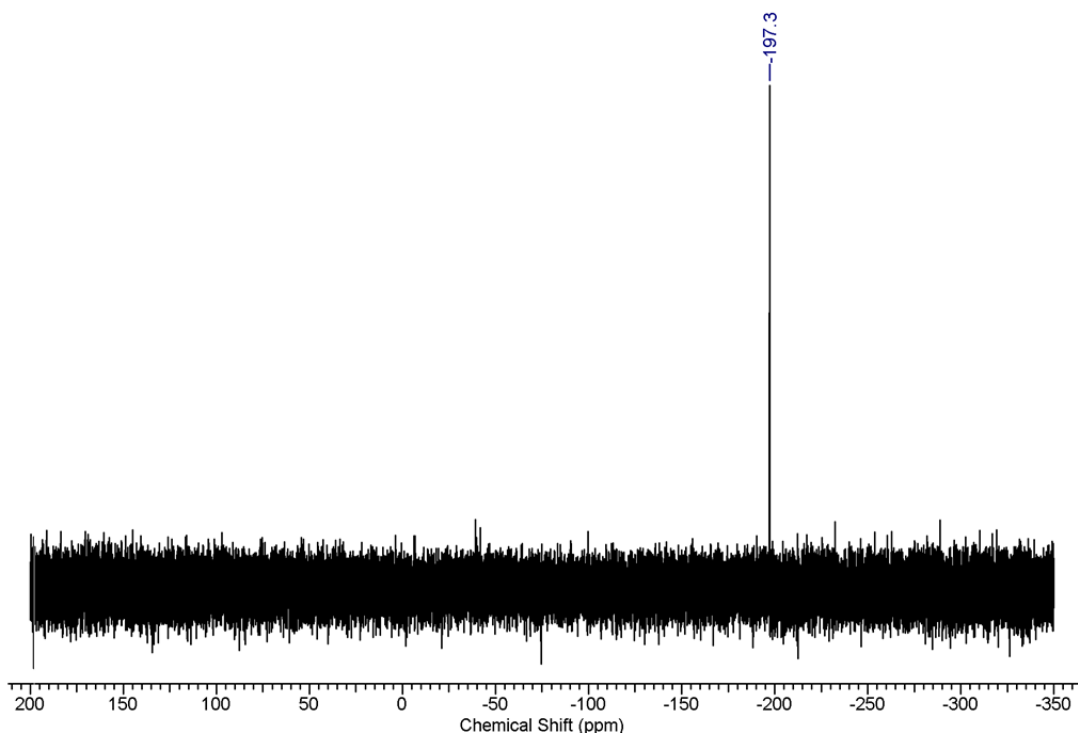
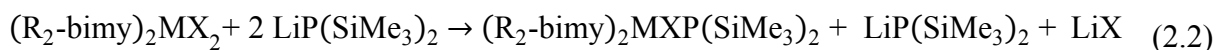


Figure 2.15: $^{31}\text{P}\{^1\text{H}\}$ NMR spectrum of complex $[\text{NiBr}(\text{iPr}_2\text{-bimy})_2\{\text{P}(\text{SiMe}_3)_2\}]$ (*trans*-6)

All synthesized palladium(II) and nickel(II) bis(trimethylsilyl)phosphido complexes were stable at room temperature and their melting points were in the range of 105 to 120 °C. In order to obtain *trans*-[M(R₂-bimy)₂{P(SiMe₃)₂}₂], M = Ni, Pd; R = ⁱPr, ⁿBu, complexes, the additional Li[P(SiMe₃)₂] was added to the reaction solutions of *trans*-**3** to *trans*-**6** in toluene or THF. The reaction temperature was changed from -40 to 60 °C (in THF) or -40 to 95 °C (in toluene). However, the ¹H NMR spectrum did not show the expected integration for protons of M—{P(SiMe₃)₂}₂. The additional bis(trimethylsilyl)phosphido group did not react with *trans*-**3** to *trans*-**6**, in the aforementioned reaction conditions, attributed to the steric crowding of the carbene and bis(trimethylsilyl)phosphido ligands.



We found that the metal-halido-NHC complexes with isopropyl or ⁿbutyl substituents on N-heterocycles only could react with Li[P(SiMe₃)₂] in a 1:1 ratio. A bidentate NHC potentially can be helpful to achieve a metal-NHC complex bearing two bis(trimethylsilyl)phosphido ligands. The rigid framework of bis(NHCs) provides an opportunity to create a linear, monovalent, two coordinate dimetal complex. Toward this end, the digold(I) complex of [AuCl₂(ⁿBu₄-benzo(imy)₂)] was synthesised by following the procedure reported by Boydston *et al.* [38]. The reaction of [AuCl₂(ⁿBu₄-benzo(imy)₂)] with Li[P(SiMe₃)₂] in a 1:2 ratio yielded a digold(I)-di(bis(trimethylsilyl)phosphido) complex of [Au(ⁿBu₄-benz(bimy)₂){P(SiMe₃)₂}₂] (**7**).

The ^1H NMR spectrum of [7] displays a doublet signal at 0.76 ppm with $^3J_{\text{H,P}} = 4.3$ Hz assigned to a $\text{P}(\text{SiMe}_3)_2$ ligand, which is shifted downfield compared to the bis(trimethylsilyl)phosphido complexes (*trans*-3 to *trans*-6), however, perfectly matches to that of metal-bis(trimethylsilyl)phosphido complexes with terminal- $\text{P}(\text{SiMe}_3)_2$ ($\delta = 0.27\text{--}0.76$ ppm, $^3J_{\text{H,P}} = 3.4\text{--}4.9$ Hz) [2, 3, 7]. Due to the symmetrical structure of complex [7], the other peaks present in the ^1H NMR spectrum of the starting $[\text{Au}_2\text{Cl}_2(\text{}^n\text{Bu}_4\text{-benzo(imy)}_2)]$ could successfully be assigned, albeit shifted upfield [54]. In the ^{31}P NMR spectrum of [7] a main signal was recorded at -230.4 ppm assigned to $\text{P}(\text{SiMe}_3)_2$ group which again falls well within the range of reported $\text{M-P}(\text{SiMe}_3)_2$ complexes [7, 12, 60].

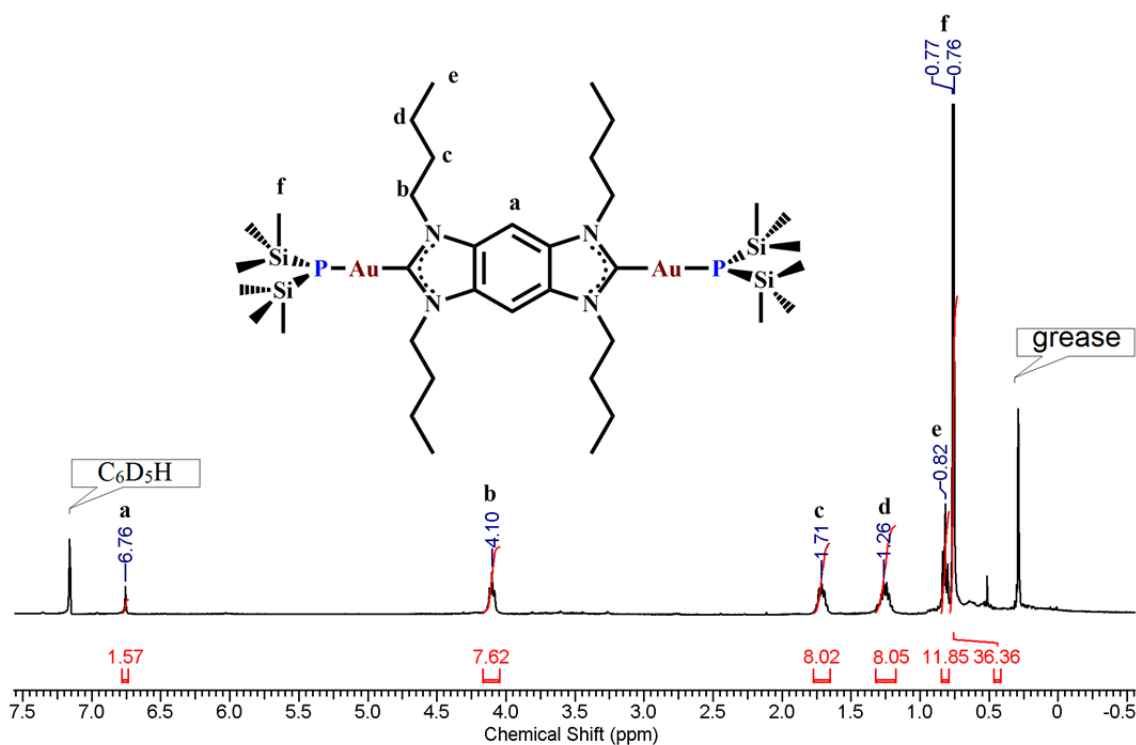


Figure 2.16: ^1H NMR spectrum of complex $[\text{Au}(\text{}^n\text{Bu}_4\text{-benz(bimy)}\{\text{P}(\text{SiMe}_3)_2\}_2)]$ (7)

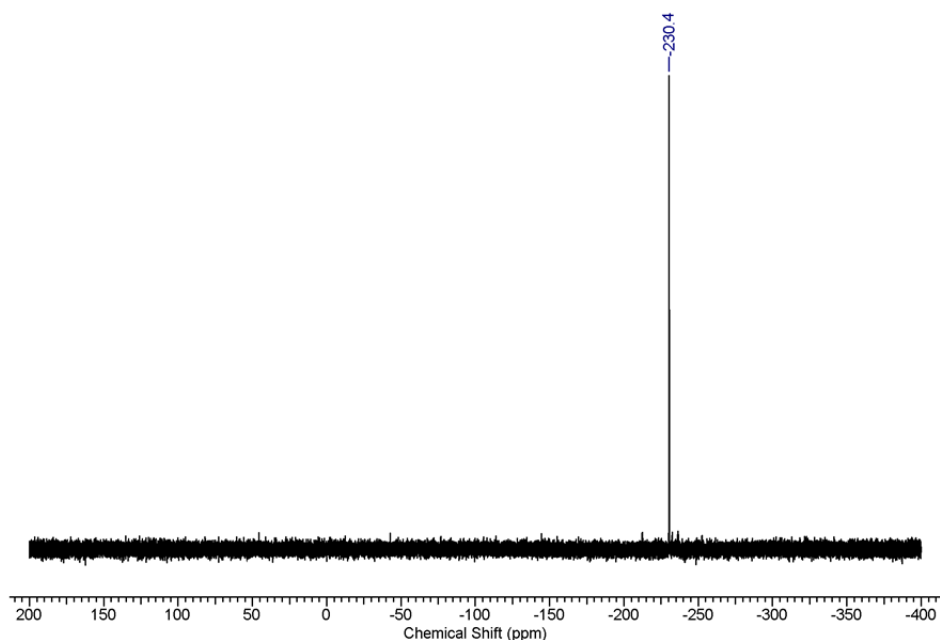


Figure 2.17: $^{31}\text{P}\{^1\text{H}\}$ NMR spectrum of complex $[\text{Au}(\text{}^n\text{Bu}_4\text{-benz(bimy)})\{\text{P}(\text{SiMe}_3)_2\}_2]$ (**7**)

2.4. CONCLUSIONS

The reaction of metal-NHC-halido complexes $\textit{trans}\text{-}[\text{MX}_2(\text{R}_2\text{-bimy})_2]$ ($\text{M} = \text{Pd, Ni, R} = \text{}^i\text{Pr, X} = \text{I}$), ($\text{M} = \text{Pd, R} = \text{}^n\text{Bu, X} = \text{I}$, [$\textit{trans}\text{-1}$]), ($\text{M} = \text{Ni, R} = \text{}^n\text{Bu, X} = \text{Br}$, [$\textit{trans}\text{-2}$]) with $\text{Li}[\text{P}(\text{SiMe}_3)_2]$, in a 1:1 ratio, resulted in the formation of a new series of room temperature-stable $\textit{trans}\text{-metal-halido-bis(trimethylsilyl)phosphido}$ complexes. $[\text{PdI}(\text{}^i\text{Pr}_2\text{-bimy})_2\{\text{P}(\text{SiMe}_3)_2\}]$ ($\textit{trans}\text{-3}$), $[\text{NiI}(\text{}^i\text{Pr}_2\text{-bimy})_2\{\text{P}(\text{SiMe}_3)_2\}]$ ($\textit{trans}\text{-4}$), $[\text{PdI}(\text{}^n\text{Bu}_2\text{-bimy})_2\{\text{P}(\text{SiMe}_3)_2\}]$ ($\textit{trans}\text{-5}$) and $[\text{NiBr}(\text{}^n\text{Bu}_2\text{-bimy})_2\{\text{P}(\text{SiMe}_3)_2\}]$ ($\textit{trans}\text{-6}$) were formed in good yield, in a temperature range from $-40\text{ }^\circ\text{C}$ to $60\text{ }^\circ\text{C}$. The reaction of $\textit{trans}\text{-3}$ to $\textit{trans}\text{-6}$ with additional $\text{Li}[\text{P}(\text{SiMe}_3)_2]$ did not result in the formation of $\text{M}\text{-}\{\text{P}(\text{SiMe}_3)_2\}_2$ complexes due to the lack of free space around the metal centers. The digold(I)-bis(trimethylsilyl)phosphido complex, $[\text{Au}_2(\text{}^n\text{Bu}_4\text{-benzo(imy)})_2]\{\text{P}(\text{SiMe}_3)_2\}$ (**7**), was

synthesized by the reaction of $[\text{Au}_2\text{Cl}_2(\text{}^n\text{Bu}_4\text{-benzo(imy)}_2)]$ with $\text{Li}[\text{P}(\text{SiMe}_3)_2]$ in a 1:2 ratio. NMR spectroscopy, X-ray crystallography, mass spectrometry and elemental analysis were used for characterization of the complexes. The aforementioned bis(trimethylsilyl)phosphido complexes (*trans*-**3** to *trans*-**7**) can participate in carbonyl addition reaction of acid chlorides to provide metal-phosphaalkene or metal-acylphosphido complexes.

3. METAL-DIACYLPHOSPHIDO COMPLEXES

3.1. INTRODUCTION

Due to the different electronegativities of silicon and phosphorus atoms, the polar Si–P bond in disilylalkylsilylphosphines could be easily cleaved in the presence of suitable polar organic compounds [1]. The reaction of acid chlorides with disilylalkylsilylphosphines resulted in the formation of compounds with phosphorus-carbon double bond (P=C) in phosphalkenes and/or phosphorus-carbon single bond (C–P) in diacylphosphines [1, 40]. In 1976, Becker synthesized the first phosphalkene compound with a localized C=P bond by the reaction of an organic silylphosphine compound with acid chloride [40-44]. By following Becker's route and using various acid chlorides, Weber *et al.* succeeded in synthesizing metal-phosphalkenes $[(\eta^5\text{-C}_5\text{H}_5)(\text{CO})_2\text{MP}=\text{C}(\text{OSiMe}_3)\text{R}]$ and metal-diacylphosphidos $[(\eta^5\text{-C}_5\text{H}_5)(\text{CO})_2\text{MP}\{\text{C}(\text{O})\text{R}\}_2]$; (M = Fe, Ru; R = Ph, 2,4,6-Me₃C₆H₂, ^tBu) [47, 48, 61]. In 2006, Gates *et al.* [51] introduced a new series of π -conjugated polymers and molecules composed of phosphalkene by means of diacid dichlorides. The reaction of bifunctional silylphosphines, 1,4-C₆R₄[P(SiMe₃)₂]₂, with 1,4-C₆R'₄[COCl]₂ (R = H, Me; R' = H, Me) resulted in the formation of poly(p-phenylenephosphalkene)s (PPP)s, while monofunctional silylphosphines with acid chlorides or diacid dichloride yielded mono(phosphalkene) or bis(phosphalkene) [51].

Herein, by following Weber's synthetic route [50], the cleavage of Si–P bonds in $[\text{PdI}(\text{iPr}_2\text{-bimy})_2\{\text{P}(\text{SiMe}_3)_2\}]$ (*trans*-**3**) and $[\text{NiI}(\text{iPr}_2\text{-bimy})_2\{\text{P}(\text{SiMe}_3)_2\}]$ (*trans*-**4**) is demonstrated by means of benzoyl chloride ($\text{PhC}(\text{O})\text{Cl}$). The structure of two new dibenzoylphosphido complexes are studied by NMR spectroscopy, X-ray analysis and mass spectrometry.

3.2. EXPERIMENTAL

3.2.1. General Synthetic Techniques and Starting Materials

All reactions have been performed using standard Schlenk techniques under a dry nitrogen atmosphere unless otherwise stated. Non-chlorinated solvents (toluene, tetrahydrofuran (THF), hexane, heptane, diethyl ether and pentane) were dried by passage through packed columns of activated alumina using a commercially available MBraun MB-SP Series solvent purification system. Chemicals were purchased from Aldrich and/or VWR. Benzene- d_6 and benzoyl chloride were dried and distilled over Na/K and CaH_2 , respectively.

^1H , $^{13}\text{C}\{^1\text{H}\}$ and $^{31}\text{P}\{^1\text{H}\}$ NMR spectra were recorded on a Varian Mercury 400 MHz, Inova 400 and 600 MHz spectrometer and the chemical shifts (δ) were internally referenced by the residual solvents signals (benzene- d_6 and chloroform- d) relative to tetramethylsilane (SiMe_4) (^1H and ^{13}C) or 85% H_3PO_4 (^{31}P). Single crystal X-ray diffraction measurements were performed on a Bruker APEXII diffractometer, with the molecular structures determined via direct methods using the SHELX suite of crystallographic programs [55]. All samples were mounted on a Mitegen polyimide micromount with a small

amount of Paratone N oil. Mass spectrometry and exact mass determinations were performed on a Bruker micrOTOF II instrument or Finningan MAT 8400.

3.2.2. [PdI(ⁱPr₂-bimy)₂P{C(O)Ph}₂] (*trans*-8)

To a cooled (-25 °C) solution of [PdI(ⁱPr₂-bimy)₂{P(SiMe₃)₂}] (*trans*-3) (0.20 g, 0.26 mmol) in toluene (10 mL) was added dropwise a solution of PhC(O)Cl (0.07 mL, 0.57 mmol) in toluene (5 mL). After the addition was complete, the reaction was warmed up to room temperature and stirred for 1h. ³¹P NMR of an aliquot removed from the reaction mixture confirmed that the reaction was completed. The reaction mixture was concentrated under vacuum and residual was taken up in Et₂O (20 mL). Insoluble material was filtered off and the filtrate was concentrated to obtain a pale yellow solid. Yield: 0.16 g (70%). ¹H NMR (600 MHz, C₆D₆, 23 °C) δ = 7.83 (m, 4H, o-Ph), 7.24 (dd, 4H, Ar-H), 6.91 (dd, 4H, Ar-H), 6.83 (m, 2H, p-Ph), 6.77 (m, 4H, m-Ph), 6.19 (sept, 4H, ³J_{H,H} = 7.0 Hz, NCH(CH₃)₂), 1.78 (d, 12H, ³J_{H,H} = 7.0, CH₃), 1.58 (d, 12H, ³J_{H,H} = 7.0, CH₃). ¹³C {¹H} NMR (600 MHz, CDCl₃, 23 °C) δ = 220.4 (d, ¹J_{C,P} = 42.1 Hz, P(CO)), 184.3 (s, CNC), 143.5 (d, ²J_{C,P} = 27.5 Hz, Ph-C), 134.5, 130.0 (s, Ph-C), 127.2, 120.4, 111.9 (s, Ar-C), 53.8 (s, NCH(CH₃)₂), 20.2 (s, CH₃). ³¹P {¹H} NMR (C₆D₆, 23 °C) δ = 51.4. m.p. (decomp) = 112-115 °C.

3.2.3. [NiI(ⁱPr₂-bimy)₂{P(C(O)Ph)₂}] (*trans*-9)

Complex **9** was prepared as for **8** from [NiI(ⁱPr₂-bimy)₂{P(SiMe₃)₂}] (*trans*-4) (0.14 g, 0.18 mmol) and PhC(O)Cl (0.04 mL, 0.36 mmol) in toluene (20 mL). Yield: 0.15 g (61%). Slow evaporation of Et₂O solution at -5 °C afforded the product as red needle crystals of **9** suitable for X-ray crystallography. ¹H NMR (600 MHz, C₆D₆, 23 °C) δ = 7.63 (m, 4H, o-Ph),

7.20 (dd, 4H, Ar-H), 6.91 (m, 4H, m-Ph, Ar-H), 6.70 (m, 10H, p-Ph, NCH(CH₃)₂), 1.83 (d, ³J_{H,H} = 7.0 Hz, 12H, CH₃), 1.67 (d, ³J_{H,H} = 7.0 Hz, 12H, CH₃). ³¹P{¹H} NMR (C₆D₆, 23 °C) δ = 72.7. ¹³C{¹H} NMR (600 MHz, CDCl₃, 23 °C) δ = 221.5 (d, ¹J_{C,P} = 45.6 Hz, P(CO)), 185.3 (s, CNC), 145.0 (d, ²J_{C,P} = 25.4 Hz, Ph-C), 135.0, 130.6 (s, Ph-C), 127.5, 121.3, 112.2 (s, Ar-C), 54.1 (s, NCH(CH₃)₂), 20.6 (s, CH₃). m.p. (decomp) = 107-109 °C. HRMS (EI): m/z calcd for C₄₀H₄₆IN₄NaO₂P[⁵⁸Ni]: 853.16566 [M]⁺; found: 853.16684. Anal. Calc for C₄₀H₄₆IN₄NiO₂P (923.52): C 57.79, H 5.58, N 6.74. Found: C 57.81, H 5.89, N 5.73. Crystal data for [*trans*-9].C₇H₈ : M = 923.52, T = 110 K, λ = 0.71073 Å, μ(Mo Kα) = 1.376 cm⁻¹, monoclinic, a = 12.750(3), b = 9.244(2), c = 38.007(11) Å, β = 95.444(18)°, V = 4459(2) Å³, space group P 2₁/n, Z = 4, 73261 measured reflections, 10960 unique reflections, R₁ = 0.0391, wR₁ = 0.0959 (I ≥ 2σ(I)), wR₂ (all data) = 0.1140, GOF = 1.114, F(000) = 1904.

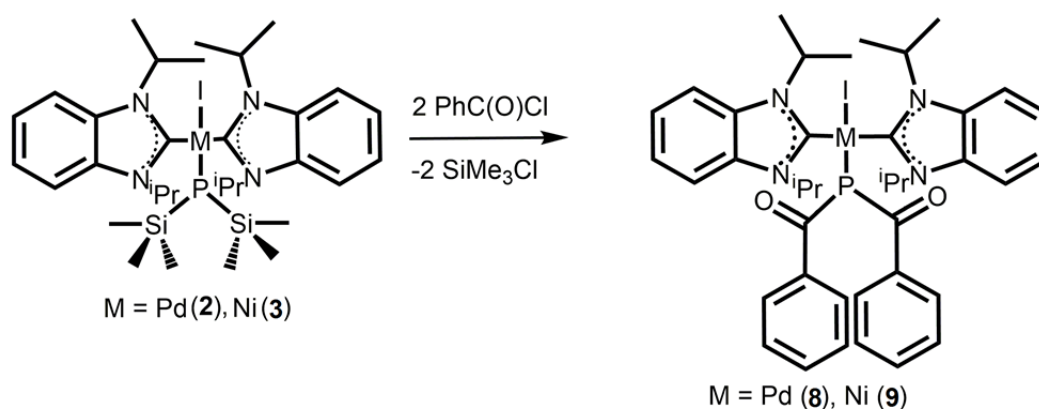
3.3. RESULTS AND DISCUSSION

3.3.1. [MI(^tPr₂-bimy)₂P{C(O)Ph}₂] Complexes, M = Pd, Ni.

In general, metal-diacylphosphido complexes are readily prepared by the reaction of metal-silylphosphido complexes with acid chlorides. Based on a previous study [61], a 1:1 ratio of [(η⁵-C₅H₅)(CO)₂Fe-P(SiMe₃)₂] to PhC(O)Cl afforded a mixture of phosphalkene [(η⁵-C₅H₅)(CO)₂Fe-P=C(OSiMe₃)Ph] and benzoylphosphido [(η⁵-C₅H₅)(CO)₂Fe-P{C(O)Ph}₂] complexes. The product ratio of phosphalkene to benzoylphosphido complex was concentration dependent and the formation of phosphalkene complex was clearly favoured in dilute solution. However, the analogous dipivaloylphosphido complex, [(η⁵-C₅H₅)(CO)₂Fe-P{C(O)^tBu}₂], was the only definable product of the reaction of [(η⁵-

$\text{C}_5\text{H}_5(\text{CO})_2\text{Fe-P}(\text{SiMe}_3)_2$] with ${}^t\text{BuC}(\text{O})\text{Cl}$. Equimolar amounts of $[(\eta^5\text{-C}_5\text{H}_5)(\text{CO})_2\text{Fe-P}(\text{SiMe}_3)_2]$ with a 2,4,6-trimethylbenzoyl chloride ($\text{MesC}(\text{O})\text{Cl}$) supplied the iron-phosphaalkene complex, $[(\eta^5\text{-C}_5\text{H}_5)(\text{CO})_2\text{Fe-P}=\text{C}(\text{OSiMe}_3)\text{Mes}]$.

The reaction of $[\text{PdI}(\text{}^i\text{Pr}_2\text{-bimy})_2\{\text{P}(\text{SiMe}_3)_2\}]$ (*trans*-**3**) with $\text{PhC}(\text{O})\text{Cl}$ in a 1:2 ratio at room temperature yielded a palladium-dibenzoylphosphido complex, $[\text{PdI}(\text{}^i\text{Pr}_2\text{-bimy})_2\text{P}\{\text{C}(\text{O})\text{Ph}\}_2]$ (*trans*-**8**) as the only detectable product. The same reaction condition resulted in the formation of $[\text{NiI}(\text{}^i\text{Pr}_2\text{-bimy})_2\text{P}\{\text{C}(\text{O})\text{Ph}\}_2]$ (*trans*-**9**) from $[\text{PdI}(\text{}^i\text{Pr}_2\text{-bimy})_2\{\text{P}(\text{SiMe}_3)_2\}]$ (*trans*-**4**) and benzoyl chloride.



Scheme 3.1: Synthesis of $[\text{MI}(\text{R}_2\text{-bimy})_2\text{P}\{\text{C}(\text{O})\text{Ph}\}_2]$ complexes.

The metal-dibenzoylphosphido complexes were characterized by NMR spectroscopy and chemical shift data were obtained at room temperature in benzene- d^6 . ${}^1\text{H}$ NMR of the complexes, *trans*-**8** and *trans*-**9**, lacked the silylphosphido ligand signal, which stands at the range of 0.04-0.15 ppm in the precursors, *trans*-**3** and *trans*-**4**. In addition, new signals were observed in the aromatic region assigned to the resonances of ortho, para and meta protons of benzoylphosphido ligand which are in the range of those reported for $[(\eta^5\text{-$

$\text{C}_5\text{H}_5(\text{CO})_2\text{Fe}-\text{P}\{\text{C}(\text{O})\text{Ph}\}_2$ [61]. All of the assigned peaks for *trans*-**8** and *trans*-**9**, are illustrated in the spectra in Figure 3.1 and Figure 3.2, respectively.

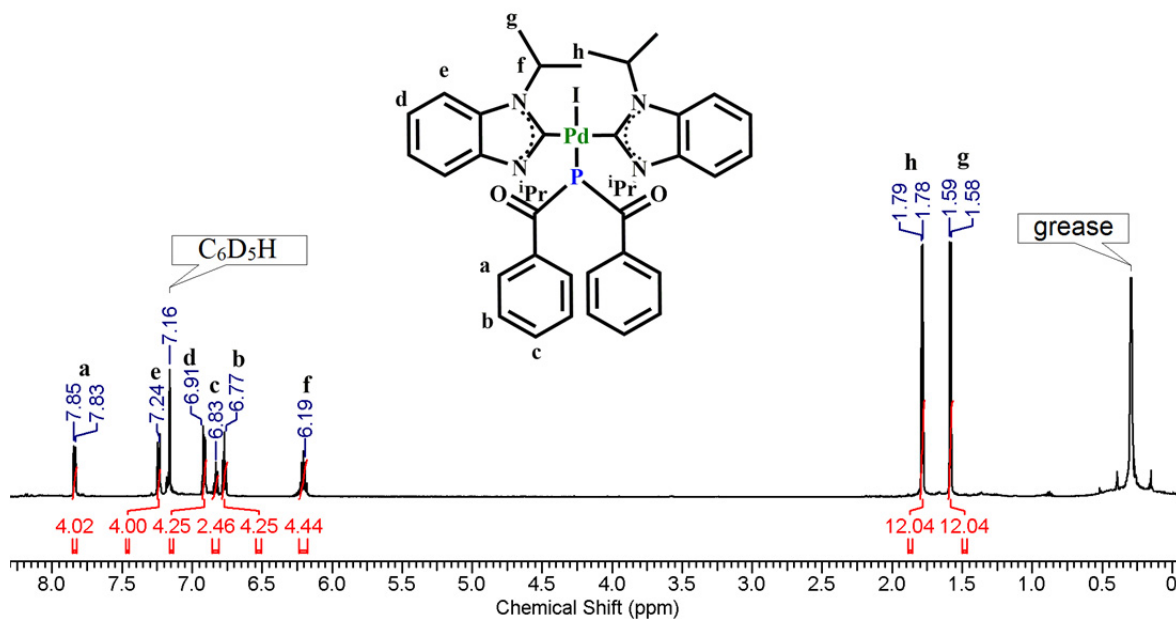


Figure 3.1: ^1H NMR spectrum of complex $[\text{PdI}(\text{iPr}_2\text{-bimy})_2\text{P}\{\text{C}(\text{O})\text{Ph}\}_2]$ (*trans*-**8**)

^{31}P NMR spectroscopy was used to monitor progress of all reactions. A significant downfield shift ($\sim\delta\Delta = 300$ ppm) is expected upon formation of metal-diacylphosphido complexes from $\text{M}-\{\text{P}(\text{SiMe}_3)_2\}$ complexes [50]. As shown in Figure 3.3, a significant signal changes was observed upon the conversion of *trans*-**3** ($\delta = -181.7$) to *trans*-**8** ($\delta = +51.4$) as a result of replacement of electron-donating trimethylsilyl groups ($\text{M}-\text{P}(\text{SiMe}_3)_2$) with the electron withdrawing benzoyl groups ($\text{M}-\text{P}\{\text{C}(\text{O})\text{Ph}\}_2$). This chemical shift is close to those reported for the iron-diacylphosphido complexes (63.1-92.6 ppm) [61]. Similar changes were observed for the nickel complex (*trans*-**9**) ($\delta = +72.7$, $\Delta\delta = 250$, Figure 3.4).

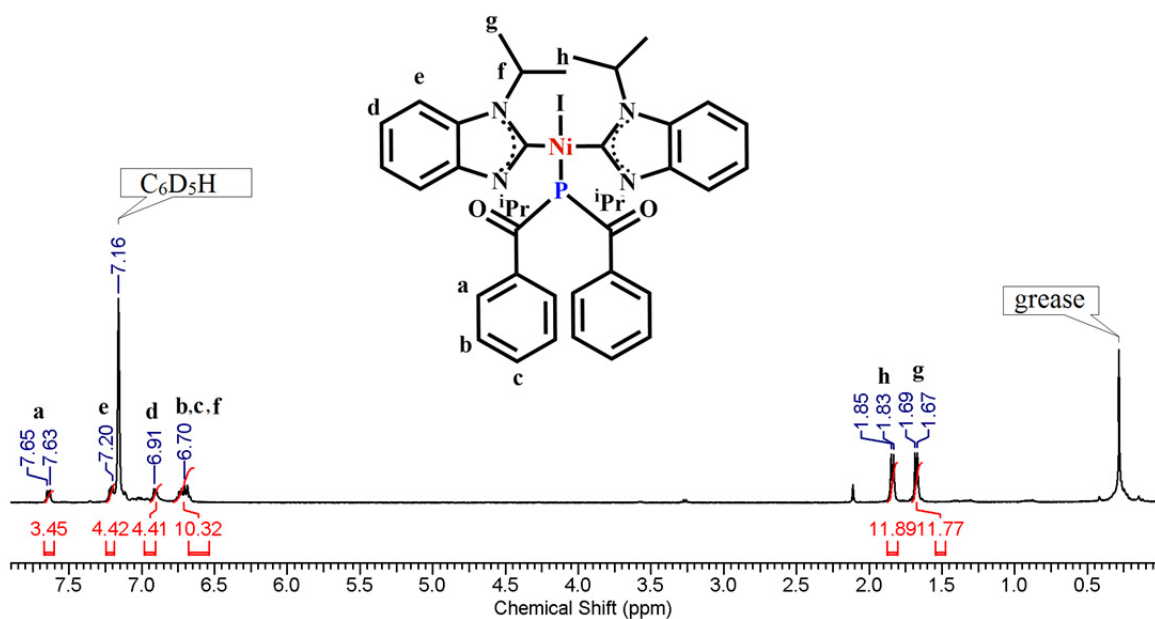


Figure 3.2: ^1H NMR spectrum of complex $[\text{Ni}(\text{iPr}_2\text{-bimy})_2\text{P}\{\text{C}(\text{O})\text{Ph}\}_2]$ (*trans-9*)

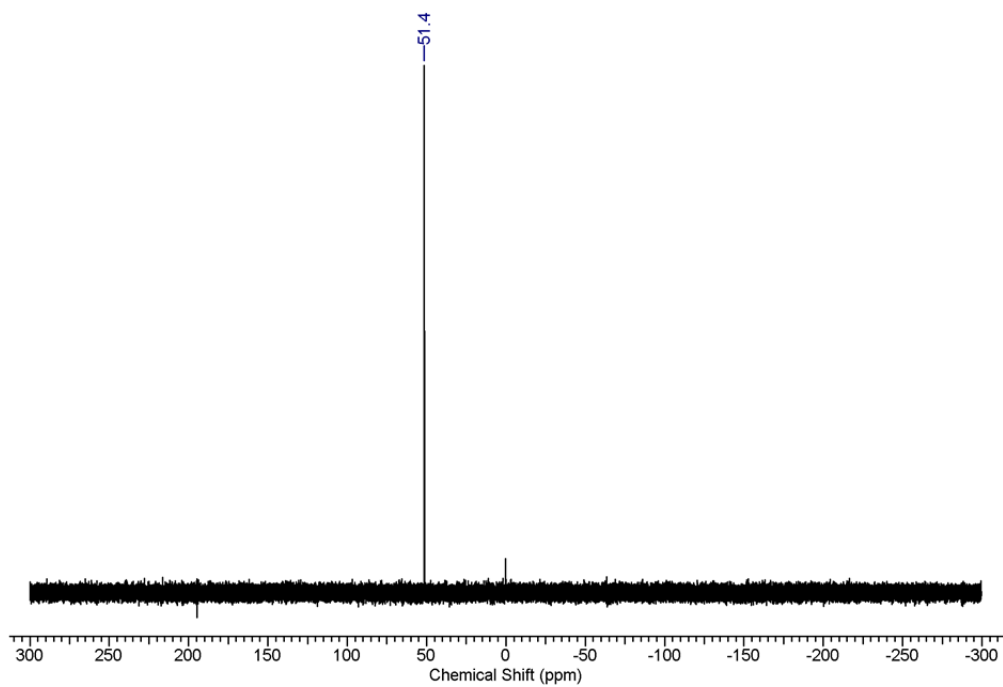


Figure 3.3: $^{31}\text{P}\{^1\text{H}\}$ NMR spectrum of complex $[\text{Pd}(\text{iPr}_2\text{-bimy})_2\text{P}\{\text{C}(\text{O})\text{Ph}\}_2]$ (*trans-8*)

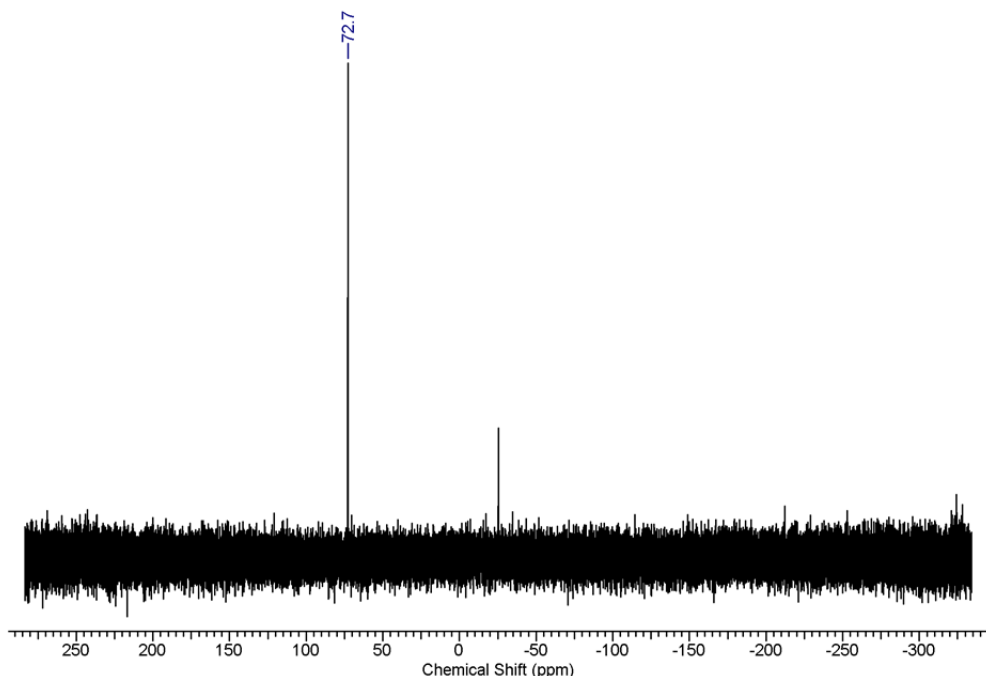


Figure 3.4: $^{31}\text{P}\{^1\text{H}\}$ NMR spectrum of complex $[\text{Ni}(\text{iPr}_2\text{-bimy})_2\text{P}\{\text{C}(\text{O})\text{Ph}\}_2]$ (*trans-9*)

In the ^{13}C NMR spectra of the both dibenzoylphosphido complexes, all peaks of the NHC ligands were shifted upfield. The resonance of the carbonyl carbon atom ($\text{P}-\{\text{C}(\text{O})\text{Ph}\}_2$) were observed as a doublet signal at 220.3 ppm ($^1J_{\text{C,P}} = 42.1$ Hz) in *trans-8* and at 221.5 ppm ($^1J_{\text{C,P}} = 45.6$ Hz) in *trans-9*, consistent with the reported range for carbonyl carbon of diacylphosphido complexes in previous studies ($\delta = 224.4\text{--}235.9$) [50, 61]. The characteristic doublet of the ipso-carbon atom of $\text{P}\{\text{C}(\text{O})\text{Ph}\}_2$ was emerged at 143.5 ($^2J_{\text{C,P}} = 27.5$ Hz, in *trans-8*) and 145.0 ppm ($^2J_{\text{C,P}} = 25.4$ Hz, in *trans-9*) were also observed [50].

The formation of *trans-9* was ultimately confirmed by single crystal X-ray diffraction studies. Needle crystals of this complex were obtained by slow evaporation of a concentrated ether solution at -5 °C. Complex *trans-9* crystallizes in the orthorhombic space group $\text{P}2_1/n$ with 4 molecules in the unit cell ($Z = 4$). The inversion center, 2-fold screw axis and n-glide

present in the unit cell of *trans-9*. Based on the crystallographic data for *trans-9*, the nickel atom displayed nearly planar geometry, coordinated to two 1,3-diisopropyl(benz)imidazole, one iodo and one phosphido ligands. The bond distances for Ni(1)-C(1), Ni(1)-C(14), Ni(1)-I(1) and Ni(1)-P(1) are 1.896(3) 1.903(3), 2.5326(6) and 2.1888(10) Å, respectively. In comparison with [Ni(PEt₃)₂{P(SiMe₃)₂}₂] bond distances [62], the Ni(1)-P(1) bond in *trans-9* (2.1888(10) Å) is shorter than those of the nickel-di(bis(trimethylsilyl)phosphido) complex (2.236(2) and 2.258(2) Å). The bond angles of C(1)-Ni(1)-C(14), I(1)-Ni(1)-P(1), I(1)-Ni(1)-C(1) and C(1)-Ni(1)-P(1) are 176.50(11), 170.15(3), 87.23(9) and 92.29(9)°, correspondingly. The phosphorus atom in *trans-9* shows a slightly distorted tetrahedral (103.22(14)°) geometry. Two images of the *trans-9* with selected bond distances and angles are shown in Figure 3.5.

The complex *trans-8* is thermally stable to 112 °C and decomposes at the range of 112-115 °C to yield a brownish solid. Similar behaviour was observed for single crystals of *trans-9* at lower temperatures, which decomposed to a black compound at 107-109 °C. An ether solution of both complexes was kept for one month at room temperature and no changes were observed in their NMR spectroscopy. The stability of diacylphosphido complexes is much greater than that of phosphalkene complexes. According to the work of Weber *et al.* [50], the iron-phosphalkenes decomposed rapidly in air. They are extremely sensitive to hydrolysis in solution and traces of moisture in the presentation and processing of these compounds lead to contamination by transition iron-substituted acylphosphine [(η⁵-C₅H₅)(CO)₂FeP(H)-C(O)R]; R = Mes, Ph, ^tBu, [50].

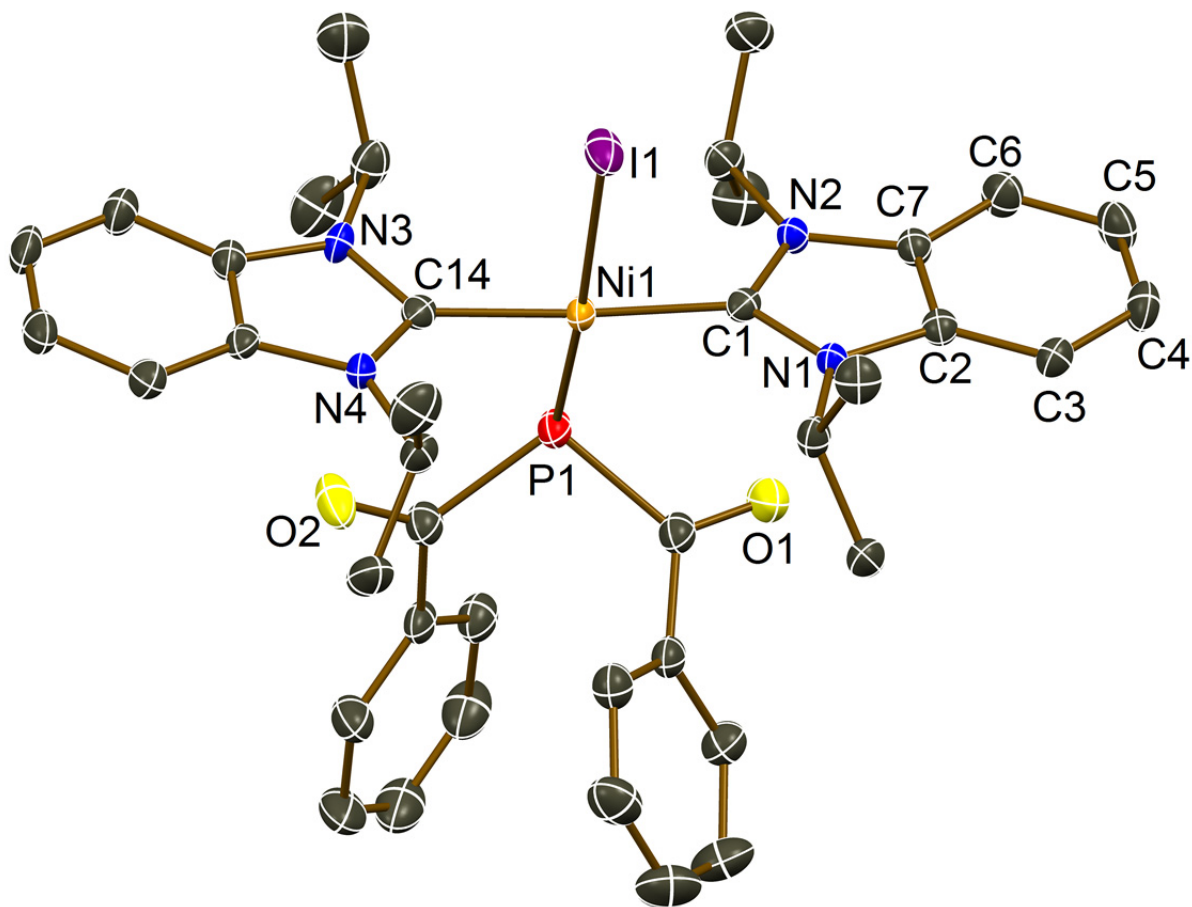


Figure 3.5: Molecular structure of complex $[\text{NiI}(\text{}^i\text{Pr}_2\text{-bimy})_2\text{P}\{\text{C}(\text{O})\text{Ph}\}_2]$ (*trans*-**9**) (50% probability). All hydrogen atoms and solvent (toluene) molecules are omitted for clarity. Selected bond lengths (Å) and angles (°) of complex **9**: Ni1-I1 (2.5326(6)), Ni1-P1 (2.1888(10)), Ni1-C1 (1.896 (3)), Ni1-C14 (1.903 (3)), I1-Ni1-P1 (170.15(3)), I1-Ni1-C1 (87.23(9)), I1-Ni1-C14 (89.81(8)), P1-Ni1-C1 (92.29(9)), P1-Ni1-C14 (90.31(9)), C1-Ni1-C14 (176.50(11)).

3.4. CONCLUSIONS

The cleavage of the silicon-phosphorus polar bond in the $[\text{PdI}(\text{}^i\text{Pr}_2\text{-bimy})_2\{\text{P}(\text{SiMe}_3)_2\}]$ (*trans*-**3**) and $[\text{NiI}(\text{}^i\text{Pr}_2\text{-bimy})_2\{\text{P}(\text{SiMe}_3)_2\}]$ (*trans*-**4**) by means of benzoyl chloride resulted in formation of metal-dibenzoylphosphido complexes $[\text{PdI}(\text{}^i\text{Pr}_2\text{-$

bimy)₂P{C(O)Ph}₂] (*trans*-**8**) and [Ni(ⁱPr₂-bimy)₂P{C(O)Ph}₂] (*trans*-**9**), respectively. The progress of the reactions was monitored by NMR spectroscopy. A significant downfield shift of the phosphorus signal was observed upon the formation of metal-dibenzoylphosphido complexes (~Δδ = 300 ppm). X-ray diffraction study was applied for extra characterization of nickel-dibenzoylphosphido complex (*trans*-**9**). The molecular structure of *trans*-**9** showed that nickel atom has *trans*-square planar configuration with two NHCs, one iodo and one benzoylphosphido ligands.

4. CONCLUSIONS AND RECOMMENDATIONS FOR FUTURE WORK

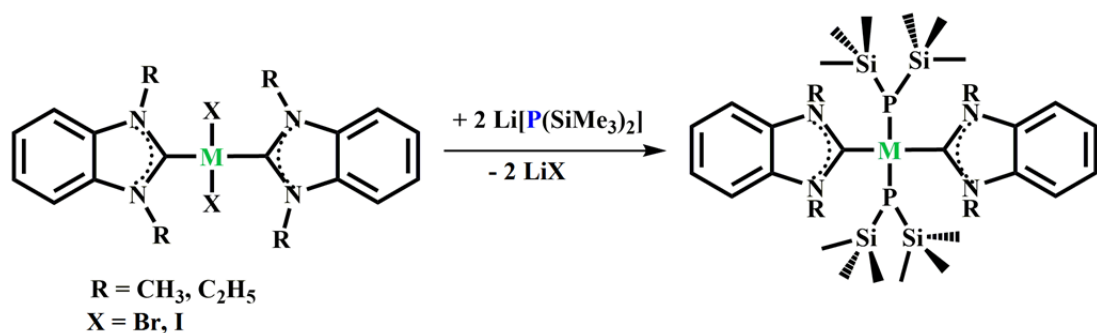
4.1. CONCLUSIONS

We have demonstrated a straightforward synthesis of a novel series of room temperature-stable *trans*-metal-bis(trimethylsilyl)phosphido complexes. The reaction of metal-dicarbene-dihalide complexes, *trans*-[M₂(ⁱPr₂-bimy)₂] (M = Pd, Ni), PdI₂(ⁿBu₂-bimy)₂ (*trans*-**1**) and [NiBr₂(ⁿBu₂-bimy)₂] (*trans*-**2**) with Li[P(SiMe₃)₂], in a 1:1 ratio, resulted in delivery of the P(SiMe₃)₂ group to the palladium(II) and nickel(II) complexes. The silylated complexes PdI(ⁱPr₂-bimy)₂{P(SiMe₃)₂} (*trans*-**3**), [NiI(ⁱPr₂-bimy)₂{P(SiMe₃)₂}] (*trans*-**4**), PdI(ⁿBu₂-bimy)₂{P(SiMe₃)₂} (*trans*-**5**) and NiBr(ⁿBu₂-bimy)₂{P(SiMe₃)₂} (*trans*-**6**) were obtained in good yield and characterized by ¹H, ¹³C{¹H}, ³¹P{¹H} NMR spectroscopy and single-crystal X-ray analysis. Furthermore, the synthesized *trans*-metal-bis(trimethylsilyl)phosphido complexes (*trans*-**3** to *trans*-**6**) were reacted with additional Li[P(SiMe₃)₂] to form metal-{P(SiMe₃)₂}₂ complexes. However, due to the lack of free space around the metal centers in *trans*-**3** to *trans*-**6**, an additional P(SiMe₃)₂ could not be transferred to the metal-bis(trimethylsilyl)phosphido complexes. In contrast, the reaction of linear, monovalent, two coordinate gold(I) complex, [Au₂Cl₂(ⁿBu₄-benzo(imy)₂)] with Li[P(SiMe₃)₂] in a 1:2 ratio, yielded the first gold-di(bis(trimethylsilyl)phosphido complex, [Au₂(bis-NHC){P(SiMe₃)₂] (**7**).

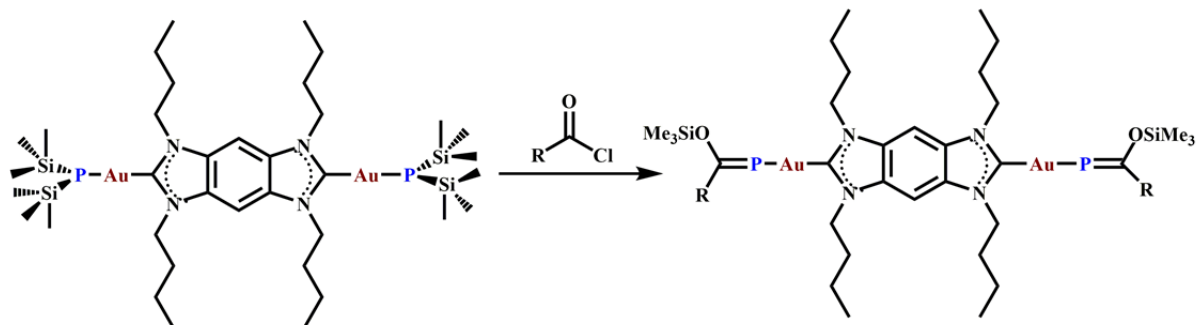
The cleavage of P-Si bond in palladium(II)- and nickel(II)-bis(trimethylsilyl)phosphine complexes (*trans*-**3** and *trans*-**4**) by means of benzoyl chloride, in a 1:2 ratio, resulted in the formation of the first square planar dibenzoylphosphido complexes $[\text{PdI}(\text{}^i\text{Pr}_2\text{-bimy})_2\text{P}\{\text{C}(\text{O})\text{Ph}\}_2]$ (*trans*-**8**) and $[\text{NiI}(\text{}^i\text{Pr}_2\text{-bimy})_2\text{P}\{\text{C}(\text{O})\text{Ph}\}_2]$ (*trans*-**9**). The progress of the reactions was monitored by NMR spectroscopy. The formation of *trans*-**9** was further confirmed by single-crystal X-ray analysis and mass spectrometry.

4.2. RECOMMENDATIONS FOR FUTURE WORK

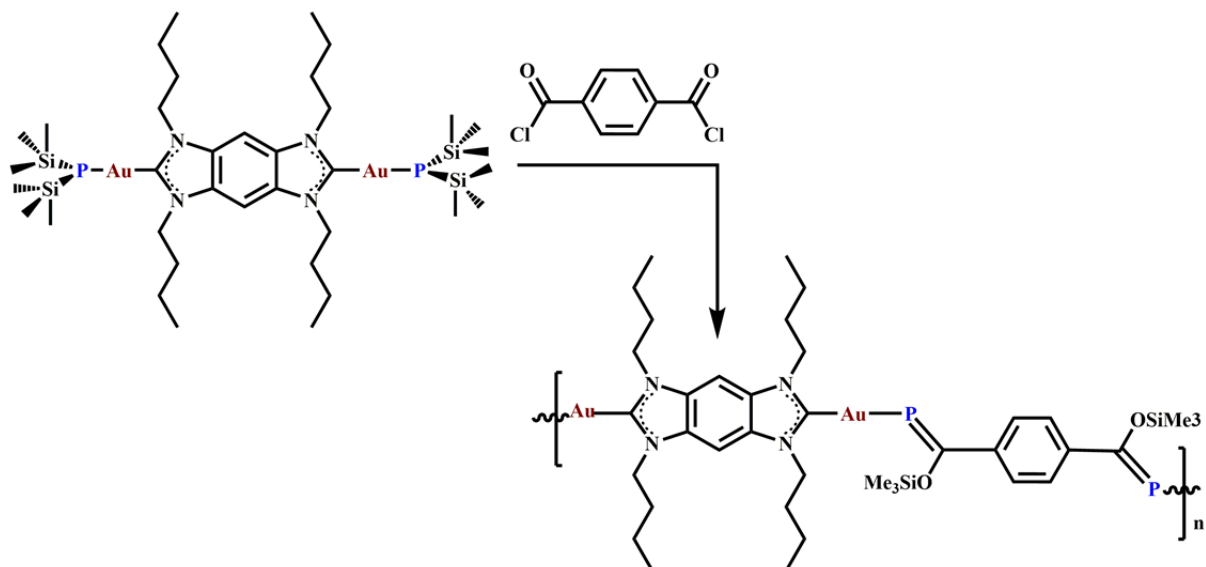
N-heterocyclic carbenes with smaller substituents on the N-heterocycles such as methyl and ethyl groups can decrease the steric bulk [15, 16] and increase free space in $[\text{MX}_2(\text{NHC})_2]$ complexes [63, 64]. Therefore, the reaction of these complexes with $\text{Li}[\text{P}(\text{SiMe}_3)_2]$, in a 1:2 ratio, is suggested as a route to provide *trans*-di(bis(trimethylsilyl)phosphido) complexes.



It is also recommended to investigate the reaction of $[\text{Au}_2(\text{}^t\text{Bu}_4\text{-benzo(imy)}_2)\{\text{P}(\text{SiMe}_3)_2\}_2]$ (**7**) with $\text{RC}(\text{O})\text{Cl}$ ($\text{R} = \text{Ph}, \text{}^t\text{Bu}, \text{Mes}$), in a 1:2 ratio, to yield phosphalkene complexes.



Furthermore, it is worth trying the polymerization reaction of $[\text{Au}_2(\text{}^n\text{Bu}_4\text{-benzo(imy)}_2)\{\text{P}(\text{SiMe}_3)_2\}_2]$ (7) with 1,4- $[\text{C}(\text{O})\text{Cl}]\text{-C}_6\text{H}_4$, in a 1:1 ratio.



REFERENCES

- [1] G. Fritz, P. Scheer, *Chem. Rev.*, 100 (2000) 3341-3402.
- [2] S.C. Goel, M.Y. Chiang, D.J. Rauscher, W.E. Buhro, *J. Am. Chem. Soc.*, 115 (1993) 160-169.
- [3] F. Lindenberg, E. Hey-Hawkins, *J. Organomet. Chem.*, 435 (1992) 291-297.
- [4] S.C. Goel, M.Y. Chiang, W.E. Buhro, *J. Am. Chem. Soc.*, 112 (1990) 5636-5637.
- [5] R. Waterman, *Dalton Trans.*, (2009) 18-26.
- [6] R.L. Wells, R.A. Baldwin, P.S. White, W.T. Pennington, A.L. Rheingold, G.P. Yap, *Organometallics*, 15 (1996) 91-97.
- [7] H. Schäfer, *Z. Anorg. Allg. Chem.*, 467 (1980) 105-122.
- [8] H. Schäfer, D. Binder, B. Deppisch, G. Mattern, *Z. Anorg. Allg. Chem.*, 546 (1987) 79-98.
- [9] G. Fritz, W. Hölderich, *Z. Anorg. Allg. Chem.*, 422 (1976) 104-114.
- [10] K.L. Antcliff, R.J. Baker, C. Jones, D.M. Murphy, R.P. Rose, *Inorg. Chem.*, 44 (2005) 2098-2105.
- [11] H. Schäfer, D. Binder, *Z. Anorg. Allg. Chem.*, 560 (1988) 65-79.
- [12] H. Schäfer, D. Binder, *Z. Anorg. Allg. Chem.*, 546 (1987) 55-78.
- [13] C.A. Tolman, *Chem. Rev.*, 77 (1977) 313-348.
- [14] H. Clavier, S.P. Nolan, *Chem. Comm.*, 46 (2010) 841-861.
- [15] A.C. Hillier, W.J. Sommer, B.S. Yong, J.L. Petersen, L. Cavallo, S.P. Nolan, *Organometallics*, 22 (2003) 4322-4326.
- [16] D.G. Gusev, *Organometallics*, 28 (2009) 6458-6461.
- [17] H.V. Huynh, Y. Han, J.H.H. Ho, G.K. Tan, *Organometallics*, 25 (2006) 3267-3274.
- [18] H.V. Huynh, T.C. Neo, G.K. Tan, *Organometallics*, 25 (2006) 1298-1302.
- [19] Y. Han, H.V. Huynh, L.L. Koh, *J. Organomet. Chem.*, 692 (2007) 3606-3613.
- [20] Y. Han, H.V. Huynh, G.K. Tan, *Organometallics*, 26 (2007) 4612-4617.

- [21] Y. Han, Y.-T. Hong, H.V. Huynh, *J. Organomet. Chem.*, 693 (2008) 3159-3165.
- [22] T. Weskamp, W.C. Schattenmann, M. Spiegler, W.A. Herrmann, *Angew. Chem. Int. Ed. Engl.*, 37 (1998) 2490-2493.
- [23] L. Jafarpour, S.P. Nolan, *J. Organomet. Chem.*, 617 (2001) 17-27.
- [24] M. Scholl, T.M. Trnka, J.P. Morgan, R.H. Grubbs, *Tetrahedron Lett.*, 40 (1999) 2247-2250.
- [25] H.V. Huynh, L.R. Wong, P.S. Ng, *Organometallics*, 27 (2008) 2231-2237.
- [26] J. Berding, J.A. van Paridon, V.H.S. van Rixel, E. Bouwman, *Eur. J. Inorg. Chem.*, 2011 (2011) 2450-2458.
- [27] S. Guo, H.V. Huynh, *Organometallics*, 31 (2012) 4565-4573.
- [28] M. Koch, J.A. Garg, O. Blacque, K. Venkatesan, *J. Organomet. Chem.*, 700 (2012) 154-159.
- [29] V.W.-W. Yam, C.-H. Tao, L. Zhang, K.M.-C. Wong, K.-K. Cheung, *Organometallics*, 20 (2001) 453-459.
- [30] C. Desmarets, S. Kuhl, R. Schneider, Y. Fort, *Organometallics*, 21 (2002) 1554-1559.
- [31] D.S. McGuinness, W. Mueller, P. Wasserscheid, K.J. Cavell, B.W. Skelton, A.H. White, U. Englert, *Organometallics*, 21 (2002) 175-181.
- [32] X. Wang, S. Liu, G.-X. Jin, *Organometallics*, 23 (2004) 6002-6007.
- [33] E.A.B. Kantchev, C.J. O'Brien, M.G. Organ, *Angew. Chem. Int. Ed. Engl.*, 46 (2007) 2768-2813.
- [34] T. Schaub, M. Backes, U. Radius, *Organometallics*, 25 (2006) 4196-4206.
- [35] D.M. Khramov, A.J. Boydston, C.W. Bielawski, *Angew. Chem.*, 118 (2006) 6332-6335.
- [36] F.E. Hahn, C. Radloff, T. Pape, A. Hepp, *Organometallics*, 27 (2008) 6408-6410.
- [37] A.J. Boydston, C.W. Bielawski, *Dalton Trans.*, (2006) 4073-4077.
- [38] A.J. Boydston, K.A. Williams, C.W. Bielawski, *J. Am. Chem. Soc.*, 127 (2005) 12496-12497.
- [39] L. Mercs, A. Neels, M. Albrecht, *Dalton Trans.*, (2008) 5570-5576.
- [40] G. Becker, *Z. Anorg. Allg. Chem.*, 423 (1976) 242-254.

- [41] G. Becker, H. Schmidt, G. Uhl, W. Uhl, M. Regitz, W. Rösch, U.-J. Vogelbacher, *John Wiley & Sons, Inc.*, (2007) 243-249.
- [42] G. Becker, H.P. Beck, *Z. Anorg. Allg. Chem.*, 430 (1977) 77-90.
- [43] G. Becker, K. Hübler, J. Weidlein, *Z. Anorg. Allg. Chem.*, 620 (1994) 16-28.
- [44] G. Becker, O. Mundt, *Z. Anorg. Allg. Chem.*, 443 (1978) 53-69.
- [45] R. Appel, F. Knoll, I. Ruppert, *Angew. Chem. Int. Ed. Engl.*, 20 (1981) 731-744.
- [46] L. Weber, K. Reizig, R. Boese, M. Polk, *Angew. Chem. Int. Ed. Engl.*, 24 (1985) 604-605.
- [47] L. Weber, K. Reizig, M. Frebel, R. Boese, M. Polk, *J. Organomet. Chem.*, 306 (1986) 105-114.
- [48] L. Weber, K. Reizig, R. Boese, *Angew. Chem. Int. Ed. Engl.*, 25 (1986) 755-757.
- [49] L. Weber, K. Reizig, *Angew. Chem.*, 97 (1985) 53-54.
- [50] L. Weber, K. Reizig, M. Frebel, *Chem. Ber.*, 119 (1986) 1857-1867.
- [51] V.A. Wright, B.O. Patrick, C. Schneider, D.P. Gates, *J. Am. Chem. Soc.*, 128 (2006) 8836-8844.
- [52] H.H. Karsch, F. Bienlein, T. Rupprich, F. Uhlig, E. Herrmann, M. Scheer, *Synthetic Methods of Organometallic and Inorganic Chemistry* (1996) 58-65.
- [53] W. Huang, J. Guo, Y. Xiao, M. Zhu, G. Zou, J. Tang, *Tetrahedron*, 61 (2005) 9783-9790.
- [54] C. Radloff, J.J. Weigand, F.E. Hahn, *Dalton Trans.*, 43 (2009) 9392-9394.
- [55] G.M. Sheldrick, *Acta Crystallogr. Sec. A*, 64 (2008) 112-122.
- [56] M. Brookhart, M.L.H. Green, *J. Organomet. Chem.*, 250 (1983) 395-408.
- [57] M. Bortolin, U.E. Bucher, H. Ruediger, L.M. Venanzi, A. Albinati, F. Lianza, S. Trofimenko, *Organometallics*, 11 (1992) 2514-2521.
- [58] W. Yao, O. Eisenstein, R.H. Crabtree, *Inorg. Chim. Acta*, 254 (1997) 105-111.
- [59] J.C. Lewis, J. Wu, R.G. Bergman, J.A. Ellman, *Organometallics*, 24 (2005) 5737-5746.
- [60] J. Goubeau, H. Schäfer, G. Rienäcker, *Z. Anorg. Allg. Chem.*, 459 (1979) 5-6.

- [61] L. Weber, K. Reizig, R. Boese, *Organometallics*, 4 (1985) 1890-1891.
- [62] B. Deppisch, H. Schäfer, *Acta Crystallogr. Sect. B*, 38 (1982) 748-752.
- [63] H.M. Wang, I.J. Lin, *Organometallics*, 17 (1998) 972-975.
- [64] H.V. Huynh, J.H.H. Ho, T.C. Neo, L.L. Koh, *J. Organomet. Chem.*, 690 (2005) 3854-3860.

APPENDICES

Appendix A: Crystal data and structure refinement for [PdI₂(ⁿBu₂-bimy)₂] (*trans*-1)

Formula	C ₃₀ H ₄₄ I ₂ N ₄ Pd
Formula Weight (<i>g/mol</i>)	820.89
Crystal Dimensions (<i>mm</i>)	0.293 × 0.156 × 0.045
Crystal Color and Habit	yellow Plate
Crystal System	monoclinic
Space Group	P 2 ₁
Flack (<i>x</i>)	0.335(10)
Temperature, K	113(2)
<i>a</i> , Å	10.790(3)
<i>b</i> , Å	20.017(6)
<i>c</i> , Å	15.036(4)
α, °	90
β, °	96.577(6)
γ, °	90
<i>V</i> , Å ³	3226.1(16)
Number of reflections to determine final unit cell	9685
Min and Max 2θ for cell determination, °	5.82, 74.98
<i>Z</i>	4
F(000)	1616
ρ (<i>g/cm</i>)	1.690
λ, Å, (MoKα)	0.71073
μ, (<i>cm</i> ⁻¹)	2.513
Diffractometer Type	Bruker APEX-II CCD
Scan Type(s)	ω and φ scans
Max 2θ for data collection, °	75.74
Measured fraction of data	0.997
Number of reflections measured	113233
Unique reflections measured	34320
R _{merge}	0.0353
Number of reflections included in refinement	34320
Cut off Threshold Expression	I > 2sigma(I)
Structure refined using	full matrix least-squares using F ²

Weighting Scheme	$w=1/[\sigma^2(F_o^2)+(0.0203P)^2]$ where $P=(F_o^2+2F_c^2)/3$
Number of parameters in least-squares	676
R ₁	0.0314
wR ₂	0.0501
R ₁ (all data)	0.0427
wR ₂ (all data)	0.0532
GOF	1.014
Maximum shift/error	0.002
Min & Max peak heights on final ΔF Map (e ⁻ /Å)	-1.018, 1.684

Where:

$$R_1 = \sum (|F_o| - |F_c|) / \sum F_o$$

$$wR_2 = [\sum w (F_o^2 - F_c^2)^2 / \sum w F_o^4]^{1/2}$$

$$GOF = [\sum w (F_o^2 - F_c^2)^2 / (\text{No. of reflns.} - \text{No. of params.})]^{1/2}$$

Appendix B: Atomic coordinates for [PdI₂(ⁿBu₂-bimy)₂] (*trans*-1)

Atom	x	y	z	U _{iso} /equiv
Pd1	0.37685(2)	0.20973(2)	0.62773(2)	0.01052(3)
I1	0.42279(2)	0.11260(2)	0.52055(2)	0.01548(4)
I2	0.32881(2)	0.30642(2)	0.73464(2)	0.01565(4)
N1	0.6392(2)	0.21575(12)	0.72694(16)	0.0121(4)
N2	0.6279(2)	0.27024(12)	0.60187(15)	0.0127(4)
N3	0.1151(2)	0.20673(12)	0.52938(16)	0.0127(4)
N4	0.1245(2)	0.15207(12)	0.65461(16)	0.0124(4)
C1	0.5604(3)	0.23191(15)	0.6529(2)	0.0123(5)
C2	0.7557(3)	0.24481(14)	0.72375(19)	0.0127(5)
C3	0.8652(3)	0.24272(15)	0.7822(2)	0.0163(6)
C4	0.9665(3)	0.27840(17)	0.7569(2)	0.0183(6)
C5	0.9574(3)	0.31517(16)	0.6779(2)	0.0182(6)
C6	0.8483(3)	0.31681(15)	0.6196(2)	0.0166(6)
C7	0.7483(2)	0.28044(14)	0.64395(18)	0.0121(5)
C8	0.6042(3)	0.17388(14)	0.79974(19)	0.0140(5)
C9	0.6283(3)	0.09988(15)	0.7871(2)	0.0162(6)
C10	0.5877(3)	0.06041(16)	0.8658(2)	0.0203(6)
C11	0.6134(4)	-0.01374(18)	0.8596(3)	0.0355(9)
C12	0.5799(3)	0.30079(15)	0.51622(18)	0.0149(5)
C13	0.5415(3)	0.37261(15)	0.5278(2)	0.0193(6)
C14	0.5094(3)	0.40884(18)	0.4391(2)	0.0226(7)
C15	0.6215(4)	0.4231(2)	0.3903(3)	0.0279(8)
C16	0.1928(3)	0.18884(14)	0.6030(2)	0.0113(5)
C17	-0.0031(3)	0.17999(14)	0.53339(19)	0.0125(5)
C18	-0.1129(3)	0.18353(15)	0.4753(2)	0.0161(5)
C19	-0.2142(3)	0.14994(16)	0.5004(2)	0.0187(6)
C20	-0.2088(3)	0.11279(15)	0.5792(2)	0.0178(6)
C21	-0.0994(3)	0.10944(15)	0.6380(2)	0.0161(5)
C22	0.0032(3)	0.14461(14)	0.61276(19)	0.0126(5)
C23	0.1509(3)	0.24662(14)	0.45448(19)	0.0135(5)
C24	0.1235(3)	0.32072(14)	0.4615(2)	0.0155(5)
C25	0.1574(3)	0.35606(15)	0.3778(2)	0.0167(5)
C26	0.1368(4)	0.43157(18)	0.3796(3)	0.0356(9)
C27	0.1713(3)	0.11919(14)	0.73861(17)	0.0142(5)
C28	0.2115(3)	0.04753(15)	0.7224(2)	0.0194(6)

C29	0.2360(3)	0.00673(18)	0.8090(2)	0.0229(7)
C30	0.1178(3)	-0.0131(2)	0.8472(3)	0.0290(8)
Pd2	-0.13183(2)	0.20519(2)	0.12303(2)	0.01103(4)
I3	-0.08405(2)	0.12729(2)	-0.00831(2)	0.01577(4)
I4	-0.17763(2)	0.28316(2)	0.25419(2)	0.01691(4)
N5	0.1355(2)	0.17405(12)	0.20333(16)	0.0124(4)
N6	0.1186(2)	0.27425(12)	0.14746(16)	0.0127(4)
N7	-0.3797(2)	0.13462(12)	0.09909(16)	0.0130(4)
N8	-0.4019(2)	0.23508(12)	0.04535(16)	0.0121(4)
C31	0.0534(3)	0.21741(14)	0.1590(2)	0.0124(5)
C32	0.2524(2)	0.20390(15)	0.22164(18)	0.0125(5)
C33	0.3638(3)	0.18074(16)	0.26759(19)	0.0170(6)
C34	0.4637(3)	0.22461(17)	0.2741(2)	0.0202(6)
C35	0.4544(3)	0.28848(17)	0.2368(2)	0.0201(6)
C36	0.3422(3)	0.31147(16)	0.19187(19)	0.0161(5)
C37	0.2419(3)	0.26760(14)	0.18560(19)	0.0124(5)
C38	0.1091(3)	0.10460(14)	0.22490(19)	0.0151(5)
C39	0.0912(3)	0.09372(15)	0.3229(2)	0.0155(5)
C40	0.0830(3)	0.01984(16)	0.3459(2)	0.0217(6)
C41	0.0570(4)	0.00876(18)	0.4423(2)	0.0294(8)
C42	0.0674(3)	0.33497(14)	0.10469(19)	0.0147(5)
C43	0.1087(3)	0.34710(16)	0.0129(2)	0.0190(6)
C44	0.0566(3)	0.41273(18)	-0.0273(2)	0.0242(7)
C45	0.1078(4)	0.4312(2)	-0.1137(2)	0.0297(8)
C46	-0.3174(3)	0.19200(15)	0.0882(2)	0.0128(5)
C47	-0.5043(3)	0.14015(15)	0.06359(19)	0.0142(5)
C48	-0.6026(3)	0.09502(16)	0.0584(2)	0.0175(6)
C49	-0.7162(3)	0.11702(18)	0.0159(2)	0.0198(6)
C50	-0.7292(3)	0.18114(18)	-0.0211(2)	0.0206(6)
C51	-0.6314(3)	0.22605(16)	-0.01635(19)	0.0164(5)
C52	-0.5180(3)	0.20424(15)	0.02792(19)	0.0135(5)
C53	-0.3262(3)	0.07450(14)	0.1438(2)	0.0162(5)
C54	-0.3543(3)	0.06851(15)	0.2401(2)	0.0190(6)
C55	-0.3047(3)	0.00347(17)	0.2818(2)	0.0242(7)
C56	-0.3334(4)	-0.00624(19)	0.3766(2)	0.0321(9)
C57	-0.3802(3)	0.30596(15)	0.02752(18)	0.0148(5)
C58	-0.3557(3)	0.32087(15)	-0.0677(2)	0.0171(6)
C59	-0.3506(3)	0.39590(16)	-0.0852(2)	0.0241(7)

C60	-0.3198(4)	0.41197(19)	-0.1798(2)	0.0342(9)
H3	0.8708	0.2182	0.8367	0.020
H4	1.0435	0.2776	0.7945	0.022
H5	1.0278	0.3397	0.6635	0.022
H6	0.8423	0.3417	0.5655	0.020
H8A	0.5144	0.1805	0.8050	0.017
H8B	0.6516	0.1887	0.8566	0.017
H9A	0.7182	0.0924	0.7832	0.019
H9B	0.5812	0.0843	0.7306	0.019
H10A	0.6323	0.0780	0.9222	0.024
H10B	0.4973	0.0673	0.8680	0.024
H11A	0.5696	-0.0315	0.8039	0.053
H11B	0.5840	-0.0367	0.9108	0.053
H11C	0.7033	-0.0210	0.8601	0.053
H12A	0.5071	0.2749	0.4889	0.018
H12B	0.6451	0.2990	0.4750	0.018
H13A	0.6103	0.3966	0.5636	0.023
H13B	0.4680	0.3737	0.5617	0.023
H14A	0.4493	0.3814	0.4000	0.027
H14B	0.4679	0.4516	0.4504	0.027
H15A	0.6828	0.4491	0.4291	0.042
H15B	0.5952	0.4486	0.3358	0.042
H15C	0.6592	0.3809	0.3743	0.042
H18	-0.1175	0.2080	0.4209	0.019
H19	-0.2910	0.1521	0.4627	0.022
H20	-0.2808	0.0894	0.5930	0.021
H21	-0.0946	0.0847	0.6921	0.019
H23A	0.1059	0.2293	0.3981	0.016
H23B	0.2413	0.2407	0.4511	0.016
H24A	0.1728	0.3396	0.5153	0.019
H24B	0.0339	0.3275	0.4674	0.019
H25A	0.1066	0.3371	0.3248	0.020
H25B	0.2462	0.3472	0.3713	0.020
H26A	0.0483	0.4409	0.3832	0.053
H26B	0.1618	0.4515	0.3249	0.053
H26C	0.1869	0.4508	0.4318	0.053
H27A	0.1052	0.1190	0.7792	0.017
H27B	0.2433	0.1446	0.7682	0.017

H28A	0.2884	0.0484	0.6923	0.023
H28B	0.1456	0.0252	0.6818	0.023
H29A	0.2828	-0.0342	0.7968	0.027
H29B	0.2888	0.0333	0.8541	0.027
H30A	0.0742	0.0272	0.8639	0.044
H30B	0.1388	-0.0410	0.9003	0.044
H30C	0.0637	-0.0382	0.8022	0.044
H33	0.3708	0.1373	0.2930	0.020
H34	0.5411	0.2107	0.3050	0.024
H35	0.5256	0.3168	0.2421	0.024
H36	0.3348	0.3550	0.1668	0.019
H38A	0.1788	0.0762	0.2098	0.018
H38B	0.0327	0.0900	0.1871	0.018
H39A	0.0138	0.1164	0.3359	0.019
H39B	0.1620	0.1141	0.3612	0.019
H40A	0.0158	-0.0011	0.3050	0.026
H40B	0.1625	-0.0023	0.3365	0.026
H41A	0.1248	0.0281	0.4832	0.044
H41B	0.0515	-0.0393	0.4539	0.044
H41C	-0.0219	0.0303	0.4519	0.044
H42A	0.0931	0.3735	0.1437	0.018
H42B	-0.0248	0.3324	0.0988	0.018
H43A	0.0797	0.3098	-0.0274	0.023
H43B	0.2010	0.3483	0.0179	0.023
H44A	-0.0353	0.4092	-0.0388	0.029
H44B	0.0765	0.4490	0.0168	0.029
H45A	0.1986	0.4357	-0.1026	0.045
H45B	0.0711	0.4736	-0.1360	0.045
H45C	0.0866	0.3961	-0.1583	0.045
H48	-0.5926	0.0513	0.0828	0.021
H49	-0.7863	0.0881	0.0119	0.024
H50	-0.8081	0.1943	-0.0505	0.025
H51	-0.6409	0.2694	-0.0419	0.020
H53A	-0.2347	0.0750	0.1427	0.019
H53B	-0.3596	0.0347	0.1101	0.019
H54A	-0.3157	0.1065	0.2753	0.023
H54B	-0.4456	0.0707	0.2420	0.023
H55A	-0.3411	-0.0341	0.2448	0.029

H55B	-0.2132	0.0021	0.2809	0.029
H56A	-0.2962	0.0302	0.4141	0.048
H56B	-0.2986	-0.0490	0.3995	0.048
H56C	-0.4240	-0.0063	0.3780	0.048
H57A	-0.3079	0.3215	0.0688	0.018
H57B	-0.4541	0.3319	0.0409	0.018
H58A	-0.4225	0.3006	-0.1098	0.020
H58B	-0.2755	0.3003	-0.0789	0.020
H59A	-0.2866	0.4164	-0.0411	0.029
H59B	-0.4322	0.4160	-0.0766	0.029
H60A	-0.2387	0.3926	-0.1885	0.051
H60B	-0.3167	0.4605	-0.1876	0.051
H60C	-0.3844	0.3931	-0.2238	0.051

Appendix C: Crystal data and structure refinement for [NiBr₂(ⁿBu₂-bimy)₂] (*trans-2*)

Formula	C ₃₀ H ₄₄ Br ₂ N ₄ Ni
Formula Weight (<i>g/mol</i>)	679.22
Crystal Dimensions (<i>mm</i>)	0.123 × 0.062 × 0.026
Crystal Color and Habit	orange plate
Crystal System	monoclinic
Space Group	P 2 ₁ /c
Temperature, K	110(2)
<i>a</i> , Å	13.854(9)
<i>b</i> , Å	8.690(7)
<i>c</i> , Å	14.383(8)
α, °	90
β, °	117.652(17)
γ, °	90
<i>V</i> , Å ³	1533.9(18)
Number of reflections to determine final unit cell	2800
Min and Max 2θ for cell determination, °	5.68, 50.74
<i>Z</i>	2
F(000)	700
ρ (<i>g/cm</i>)	1.471
λ, Å, (MoKα)	0.71073
μ, (<i>cm</i> ⁻¹)	3.262
Diffractometer Type	Bruker APEX-II CCD
Scan Type(s)	ω and φ scans
Max 2θ for data collection, °	61.342
Measured fraction of data	0.998
Number of reflections measured	26784
Unique reflections measured	4691
R _{merge}	0.0901
Number of reflections included in refinement	4691
Cut off Threshold Expression	I > 2σ(I)
Structure refined using	full matrix least-squares using F ²
Weighting Scheme	w=1/[σ(F ²)+(0.0327P) ²] where P=(F ² +2Fc ²)/3
Number of parameters in least-squares	171
R ₁	0.0436

wR ₂	0.0795
R ₁ (all data)	0.0937
wR ₂ (all data)	0.0952
GOF	0.995
Maximum shift/error	0.000
Min & Max peak heights on final ΔF Map (e ⁻ /Å)	-0.911, 0.754

Where:

$$R_1 = \sum (|F_o| - |F_c|) / \sum F_o$$

$$wR_2 = [\sum w (F_o^2 - F_c^2)^2 / \sum w F_o^4]^{1/2}$$

$$GOF = [\sum w (F_o^2 - F_c^2)^2 / (\text{No. of reflns.} - \text{No. of params.})]^{1/2}$$

Appendix D: Atomic coordinates for [NiBr₂(ⁿBu₂-bimy)₂] (*trans-2*)

Atom	x	y	z	U _{iso} /equiv
Ni1	0.0000	0.5000	0.0000	0.01471(13)
Br1	0.01355(3)	0.76561(3)	0.00780(2)	0.02197(10)
C1	-0.0959(2)	0.5118(3)	0.0609(2)	0.0162(6)
N1	-0.0742(2)	0.4831(3)	0.16168(17)	0.0161(5)
C2	-0.1661(2)	0.5117(3)	0.1750(2)	0.0175(6)
C3	-0.1842(3)	0.5021(3)	0.2625(2)	0.0222(7)
C4	-0.2878(3)	0.5372(4)	0.2473(2)	0.0245(7)
C5	-0.3706(3)	0.5797(4)	0.1490(2)	0.0254(7)
C6	-0.3533(3)	0.5902(4)	0.0618(2)	0.0214(7)
C7	-0.2488(2)	0.5559(3)	0.0776(2)	0.0163(6)
N2	-0.20173(19)	0.5565(3)	0.01000(17)	0.0160(5)
C8	0.0301(2)	0.4300(4)	0.2452(2)	0.0169(6)
C9	0.1038(2)	0.5606(4)	0.3110(2)	0.0181(6)
C10	0.2018(2)	0.5000(4)	0.4082(2)	0.0213(7)
C11	-0.2766(3)	0.1307(4)	0.0268(3)	0.0315(8)
C12	-0.2625(2)	0.5922(4)	-0.1024(2)	0.0202(7)
C13	-0.3280(2)	0.4553(4)	-0.1665(2)	0.0209(7)
C14	-0.4025(3)	0.4989(4)	-0.2806(2)	0.0276(8)
C15	-0.4684(3)	0.3619(4)	-0.3449(2)	0.0328(8)
H3	-0.1279	0.4729	0.3295	0.027
H4	-0.3030	0.5322	0.3051	0.029
H5	-0.4409	0.6022	0.1417	0.030
H6	-0.4097	0.6193	-0.0051	0.026
H8A	0.0685	0.3708	0.2135	0.020
H8B	0.0163	0.3595	0.2918	0.020
H9A	0.1292	0.6203	0.2679	0.022
H9B	0.0615	0.6309	0.3326	0.022
H10A	0.2434	0.4285	0.3866	0.026
H10B	0.1764	0.4419	0.4518	0.026
H11A	-0.2362	0.2002	0.0037	0.047
H11B	-0.3024	0.1879	0.0697	0.047
H11C	-0.3391	0.0878	-0.0347	0.047
H12A	-0.2106	0.6246	-0.1282	0.024
H12B	-0.3125	0.6792	-0.1126	0.024
H13A	-0.3726	0.4140	-0.1349	0.025

H13B	-0.2774	0.3732	-0.1642	0.025
H14A	-0.4529	0.5812	-0.2829	0.033
H14B	-0.3578	0.5399	-0.3123	0.033
H15A	-0.4187	0.2799	-0.3425	0.049
H15B	-0.5136	0.3938	-0.4178	0.049
H15C	-0.5152	0.3238	-0.3156	0.049

Appendix E: Crystal data and structure refinement for $[\text{PdI}(\text{Pr}_2\text{-bimy})_2\{\text{P}(\text{SiMe}_3)_2\}]\cdot\text{C}_5\text{H}_{12}$ (*trans-3*)

Formula	$\text{C}_{37}\text{H}_{66}\text{IN}_4\text{PPdSi}_2$
Formula Weight (<i>g/mol</i>)	887.38
Crystal Dimensions (<i>mm</i>)	$0.184 \times 0.150 \times 0.089$
Crystal Color and Habit	yellow needle
Crystal System	monoclinic
Space Group	$\text{P } 2_1/c$
Temperature, K	110(2)
<i>a</i> , Å	21.223(4)
<i>b</i> , Å	10.532(2)
<i>c</i> , Å	21.304(5)
α , °	90
β , °	116.819(7)
γ , °	90
<i>V</i> , Å ³	4249.9(16)
Number of reflections to determine final unit cell	4477
Min and Max 2θ for cell determination, °	5.44, 48.84
<i>Z</i>	4
F(000)	1832
ρ (<i>g/cm</i>)	1.387
λ , Å, (MoK α)	0.71073
μ , (<i>cm</i> ⁻¹)	1.286
Diffractometer Type	Bruker APEX-II CCD
Scan Type(s)	ω and φ scans
Max 2θ for data collection, °	61.158
Measured fraction of data	0.998
Number of reflections measured	20403
Unique reflections measured	15254
Number of reflections included in refinement	20403
Cut off Threshold Expression	$I > 2\sigma(I)$
Structure refined using	full matrix least-squares using F^2
Weighting Scheme	$w=1/[\sigma^2(\text{Fo}^2)+(0.0397\text{P})^2+3.123\text{P}]$ where $\text{P}=(\text{Fo}^2+2\text{Fc}^2)/3$
Number of parameters in least-squares	432
R_1	0.0493
wR_2	0.0913

R ₁ (all data)	0.0793
wR ₂ (all data)	0.1012
GOF	1.017
Maximum shift/error	0.001
Min & Max peak heights on final ΔF Map (e ⁻ /Å)	-0.981, 0.943

Where:

$$R_1 = \sum (|F_o| - |F_c|) / \sum F_o$$

$$wR_2 = [\sum w (F_o^2 - F_c^2)^2 / \sum w F_o^4]^{1/2}$$

$$GOF = [\sum w (F_o^2 - F_c^2)^2 / (\text{No. of reflns.} - \text{No. of params.})]^{1/2}$$

Appendix F: Atomic coordinates for [PdI(ⁱPr₂-bimy)₂{P(SiMe₃)₂}].C₅H₁₂ (*trans*-3)

Atom	x	y	z	U _{iso} /equiv
Pd1	0.20794(2)	0.74344(3)	0.41654(2)	0.01280(6)
I1	0.13866(2)	0.77045(3)	0.27545(2)	0.02232(7)
P1	0.26790(5)	0.66903(9)	0.53244(5)	0.0157(2)
Si1	0.22509(6)	0.74572(11)	0.60432(6)	0.0183(2)
Si2	0.38336(6)	0.71360(10)	0.59976(6)	0.0179(2)
N1	0.33212(17)	0.8591(3)	0.40290(18)	0.0152(7)
N2	0.32971(17)	0.6537(3)	0.39050(17)	0.0141(7)
N3	0.06613(16)	0.6353(3)	0.39396(17)	0.0142(7)
N4	0.06660(17)	0.8412(3)	0.40138(17)	0.0148(7)
C1	0.29856(19)	0.7522(3)	0.40680(19)	0.0136(7)
C2	0.3844(2)	0.8300(4)	0.3831(2)	0.0152(8)
C3	0.4323(2)	0.9045(4)	0.3713(2)	0.0197(9)
C4	0.4785(2)	0.8424(4)	0.3517(2)	0.0221(10)
C5	0.4772(2)	0.7121(4)	0.3440(2)	0.0242(10)
C6	0.4298(2)	0.6370(4)	0.3555(2)	0.0206(9)
C7	0.3831(2)	0.6981(4)	0.3751(2)	0.0153(8)
C8	0.3129(2)	0.9869(4)	0.4172(2)	0.0196(9)
C9	0.3764(2)	1.0527(4)	0.4758(2)	0.0243(10)
C10	0.2783(2)	1.0649(4)	0.3499(2)	0.0297(11)
C11	0.3053(2)	0.5217(4)	0.3851(2)	0.0184(9)
C12	0.3633(2)	0.4345(4)	0.4359(2)	0.0285(11)
C13	0.2739(2)	0.4763(4)	0.3090(2)	0.0300(11)
C14	0.10888(19)	0.7389(4)	0.4104(2)	0.0142(7)
C15	-0.0041(2)	0.6717(4)	0.3715(2)	0.0165(9)
C16	-0.0667(2)	0.6027(4)	0.3471(2)	0.0224(10)
C17	-0.1284(2)	0.6708(4)	0.3292(2)	0.0275(11)
C18	-0.1278(2)	0.8023(4)	0.3347(2)	0.0252(10)
C19	-0.0661(2)	0.8722(4)	0.3580(2)	0.0213(9)
C20	-0.0034(2)	0.8039(4)	0.3767(2)	0.0168(9)
C21	0.0918(2)	0.5033(3)	0.3997(2)	0.0177(9)
C22	0.0663(2)	0.4210(4)	0.4428(2)	0.0285(11)
C23	0.0728(2)	0.4462(4)	0.3273(2)	0.0273(11)
C24	0.0933(2)	0.9726(3)	0.4169(2)	0.0169(8)
C25	0.0734(2)	1.0344(4)	0.4700(2)	0.0226(10)
C26	0.0697(2)	1.0524(4)	0.3501(2)	0.0267(11)

C27	0.2762(2)	0.6772(4)	0.6950(2)	0.0249(10)
C28	0.2276(2)	0.9232(4)	0.6145(2)	0.0264(10)
C29	0.1319(2)	0.6929(4)	0.5764(2)	0.0273(10)
C30	0.4040(2)	0.8661(4)	0.6514(2)	0.0243(10)
C31	0.4182(2)	0.5768(4)	0.6633(2)	0.0244(10)
C32	0.4424(2)	0.7152(4)	0.5557(2)	0.0254(10)
C1S	0.6075(2)	0.7641(5)	0.2461(3)	0.0488(15)
C2S	0.6782(2)	0.7264(4)	0.3045(3)	0.0364(12)
C3S	0.6858(2)	0.7513(4)	0.3776(2)	0.0313(10)
C4S	0.7571(2)	0.7152(4)	0.4365(2)	0.0300(11)
C5S	0.7634(3)	0.7476(4)	0.5080(3)	0.0377(11)
H3A	0.4333	0.9941	0.3765	0.024
H4A	0.5118	0.8908	0.3435	0.027
H5A	0.5096	0.6731	0.3305	0.029
H6A	0.4292	0.5473	0.3502	0.025
H8A	0.2768	0.9751	0.4348	0.023
H9A	0.3982	0.9957	0.5163	0.036
H9B	0.3608	1.1305	0.4899	0.036
H9C	0.4109	1.0742	0.4587	0.036
H10A	0.2381	1.0179	0.3146	0.045
H10B	0.3128	1.0812	0.3320	0.045
H10C	0.2618	1.1459	0.3598	0.045
H11A	0.2663	0.5210	0.3992	0.022
H12A	0.3735	0.4558	0.4843	0.043
H12B	0.4061	0.4458	0.4298	0.043
H12C	0.3476	0.3461	0.4261	0.043
H13A	0.2363	0.5346	0.2790	0.045
H13B	0.2543	0.3909	0.3056	0.045
H13C	0.3109	0.4744	0.2935	0.045
H16A	-0.0671	0.5129	0.3428	0.027
H17A	-0.1720	0.6267	0.3130	0.033
H18A	-0.1711	0.8457	0.3220	0.030
H19A	-0.0662	0.9622	0.3611	0.026
H21A	0.1445	0.5063	0.4258	0.021
H22A	0.0724	0.4673	0.4851	0.043
H22B	0.0939	0.3423	0.4565	0.043
H22C	0.0163	0.4005	0.4145	0.043
H23A	0.0889	0.5031	0.3011	0.041

H23B	0.0215	0.4356	0.3013	0.041
H23C	0.0958	0.3634	0.3331	0.041
H24A	0.1460	0.9680	0.4391	0.020
H25A	0.0806	0.9737	0.5075	0.034
H25B	0.0236	1.0599	0.4464	0.034
H25C	0.1030	1.1094	0.4902	0.034
H26A	0.0848	1.0111	0.3179	0.040
H26B	0.0910	1.1370	0.3624	0.040
H26C	0.0181	1.0602	0.3272	0.040
H27A	0.2543	0.7036	0.7248	0.037
H27B	0.3250	0.7079	0.7154	0.037
H27C	0.2759	0.5843	0.6921	0.037
H28A	0.1940	0.9492	0.6319	0.040
H28B	0.2149	0.9633	0.5688	0.040
H28C	0.2753	0.9497	0.6480	0.040
H29A	0.1163	0.7221	0.6108	0.041
H29B	0.1295	0.6001	0.5736	0.041
H29C	0.1011	0.7290	0.5302	0.041
H30A	0.4551	0.8808	0.6737	0.037
H30B	0.3877	0.8601	0.6876	0.037
H30C	0.3799	0.9368	0.6196	0.037
H31A	0.4686	0.5893	0.6941	0.037
H31B	0.4113	0.4974	0.6370	0.037
H31C	0.3927	0.5725	0.6918	0.037
H32A	0.4916	0.7249	0.5913	0.038
H32B	0.4294	0.7863	0.5226	0.038
H32C	0.4371	0.6352	0.5303	0.038
H1S1	0.5700	0.7179	0.2511	0.073
H1S2	0.6061	0.7434	0.2006	0.073
H1S3	0.6006	0.8556	0.2485	0.073
H2S1	0.7157	0.7734	0.2988	0.044
H2S2	0.6858	0.6347	0.3000	0.044
H3S1	0.6487	0.7033	0.3834	0.038
H3S2	0.6775	0.8428	0.3817	0.038
H4S1	0.7645	0.6228	0.4343	0.036
H4S2	0.7946	0.7601	0.4298	0.036
H5S1	0.7577	0.8394	0.5110	0.057
H5S2	0.8100	0.7216	0.5443	0.057

H5S3	0.7266	0.7029	0.5151	0.057
------	--------	--------	--------	-------

Appendix G: Crystal data and structure refinement for [PdI(ⁿBu₂-bimy)₂{P(SiMe₃)₂}]. [Li(THF)₃I] (*trans-5*)

Formula	C ₄₈ H ₈₆ I ₂ LiN ₄ O ₃ PPdSi ₂
Formula Weight (g/mol)	1221.50
Crystal Dimensions (mm)	0.22 × 0.19 × 0.04
Crystal Color and Habit	orange plate
Crystal System	Monoclinic
Space Group	P2(1)/c
Temperature, K	110(2)
<i>a</i> , Å	23.826(9)
<i>b</i> , Å	10.960(4)
<i>c</i> , Å	21.942(9)
α , °	90.00
β , °	99.762(11)
γ , °	90.00
<i>V</i> , Å ³	5647(4)
Number of reflections to determine final unit cell	9780
Min and Max 2 θ for cell determination, °	5.3, 56.2
<i>Z</i>	4
F(000)	2496
ρ (g/cm ³)	1.437
λ , Å, (MoK α)	0.71073
μ , (cm ⁻¹)	1.532
Diffractometer Type	Bruker APEX-II CCD
Scan Type(s)	ω and ϕ scans
Max 2 θ for data collection, °	49.0
Measured fraction of data	0.970
Number of reflections measured	55222
Unique reflections measured	9108
Rmerge	0.0590
Number of reflections included in refinement	9108
Cut off Threshold Expression	>2sigma(I)
Structure refined using	full matrix least-squares using F ²
Weighting Scheme	w=1/[sigma ² (Fo ²)+(0.0865P) ² +0.0000P] where P=(Fo ² +2Fc ²)/3

Number of parameters in least-squares	559
R ₁	0.0367
wR ₂	0.0975
R ₁ (all data)	0.0668
wR ₂ (all data)	0.1407
GOF	1.056
Maximum shift/error	0.001
Min & Max peak heights on final ΔF Map (e ⁻ /Å)	-1.341, 0.847

Where:

$$R_1 = \sum (|F_o| - |F_c|) / \sum F_o$$

$$wR_2 = [\sum w (F_o^2 - F_c^2)^2 / \sum w F_o^4]^{1/2}$$

$$GOF = [\sum w (F_o^2 - F_c^2)^2 / (\text{No. of reflns.} - \text{No. of params.})]^{1/2}$$

Appendix H: Atomic coordinates for [PdI(ⁿBu₂-bimy)₂{P(SiMe₃)₂}]. [Li (THF)₃I] (*trans*-5)

Atom	x	y	z	Uiso/equiv
Pd1	0.321725(18)	0.17931(4)	0.643598(19)	0.01438(14)
I1	0.266852(17)	-0.03544(4)	0.646506(19)	0.02439(14)
N1	0.20869(19)	0.3047(4)	0.6007(2)	0.0144(11)
N2	0.22357(19)	0.2821(4)	0.7006(2)	0.0171(11)
N3	0.4403(2)	0.0681(4)	0.6832(2)	0.0158(11)
N4	0.4057(2)	0.0172(4)	0.5887(2)	0.0168(11)
P1	0.37431(7)	0.36325(14)	0.65067(7)	0.0165(4)
Si1	0.32897(7)	0.54319(15)	0.65079(8)	0.0194(4)
Si2	0.41198(7)	0.38120(15)	0.56413(8)	0.0200(4)
C1	0.2475(2)	0.2643(5)	0.6493(3)	0.0177(13)
C2	0.1603(3)	0.3495(5)	0.6208(3)	0.0187(14)
C3	0.1101(2)	0.3999(6)	0.5890(3)	0.0244(15)
C4	0.0702(3)	0.4329(6)	0.6244(3)	0.0247(15)
C5	0.0791(3)	0.4179(6)	0.6882(3)	0.0245(15)
C6	0.1294(3)	0.3673(5)	0.7198(3)	0.0232(15)
C7	0.1693(2)	0.3339(5)	0.6853(3)	0.0197(14)
C8	0.3945(2)	0.0837(5)	0.6374(3)	0.0166(13)
C9	0.4806(2)	-0.0063(5)	0.6634(3)	0.0167(13)
C10	0.5336(3)	-0.0469(5)	0.6927(3)	0.0225(15)
C11	0.5643(3)	-0.1163(6)	0.6571(3)	0.0251(15)
C12	0.5425(3)	-0.1461(6)	0.5961(3)	0.0262(16)
C13	0.4897(3)	-0.1072(6)	0.5674(3)	0.0247(15)
C14	0.4591(2)	-0.0377(5)	0.6026(3)	0.0167(14)
C15	0.2134(3)	0.2879(6)	0.5355(3)	0.0212(14)
C16	0.1792(3)	0.1768(6)	0.5080(3)	0.0212(14)
C17	0.1911(3)	0.1471(6)	0.4433(3)	0.0300(16)
C18	0.1547(3)	0.0401(7)	0.4146(3)	0.044(2)
C19	0.2512(2)	0.2507(6)	0.7636(2)	0.0197(14)
C20	0.2248(3)	0.1400(6)	0.7901(3)	0.0238(15)
C21	0.2591(3)	0.1046(6)	0.8530(3)	0.0268(16)
C22	0.2346(3)	-0.0044(7)	0.8821(3)	0.0360(18)
C23	0.4457(3)	0.1212(5)	0.7459(3)	0.0205(14)
C24	0.4098(3)	0.0515(6)	0.7860(3)	0.0241(15)
C25	0.4250(3)	-0.0824(6)	0.7951(3)	0.0307(16)
C26	0.3855(3)	-0.1499(7)	0.8319(4)	0.047(2)

C27	0.3679(3)	0.0060(6)	0.5289(2)	0.0204(14)
C28	0.3483(3)	-0.1245(6)	0.5133(3)	0.0260(16)
C29	0.2976(3)	-0.1316(7)	0.4604(3)	0.0378(18)
C30	0.3085(3)	-0.0742(8)	0.4018(3)	0.049(2)
C31	0.2829(3)	0.5910(6)	0.5769(3)	0.0292(16)
C32	0.2847(3)	0.5502(6)	0.7137(3)	0.0335(17)
C33	0.3842(3)	0.6634(5)	0.6738(3)	0.0244(15)
C34	0.3615(3)	0.3519(6)	0.4910(3)	0.0267(16)
C35	0.4742(2)	0.2744(6)	0.5664(3)	0.0240(15)
C36	0.4412(3)	0.5377(6)	0.5541(3)	0.0364(18)
I1S	-0.065169(18)	0.63518(4)	0.62517(2)	0.02959(15)
Li1	0.0341(5)	0.7491(11)	0.6192(4)	0.029(3)
O1S	0.07325(16)	0.7069(4)	0.55170(17)	0.0240(10)
O2S	0.08749(17)	0.7421(4)	0.69723(17)	0.0291(11)
O3S	0.01900(18)	0.9265(4)	0.6046(2)	0.0325(11)
C1S	0.1320(3)	0.7025(6)	0.5430(3)	0.0269(16)
C2S	0.1308(3)	0.6753(6)	0.4747(3)	0.0308(16)
C3S	0.0721(3)	0.7149(7)	0.4450(3)	0.0305(16)
C4S	0.0374(3)	0.6813(6)	0.4939(3)	0.0261(15)
C5S	0.0724(3)	0.7316(8)	0.7579(3)	0.048(2)
C6S	0.1253(3)	0.7550(10)	0.8019(3)	0.064(3)
C7S	0.1724(3)	0.7181(10)	0.7698(3)	0.064(3)
C8S	0.1484(3)	0.7241(7)	0.7019(3)	0.0363(18)
C9S	0.0037(3)	0.9915(7)	0.6561(3)	0.0393(18)
C10S	0.0559(4)	1.0624(9)	0.6829(4)	0.070(3)
C11S	0.0886(4)	1.0743(8)	0.6325(4)	0.062(3)
C12S	0.0589(4)	1.0021(7)	0.5807(4)	0.051(2)
H3A	0.1038	0.4107	0.5454	0.029
H4A	0.0352	0.4673	0.6045	0.030
H5A	0.0503	0.4425	0.7108	0.029
H6A	0.1356	0.3567	0.7634	0.028
H10A	0.5480	-0.0280	0.7347	0.027
H11A	0.6011	-0.1444	0.6749	0.030
H12A	0.5649	-0.1947	0.5735	0.031
H13A	0.4751	-0.1273	0.5256	0.030
H15A	0.2539	0.2769	0.5319	0.025
H15B	0.1992	0.3618	0.5119	0.025
H16A	0.1892	0.1055	0.5353	0.025

H16B	0.1380	0.1933	0.5057	0.025
H17A	0.2319	0.1266	0.4459	0.036
H17B	0.1830	0.2198	0.4165	0.036
H18A	0.1630	0.0238	0.3731	0.066
H18B	0.1143	0.0604	0.4117	0.066
H18C	0.1635	-0.0326	0.4404	0.066
H19A	0.2487	0.3217	0.7909	0.024
H19B	0.2920	0.2342	0.7634	0.024
H20A	0.2239	0.0705	0.7611	0.029
H20B	0.1852	0.1590	0.7947	0.029
H21A	0.2987	0.0856	0.8480	0.032
H21B	0.2604	0.1751	0.8814	0.032
H22A	0.2582	-0.0226	0.9221	0.054
H22B	0.2340	-0.0752	0.8547	0.054
H22C	0.1957	0.0143	0.8881	0.054
H23A	0.4332	0.2075	0.7426	0.025
H23B	0.4861	0.1194	0.7661	0.025
H24A	0.4141	0.0913	0.8270	0.029
H24B	0.3692	0.0579	0.7667	0.029
H25A	0.4647	-0.0894	0.8171	0.037
H25B	0.4229	-0.1217	0.7542	0.037
H26A	0.3971	-0.2356	0.8366	0.071
H26B	0.3462	-0.1448	0.8098	0.071
H26C	0.3880	-0.1124	0.8728	0.071
H27A	0.3879	0.0368	0.4960	0.024
H27B	0.3340	0.0580	0.5293	0.024
H28A	0.3377	-0.1630	0.5506	0.031
H28B	0.3804	-0.1715	0.5018	0.031
H29A	0.2875	-0.2184	0.4522	0.045
H29B	0.2645	-0.0909	0.4734	0.045
H30A	0.2743	-0.0814	0.3701	0.074
H30B	0.3404	-0.1158	0.3877	0.074
H30C	0.3179	0.0121	0.4092	0.074
H31A	0.2656	0.6703	0.5827	0.044
H31B	0.2529	0.5302	0.5651	0.044
H31C	0.3062	0.5974	0.5442	0.044
H32A	0.2656	0.6296	0.7126	0.050
H32B	0.3093	0.5396	0.7540	0.050

H32C	0.2561	0.4851	0.7076	0.050
H33A	0.3657	0.7431	0.6743	0.037
H33B	0.4106	0.6648	0.6441	0.037
H33C	0.4053	0.6452	0.7152	0.037
H34A	0.3814	0.3619	0.4557	0.040
H34B	0.3298	0.4100	0.4874	0.040
H34C	0.3467	0.2685	0.4914	0.040
H35A	0.4902	0.2833	0.5284	0.036
H35B	0.4614	0.1901	0.5700	0.036
H35C	0.5034	0.2941	0.6021	0.036
H36A	0.4570	0.5404	0.5157	0.055
H36B	0.4713	0.5562	0.5892	0.055
H36C	0.4106	0.5980	0.5522	0.055
H1SA	0.1528	0.6377	0.5690	0.032
H1SB	0.1510	0.7816	0.5544	0.032
H2SA	0.1604	0.7223	0.4583	0.037
H2SB	0.1366	0.5872	0.4679	0.037
H3SA	0.0590	0.6703	0.4060	0.037
H3SB	0.0706	0.8038	0.4367	0.037
H4SA	0.0021	0.7305	0.4893	0.031
H4SB	0.0270	0.5938	0.4910	0.031
H5SA	0.0577	0.6489	0.7642	0.058
H5SB	0.0428	0.7922	0.7633	0.058
H6SA	0.1260	0.7066	0.8401	0.077
H6SB	0.1284	0.8426	0.8130	0.077
H7SA	0.1853	0.6343	0.7818	0.077
H7SB	0.2051	0.7744	0.7801	0.077
H8SA	0.1656	0.7928	0.6822	0.044
H8SB	0.1563	0.6474	0.6811	0.044
H9SA	-0.0070	0.9341	0.6870	0.047
H9SB	-0.0287	1.0471	0.6423	0.047
H10B	0.0454	1.1437	0.6972	0.084
H10C	0.0782	1.0183	0.7183	0.084
H11B	0.1278	1.0435	0.6456	0.074
H11C	0.0906	1.1609	0.6202	0.074
H12B	0.0390	1.0564	0.5480	0.061
H12C	0.0864	0.9514	0.5628	0.061

Appendix I: Crystal data and structure refinement for $[\text{NiI}(\text{Pr}_2\text{-bimy})_2\text{P}\{\text{C}(\text{O})\text{Ph}\}_2]\cdot\text{C}_7\text{H}_8$ (*trans-9*)

Formula	$\text{C}_{47}\text{H}_{54}\text{IN}_4\text{NiO}_2\text{P}$
Formula Weight (<i>g/mol</i>)	923.52
Crystal Dimensions (<i>mm</i>)	$0.476 \times 0.091 \times 0.032$
Crystal Color and Habit	orange needle
Crystal System	monoclinic
Space Group	$\text{P } 2_1/n$
Temperature, K	110
<i>a</i> , Å	12.750(3)
<i>b</i> , Å	9.244(2)
<i>c</i> , Å	38.007(11)
α , °	90
β , °	95.444(18)
γ , °	90
<i>V</i> , Å ³	4459(2)
Number of reflections to determine final unit cell	9863
Min and Max 2θ for cell determination, °	4.54, 52.32
<i>Z</i>	4
F(000)	1904
ρ (<i>g/cm</i>)	1.376
λ , Å, (MoK α)	0.71073
μ , (<i>cm</i> ⁻¹)	1.204
Diffractometer Type	Bruker Kappa Axis Apex2
Scan Type(s)	ω and ϕ scans
Max 2θ for data collection, °	56.444
Measured fraction of data	0.998
Number of reflections measured	73261
Unique reflections measured	10960
R_{merge}	0.0626
Number of reflections included in refinement	10960
Cut off Threshold Expression	$I > 2\sigma(I)$
Structure refined using	full matrix least-squares using F^2
Weighting Scheme	$w=1/[\sigma^2(\text{Fo}^2)+(0.0574\text{P})^2+1.1403\text{P}]$ where $\text{P}=(\text{Fo}^2+2\text{Fc}^2)/3$

Number of parameters in least-squares	514
R ₁	0.0391
wR ₂	0.0959
R ₁ (all data)	0.0613
wR ₂ (all data)	0.1140
GOF	1.114
Maximum shift/error	0.003
Min & Max peak heights on final ΔF Map (e ⁻ /Å)	-0.921, 0.995

Where:

$$R_1 = \sum (|F_o| - |F_c|) / \sum F_o$$

$$wR_2 = [\sum (w(F_o^2 - F_c^2))^2 / \sum (w F_o^4)]^{1/2}$$

$$GOF = [\sum (w(F_o^2 - F_c^2))^2 / (\text{No. of reflns.} - \text{No. of params.})]^{1/2}$$

Appendix J: Atomic coordinates for $[\text{NiI}(\text{}^i\text{Pr}_2\text{-bimy})_2\text{P}\{\text{C}(\text{O})\text{Ph}\}_2]\cdot\text{C}_7\text{H}_8$ (*trans-9*)

Atom	x	y	z	$U_{\text{iso/equiv}}$
I1	0.46565(2)	0.55638(3)	0.68875(2)	0.02975(8)
Ni1	0.39303(3)	0.36763(4)	0.64466(2)	0.01663(9)
P1	0.34127(6)	0.17756(9)	0.61334(2)	0.02192(17)
O2	0.13356(17)	0.1567(3)	0.61752(6)	0.0332(6)
N4	0.23765(17)	0.2860(3)	0.69223(6)	0.0174(5)
N3	0.17971(18)	0.4611(3)	0.65746(6)	0.0167(5)
O1	0.49345(18)	0.1817(3)	0.56823(6)	0.0388(6)
N1	0.60854(17)	0.2806(3)	0.63935(6)	0.0189(5)
N2	0.56343(18)	0.4542(3)	0.60212(6)	0.0191(5)
C20	0.1377(2)	0.3210(3)	0.70177(7)	0.0189(6)
C19	0.0783(2)	0.2653(4)	0.72768(8)	0.0274(7)
C17	-0.0580(2)	0.4374(4)	0.70812(9)	0.0287(7)
C6	0.7395(2)	0.4740(4)	0.57535(8)	0.0240(7)
C18	-0.0203(3)	0.3259(4)	0.73025(8)	0.0301(7)
C16	0.0017(2)	0.4942(4)	0.68242(8)	0.0230(6)
C21	0.1807(2)	0.5780(3)	0.63132(7)	0.0201(6)
C7	0.6681(2)	0.4201(3)	0.59775(7)	0.0195(6)
C15	0.1004(2)	0.4325(3)	0.67958(7)	0.0183(6)
C24	0.3081(2)	0.1716(3)	0.70819(8)	0.0234(6)
C28	0.3534(2)	0.0300(4)	0.54684(8)	0.0254(7)
C2	0.6968(2)	0.3095(3)	0.62162(7)	0.0202(6)
C33	0.2917(2)	-0.0833(4)	0.55697(9)	0.0302(7)
C22	0.1881(3)	0.7243(3)	0.64932(9)	0.0279(7)
C3	0.7973(2)	0.2492(4)	0.62437(8)	0.0267(7)
C23	0.0874(2)	0.5670(4)	0.60325(8)	0.0270(7)
C25	0.3440(3)	0.2053(4)	0.74644(8)	0.0332(8)
C4	0.8676(2)	0.3035(4)	0.60193(9)	0.0293(7)
C5	0.8388(2)	0.4130(4)	0.57799(8)	0.0276(7)
C14	0.2626(2)	0.3707(3)	0.66523(7)	0.0168(6)
C32	0.2496(3)	-0.1826(4)	0.53189(11)	0.0407(9)
C29	0.3724(3)	0.0436(4)	0.51163(9)	0.0356(8)
C27	0.4048(2)	0.1374(4)	0.57282(8)	0.0252(7)
C26	0.2592(3)	0.0234(4)	0.70263(10)	0.0376(8)
C11	0.4981(2)	0.5647(4)	0.58281(8)	0.0252(7)
C34	0.1992(2)	0.1864(4)	0.59742(8)	0.0235(6)

C1	0.5271(2)	0.3670(3)	0.62696(7)	0.0183(6)
C35	0.1631(2)	0.2332(4)	0.56038(8)	0.0236(7)
C41	-0.1123(3)	0.8606(4)	0.63704(11)	0.0444(9)
C8	0.5993(2)	0.1721(4)	0.66745(8)	0.0273(7)
C40	0.0734(2)	0.1688(4)	0.54364(9)	0.0306(7)
C36	0.2128(2)	0.3425(4)	0.54352(8)	0.0283(7)
C12	0.5405(3)	0.7157(4)	0.59170(10)	0.0374(8)
C9	0.6771(3)	0.2022(5)	0.69951(9)	0.0409(9)
C13	0.4849(3)	0.5347(4)	0.54330(8)	0.0355(9)
C31	0.2683(3)	-0.1667(5)	0.49701(11)	0.0463(10)
C30	0.3295(3)	-0.0540(5)	0.48654(10)	0.0458(10)
C37	0.1719(3)	0.3905(4)	0.51037(9)	0.0379(8)
C46	-0.1870(3)	0.7605(5)	0.64330(13)	0.0520(11)
C10	0.6052(3)	0.0205(4)	0.65298(11)	0.0396(9)
C39	0.0343(3)	0.2133(5)	0.50971(10)	0.0456(10)
C38	0.0839(3)	0.3244(5)	0.49353(10)	0.0457(10)
C45	-0.2164(4)	0.7357(7)	0.67663(19)	0.0872(18)
C42	-0.0615(4)	0.9366(5)	0.66413(16)	0.0689(14)
C44	-0.1698(7)	0.8132(9)	0.70431(19)	0.106(2)
C43	-0.0917(6)	0.9122(7)	0.69825(17)	0.0941(19)
C47	-0.0835(6)	0.8927(7)	0.60023(16)	0.108(3)
H19	0.1043	0.1891	0.7429	0.033
H17	-0.1260	0.4760	0.7105	0.034
H6	0.7206	0.5495	0.5590	0.029
H18	-0.0628	0.2902	0.7475	0.036
H16	-0.0238	0.5714	0.6675	0.028
H21	0.2460	0.5657	0.6190	0.024
H24	0.3726	0.1725	0.6951	0.028
H33	0.2781	-0.0933	0.5810	0.036
H22A	0.1274	0.7377	0.6630	0.042
H22B	0.1885	0.8006	0.6314	0.042
H22C	0.2532	0.7293	0.6652	0.042
H3	0.8169	0.1743	0.6408	0.032
H23A	0.0835	0.4687	0.5936	0.041
H23B	0.0964	0.6362	0.5842	0.041
H23C	0.0222	0.5890	0.6139	0.041
H25A	0.3767	0.3013	0.7480	0.050
H25B	0.3955	0.1326	0.7557	0.050

H25C	0.2832	0.2037	0.7604	0.050
H4	0.9369	0.2648	0.6030	0.035
H5	0.8889	0.4470	0.5630	0.033
H32	0.2080	-0.2610	0.5388	0.049
H29	0.4153	0.1206	0.5046	0.043
H26A	0.2012	0.0128	0.7176	0.056
H26B	0.3125	-0.0509	0.7089	0.056
H26C	0.2322	0.0122	0.6778	0.056
H11	0.4264	0.5589	0.5914	0.030
H8	0.5272	0.1834	0.6754	0.033
H40	0.0385	0.0944	0.5552	0.037
H36	0.2753	0.3849	0.5546	0.034
H12A	0.5463	0.7298	0.6174	0.056
H12B	0.4924	0.7881	0.5803	0.056
H12C	0.6102	0.7265	0.5831	0.056
H9A	0.7489	0.1834	0.6935	0.061
H9B	0.6614	0.1390	0.7190	0.061
H9C	0.6710	0.3035	0.7066	0.061
H13A	0.5515	0.5545	0.5332	0.053
H13B	0.4295	0.5971	0.5320	0.053
H13C	0.4654	0.4331	0.5392	0.053
H31	0.2389	-0.2340	0.4799	0.056
H30	0.3420	-0.0436	0.4624	0.055
H37	0.2044	0.4687	0.4993	0.045
H46	-0.2196	0.7064	0.6240	0.062
H10A	0.5499	0.0073	0.6335	0.059
H10B	0.5953	-0.0495	0.6717	0.059
H10C	0.6743	0.0053	0.6443	0.059
H39	-0.0258	0.1675	0.4979	0.055
H38	0.0572	0.3556	0.4706	0.055
H45	-0.2685	0.6654	0.6803	0.105
H42	-0.0074	1.0037	0.6602	0.083
H44	-0.1905	0.7996	0.7274	0.127
H43	-0.0579	0.9647	0.7176	0.113
H47A	-0.0977	0.8073	0.5852	0.161
H47B	-0.0086	0.9173	0.6012	0.161
H47C	-0.1257	0.9743	0.5904	0.161

CURRICULUM VITAE

MASOOMEH MADADI

EDUCATION

M.Sc., Inorganic Chemistry

The University of Western Ontario, London, ON, Canada Jan. 2013 – Oct. 2014

M.Sc., Inorganic Chemistry

Iran University of Science and Technology, Tehran, Iran Sep. 2008 – Feb. 2011

B.Sc., Chemistry

Shahid Beheshti University, Tehran, Iran Sep. 2003 – Sep. 2007

TEACHING ASSISTANT EXPERIENCE

The University of Western Ontario, London, ON, Canada. Jan. 2013 – Jun. 2014

- General Chemistry (CHEM 1100) Winter 2013
- General Chemistry (CHEM 1301A) Fall 2013
- Organic Chemistry (CHEM 2223B) Winter 2014
- Organic Chemistry (CHEM 2213A) Summer 2014

Iran University of Science and Technology, Tehran, Iran. Sep. 2008 – Feb. 2011

- General Chemistry Winter 2009
 - Inorganics Chemistry Fall 2010 – Winter 2011
-

PEER-REVIEWED PUBLICATIONS

JOURNALS

- Masoomeh Madadi, Bahareh Khalili Najafabadi, Mahmood Azizpoor Fard and John F. Corrigan; “NHC Stabilized Bis(trimethylsilyl)phosphido Complexes of Pd(II) and Ni(II)”, *European Journal of Inorganic Chemistry*, (2014). (submitted)
- Madadi. M, Rahimi. R; “Zeolite-immobilized Mn(III), Fe(III) and Co(III) complexes with 5,10,15,20-tetra(4-methoxyphenyl)porphyrin as heterogeneous catalysts for epoxidation of (R)-(+)-limonene: Synthesis, characterization and catalytic activity”, *Journal of Reaction Kinetics, Mechanism and Catalysis*, vol. 107, no. 1, pp. 215-229, (2012).

- Madadi. M, Rahimi. R; “Zeolite-encapsulated Fe (III) complex with 5,10,15,20-tetraphenyl porphyrin as heterogeneous catalysts for epoxidation of α -pinene: Synthesis, characterization and catalytic activity”; *Journal of Chemistry and Chemical Engineering*, vol. 6, pp. 173-178, (2012).

CONFERENCES

- Madadi. M, Rahimi. R; “Host (nanocages of zeolite X)–guest (metallo and nanometallo porphyrins) nanocomposite material: An efficient catalyst for the epoxidation of (R)-(+)-limonene”, *Nanotech India 2010 Conference*, India, (2010).
 - Madadi. M, Rahimi. R; “Synthesis and Characterization of Manganese (III) tetra (4-methoxyphenyl) porphyrin encapsulated in zeolite –X: as efficient catalyst for the hydroxylation of Thymol”; *14th International Electronic Conference on Synthetic Organic Chemistry*, Spain, (2010).
 - Madadi. M, Rahimi. R; “Cationic metalloporphyrins in zeolite matrix as efficient catalysts for Monoterpenes oxidation with H₂O₂/ammonium acetate”; *The 12th Iranian Inorganic Chemistry Conference (IICC12)*, Rasht, Iran, (2010).
 - Madadi. M, Rahimi. R; “Oxidation of Terpenes with tetra-phenylporphyrin and it's different transition- metal analogues”; *The 12th Iranian Nanotechnology Conference*, Tehran, Iran (2012).
-